Pavement Deterioration Modeling Using Historical Roughness Data

by

Michelle Elizabeth Beckley

A Thesis Presented in Partial Fulfillment
of the Requirements for the Degree
Master of Science

Approved April 2016 by the
Graduate Supervisory Committee:

Kamil Kaloush, Chair
Shane Underwood
Michael Mamlouk

ARIZONA STATE UNIVERSITY

May 2016

ABSTRACT

Pavement management systems and performance prediction modeling tools are essential for maintaining an efficient and cost effective roadway network. One indicator of pavement performance is the International Roughness Index (IRI), which is a measure of ride quality and also impacts road safety. Many transportation agencies use IRI to allocate annual maintenance and rehabilitation strategies to their road network.

The objective of the work in this study was to develop a methodology to evaluate and predict pavement roughness over the pavement service life. Unlike previous studies, a unique aspect of this work was the use of non-linear mathematical function, sigmoidal growth function, to model the IRI data and provide agencies with the information needed for decision making in asset management and funding allocation. The analysis included data from two major databases (case studies): Long Term Pavement Performance (LTPP) and the Minnesota Department of Transportation MnROAD research program. Each case study analyzed periodic IRI measurements, which were used to develop the sigmoidal models.

The analysis aimed to demonstrate several concepts; that the LTPP and MnROAD roughness data could be represented using the sigmoidal growth function, that periodic IRI measurements collected for road sections with similar characteristics could be processed to develop an IRI curve representing the pavement deterioration for this group, and that pavement deterioration using historical IRI data can provide insight on traffic loading, material, and climate effects. The results of the two case studies concluded that in general, pavement sections without drainage systems, narrower lanes, higher traffic, or measured

in the outermost lane were observed to have more rapid deterioration trends than their counterparts.

Overall, this study demonstrated that the sigmoidal growth function is a viable option for roughness deterioration modeling. This research not only to demonstrated how historical roughness can be modeled, but also how the same framework could be applied to other measures of pavement performance which deteriorate in a similar manner, including distress severity, present serviceability rating, and friction loss. These sigmoidal models are regarded to provide better understanding of particular pavement network deterioration, which in turn can provide value in asset management and resource allocation planning.

DEDICATION

This thesis is dedicated to my parents, family, and friends whose continual support has helped me throughout my education and during the development of this research work. I am grateful for their unconditional love, compassion, and understanding.

ACKNOWLEDGMENTS

The author would first like to express utmost gratitude to her advisor, Professor Kamil E. Kaloush, who provided invaluable instruction, support, encouragement, and guidance from the beginning of the author's graduate program at Arizona State University. His support and guidance aided in the development of the author's interest in pavement engineering, this research topic, and the success in her graduate studies. Deepest gratitude is also due to the members of the supervisory committee, Professor Shane Underwood and Professor Michael Mamlouk, who provided instruction, guidance, and support throughout the author's graduate program and this research work.

This research was supported in part by Arizona State University funding, through a research assistantship that allowed the author to pursue her area of interest. The author is deeply appreciative for the support of the National Center of Excellence (NCE) for SMART Innovations and ASU's University Transportation Center (UTC). The author also would like to acknowledge the Long-Term Pavement Performance program (LTPP) and the Minnesota Road Research Project (MnROAD), for making available and providing the necessary data for this research.

TABLE OF CONTENTS

Page

Page

Page

LIST OF TABLES

Table Page

LIST OF FIGURES

Figure Page

DEFINITIONS

AADT	Annual Average Daily Traffic
AADTT	Annual Average Daily Truck Traffic
AC	Asphalt Concrete
ASTM	American Society for Testing and Materials
ESAL	Equivalent Single Axel Load
LISA	Lightweight Inertial Surface Analyzer
LTPP	Long Term Pavement Performance
MnDOT	Minnesota Department of Transportation
MnROAD	Minnesota Road Research Project
MEPDG	Mechanistic-Empirical Pavement Design Guide
PCI	Pavement Condition Index
PCC	Portland Cement Concrete
PMS	Pavement Management System
PSR	Present Serviceability Rating
SHRP	Strategic Highway Research Program

1. INTRODUCTION

1.1 Background

1.1.1. Pavement Management Systems

The primary goals of pavement management systems (PMS) are to maintain or improve the quality of the roadway network, while utilizing available funding in the most effective and beneficial way. Pavement management systems not only prioritize the maintenance of already deteriorated roadway segments, but also utilize historic data and deterioration modelling to plan for future conditions. There is a significant benefit to preventative pavement maintenance; as minor maintenance treatments on pavements still in good condition have a higher cost-effectiveness than major rehabilitation of a deteriorated pavement. The use of pavement management systems allows the optimum use of available resources (e.g., money and materials) while meeting set constraints of budget and time requirements (Molenaar, 2001). Pavement management systems can be used at the local, county, state, or federal level. Benchmarking and tracking the condition changes within the roadway network are important in predicting future deterioration and managing assets.

1.1.2 Pavement Roughness

Pavement roughness values are measured in the form of an international roughness index (IRI), which is a primary indication of ride quality. The IRI was developed in 1982 as part of an international experiment conducted in Brazil. It constitutes the smoothness, safety, and the ease of the driving path (Prasad et al., 2013). The IRI depends on the pavement distresses present, it is a measure of the surface texture, and it is a key indicator in driving safety. The IRI is usually correlated to roughness measurements obtained from both response-type and inertial-based profiler systems (Sayers 1990). The international roughness index is measured in units of slope, and it describes the suspension motion of a moving vehicle over a travelled distance, usually in meters per kilometer or inches per mile (Park et al., 2007). The IRI ranges from 0 m/km to 20 m/km (greatest roughness). The Federal Highway Administration (FHWA) provided guidelines on the various IRI measures as shown in the Table 1 below (FHWA 1999). IRI is also calculated in accordance with ASTM Standard E 1926 (ASTM 1999e).

Table 1: IRI and Condition (FHWA, 1999)

Condition Categories	PSR Rating		IRI Rating, m/km (in/mi)		Interstate and NHS Ride Quality
	Interstate	Other	Interstate	Other	
Very Good	≥ 4.0	≥ 4.0	< 1.0 (< 60)	< 1.0 (< 60)	Acceptable 0 – 2.0 (0 – 170) Less than Acceptable > 2.0 (> 170)
Good	3.5 – 3.9	3.5 – 3.9	1.0 – 1.5 (60 – 94)	1.0 – 1.5 (60 – 94)	
Fair	3.1 – 3.4	2.6 – 3.4	1.5 – 1.9 (95 – 119)	1.5 – 2.0 (95 – 170)	
Mediocre	2.6 – 3.0	2.1 – 2.5	1.9 – 2.0 (120 – 170)	2.0 – 3.5 (171 – 220)	
Poor	≤ 2.5	≤ 2.0	> 2.0 (> 170)	> 3.5 (> 220)	

Notes: PSR = Present serviceability rating, NHS = National Highway System.

Pavements with high IRI values can be indicative of surface distresses, uneven pavement, and low ride quality. Higher IRI values are more accepted in low volume rural areas than in high volume highways. In pavement management, surface distresses and roughness are measured periodically in order to set benchmark values and predict future conditions.

1.1.3 Sigmoidal Function

Pavement performance is dependent on traffic loading, climatic conditions, material selection, and structural composition. The general shape of the pavement performance function (loss of serviceability) is classically described as an “S” shaped curve. This deterioration pattern in pavements has been acknowledged by many researchers, including

Riggins et al. (1984) and Sotil and Kaloush (2004). The pavement performance deterioration concept is shown in Figure 1.

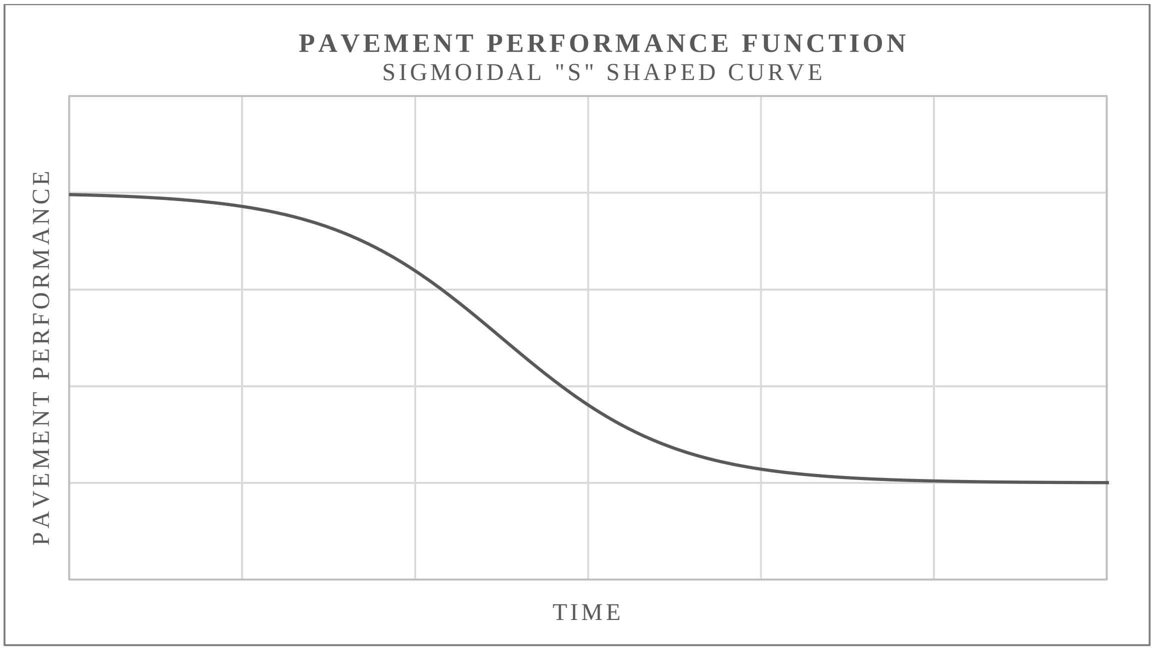

Figure 1: Pavement Performance Function, Sigmoidal "S" Shaped Curve

This concept applies to many aspects of pavement condition, including the Pavement Condition Index (PCI) and Present Serviceability Rating (PSR). These measures of pavement condition begin at a high level (desirable) and worsen to a low level over time. This trend is represented mathematically as a sigmoidal function and can take different shape forms.

The sigmodal function was selected due to its previous successful application in pavement condition modeling; it also best represents the pavement deterioration process. A similar pattern is expected in pavement roughness deterioration, except that decay is traded by growth. At the beginning of a pavement's life, the measured roughness values are low with excellent ride quality. Noticeable deterioration is not common over the first several years of pavement life. After the first few years, small distresses begin to form, which start to affect the roughness minimally. Once these distresses become apparent, the pavement begins more to deteriorate more rapidly. The deterioration slows after a certain level is reached. This trend follows the shape of the sigmoidal growth curve.

1.2 Research Objectives

The objective of the analysis in this study was to develop a methodology to evaluate and predict pavement roughness over the pavement service life. Based on historical roughness data collected, a local, county, or state agency can develop a model to predict how the pavement surface will deteriorate over time. The ability to plan for future pavement deterioration allows the jurisdiction to develop a maintenance strategy timeline.

1.3 Proposed Concept

A sigmoidal growth model to be evaluated and constructed to simulate the roughness deterioration pattern in pavements. The proposed roughness sigmoidal model is the inverse of the classic pavement performance function; the desired pavement roughness is initially low but increases over time. The analysis aims to demonstrate the following concepts:

- LTPP IRI data can be represented using a sigmoidal growth function
- IRI measurements collected for road sections with similar characteristics could be processed to develop a fitted “family” sigmoidal curve representing pavement deterioration for this group.
- Pavements separated further into subgroups can provide meaningful results which compare deterioration patterns between similar groups
- Pavement subgroups with the following characteristics will deteriorate more rapidly than their counterparts:
    - High traffic loading sections (compared to low traffic conditions)

- Freezing climate sections (compared to more moderate climates)
- Primary driving lane (outer) sections (compared to inner or passing lane)
- Standard lane-width sections compared to some wider lane-width designs
- Sections with and without adequate drainage systems

A graphical representation of the proposed concepts is shown in Figure 2.

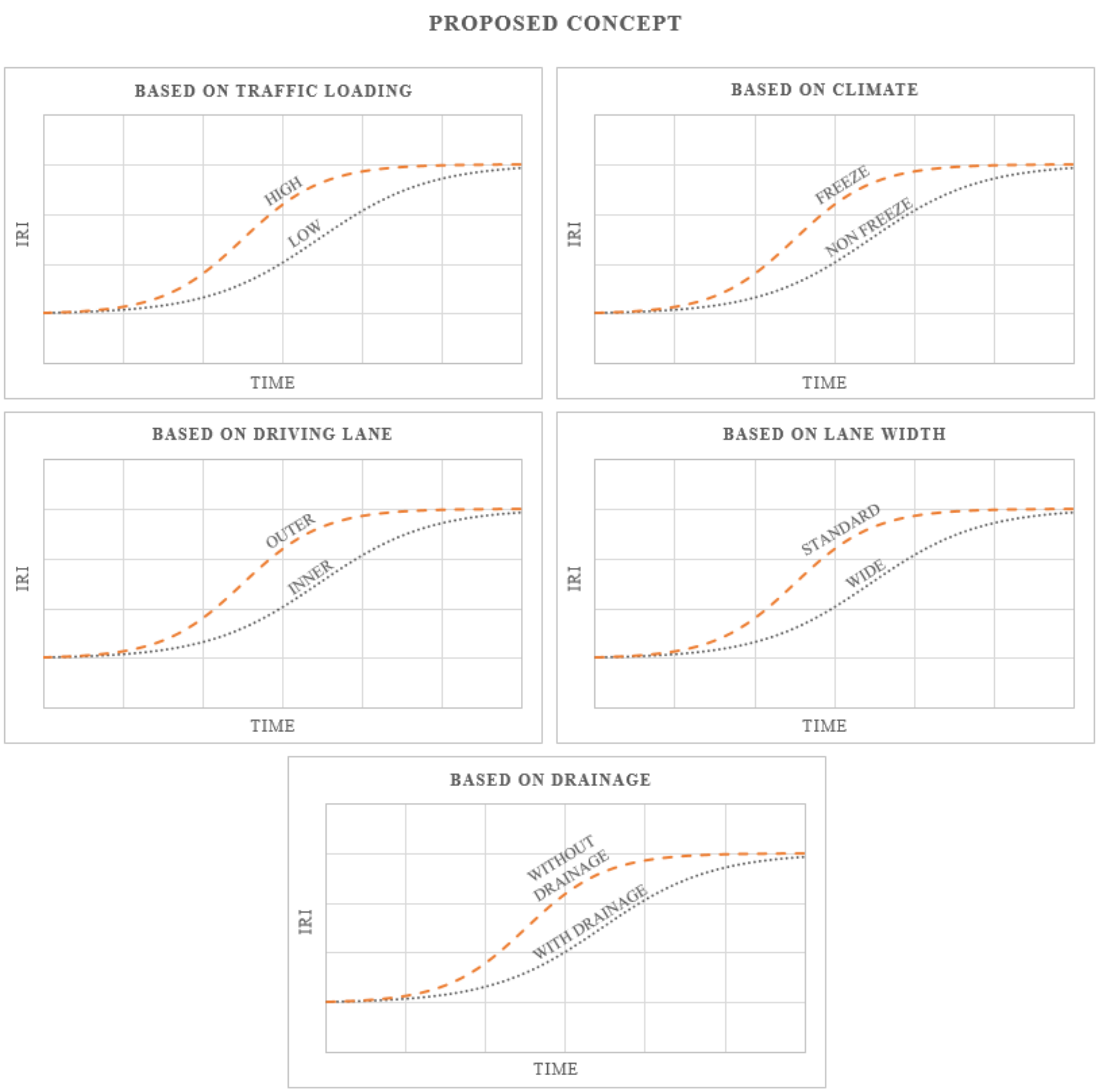

Figure 2: Proposed Deterioration between Pavement Subgroups

1.4 Scope of Research

The analysis in this study used data from the Long Term Pavement Performance (LTPP) InfoPave database and the Minnesota Road Research Program (MnROAD). To develop the methodology for predicting pavement roughness, pavement sections from Arizona (LTPP) and Minnesota (MnROAD Test Track) were used as case studies. The historical roughness (IRI) data (measured on a frequent basis, approximately once every 6-18 months) of each pavement section was analyzed to develop sigmoidal models representing deterioration. These models can then be used to predict pavement roughness over the service life if there is no planning for future maintenance action. The goal was to determine the IRI over time, demonstrate the time until the IRI reaches an unacceptable level. The process developed in this analysis can be useful for pavement management and applied to other performance measures.

1.5 Organization of Thesis

In the next chapter, a literature review outlines the concepts and theories related to pavement condition management and modeling. Past research efforts which identify current conditions and develop models to predict future pavement conditions are discussed. In Chapter 3, the methodology of this research is provided, which includes a discussion of the data sources and formats, data processing, and the conceptual framework for developing the IRI sigmoidal master curves. This process of developing sigmoidal curves is demonstrated in Chapters 4 and 5, which use historical data collected over the past 25 years from pavement test sections in Arizona and Minnesota. Chapter 4 is a case study using Arizona roadway sections from the LTPP InfoPave database, and Chapter 5 is a case study using Minnesota roadway sections provided from MnDOT's pavement test track, MnROAD. The concepts, methods, and results are concluded in Chapter 6, which also provides additional recommendations for the implementation of this research into practice.

2. LITERATURE REVIEW

2.1 Pavement Management Purpose

There are three primary objectives of a pavement management system: to implement more cost-effective treatment strategies, allocate funding to the pavement sections that will result in the best performance, and improve the quality of the pavement network (AASHTO, 2001). The goal of a pavement management system is to allocate funding in the most beneficial way towards the roadway network. The planning and scheduling of maintenance is crucial in preserving pavement condition; preventative maintenance extends the service life of a pavement and delays the need for serious rehabilitation or reconstruction. Pavement maintenance strategies can be used at either the project level, focusing on a small selection of pavement, or network level, which considers many pavement sections within an area (Haas, Hudson, & Zaniewski, 1994). The processes and methodology developed in this research is designed as a network level pavement management tool. The basic components of a network level PMS are shown in Figure 3 (FHWA, 1995).

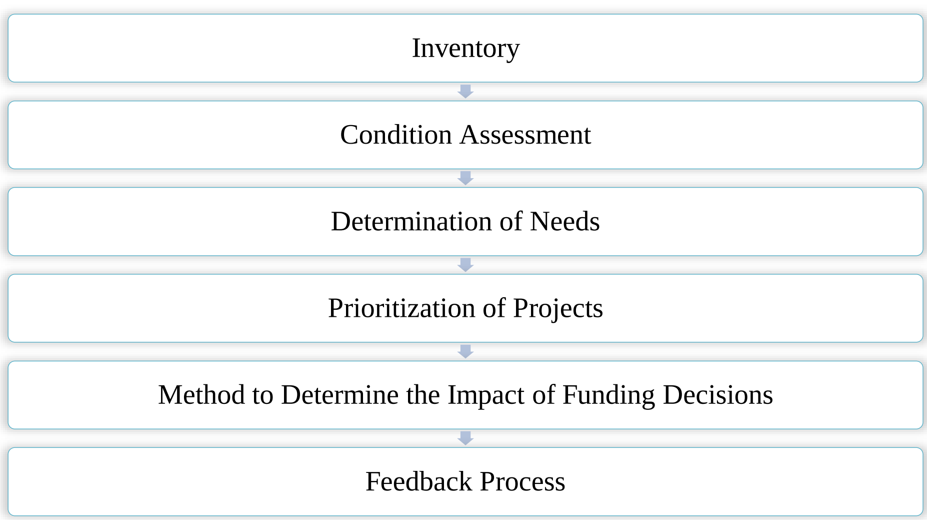

Figure 3: Network Level PMS Components

This research study will add value to the “Condition Assessment”, as future prediction will be available in addition to existing conditions. This information will better help to prioritize maintenance efforts using available funding.

2.2 IRI Measurement Process

The development of roughness testing began in the 1970’s and 1980’s with funding by the World Bank and the National Cooperative Highway Research Program (Park et al., 2007). The World Bank originally funded research to determine cost effective maintenance techniques, and it was discovered that roughness was a main source of user costs derived from poor pavement surfaces. The American Society for Testing and Materials (ASTM) has developed standard testing methods for pavement roughness using a profilograph. The testing device is a “platform comprised of dollies articulated by rigid members or trusses so that all the wheels are supporting the profilograph” (ASTM, 2012). The profilograph consists of 12 wheels, has a minimum length of 23ft, and obtains roughness measurements as it moves longitudinally across the pavement section.

More recently, there are several other common roughness measuring devices which include response-type measuring systems (Maysmeter and Roadmeter) and other inertial road profiling systems (Profiler and Profilometer) (Kaloush, 2014). Profile-measuring vehicles are most commonly utilized than truss profilographs due to the ease of use and consistency. Rather than manually translating the profilograph, an operator can measure pavement roughness simply by driving along the pavement. ASTM has also developed standards for this method of data collection, referred to as an “Accelerometer Established Inertial Profiling Reference”. This method continually measures elevation variation of the pavement surface as it moves longitudinally along the pavement (ASTM, 2009). Inertial profiling systems are able to cover a large pavement network and process data electronically. The IRI datasets included in this research work were measured using inertial profiling systems.

2.3 Pavement Condition Deterioration in Pavement Groups

Pavement performance and the rate of deterioration depend on many factors; the layer structure and materials, quality of construction, intensity of traffic loading, and the climatic conditions.

Construction variability has a significant impact on long term pavement performance (Sebaaly & Bazi, 2004). Extensive planning goes into material selection and mix design, however poor construction practices, such as uneven mixing or insufficient compaction can reduce the long term performance.

Traffic is the primarily responsible for problems associated with pavement performance (Pais, Amorim, & Minhoto, 2013). More specifically, the performance is impacted by load intensity, frequency, and axle and tire configuration. Heavy traffic causes fatigue cracking and rutting, both of which increase the IRI measurement. Trucks are of primary concern, as they carry much greater weight and axle loads. Pavement damage increases rapidly as axle loads increase. A study performed by the City of Fort Collins, Colorado, attempted to evaluate the impacts of routine garbage trucks on residential streets. This study concluded that the pavement damage caused by vehicles increases at a higher than proportional rate as vehicle size and weight increase (R3 Consulting Group, Inc., 2008). Heavier traffic loads are expected to cause more pavement deterioration than lower traffic loads.

Temperature and precipitation also affect pavement performance. The presence of freezing temperatures can cause pavement problems, including thermal, fatigue and frost related cracking, pavement rutting (due to thaw), potholes, and crack deterioration (Zubeck & Dore, 2009). Excess moisture that is not able to sufficiently drain from the pavement structure can also cause damage, even if it remains in the subgrade.

2.4 IRI Modeling Approaches

Previous studies were reviewed to develop and support methodology used in this study. Included in this review is an IRI prediction model based on the pavement properties, distresses, and external factors; and IRI backcasting model, used to linearly interpolate missing IRI data; and lastly, a sigmoidal pavement performance model representing pavement condition index (PCI) changes over time.

2.4.1 The World Bank HDM-IV Model

Pavement roughness prediction models typically predict the IRI at a certain time using a baseline IRI, the time elapsed since the baseline, pavement thickness, traffic loading, environmental factors, and pavement distress observations. The World Bank HDM-IV flexible pavement smoothness model predicts IRI using a combination of distress, environmental, traffic, structural, and material factors. The developed World Band HDM-IV Model (Watanatada, 1987, M-E PDG, 2001):

Equation 1: World Bank HDM - IV Model

$$\Delta RI = 134e^{mt}MSNK^{-5.0}\Delta NE4 + 0.114\Delta RDS = 0.0066\Delta CRX + 0.003h\Delta PAT + 0.16\Delta POT + mRI_t\Delta t$$

Where:

ΔRI	= increase in roughness period over time period Δt
$MSNK$	= a factor related to pavement thickness, structural number and cracking
$\Delta NE4$	= incremental number of equivalent standard-axle loads (ESALs) in period
Δt	= change in time
ΔRDS	= increase in rut depth, mm
ΔCRX	= percent increase in area of cracking

ΔPAT	= percent increase in surface cracking
ΔPOT	= increase in total volume of potholes, m^3/lane km
m	= environmental factor
RI_t	= roughness at time t, years
Δt	= incremental time period for analysis, years
t	= average age of pavement or overlay, years
h	= average deviation of patch from original pavement profile, mm

This method incorporates many factors and can account for daily and hourly variation in temperature, moisture, and traffic.

2.4.2 MEPDG IRI Backcasting Method

In the Mechanical-Empirical Pavement Design Guide (M-E PDG), linear modelling is expressed as a practical method in determining the initial IRI in sections which data collection began after the roadway section was opened to traffic. This method was a backcasting technique used to fill missing LTPP IRI data (M-E PDG, 2001). The basis of the model was:

Equation 2: IRI Backcasting Model

$IRI = f(age)$

The initial IRI was found by determining the location of the y-intercept of the straight line which was fit to the known points. This technique has weaknesses; however, as it was determined that the backcasted initial IRI values were significantly different than the measured initial IRI.

2.4.3 Pavement Condition Index Deterioration Superposition Model

In the previous research by Sotil and Kaloush (2004), a sigmoidal decay model was developed to predict the pavement condition index (PCI) over time. The sigmoidal function developed is as follows:

Equation 3: PCI Sigmoidal Model

$$PCI = a + \frac{b}{1 + EXP(c \cdot T + d)}$$

Where:

PCI = Condition as dependent variable

T = Reduced (shifted) time as independent variable

a = Constant representing minimum PCI value

a + *b* = Constant representing maximum PCI value

c, *d* = Parameters describing the shape of the sigmoidal function

The research described the process of developing the sigmoidal curve using the superposition of sections. This model allowed for the future PCI to be predicted in the absence of future maintenance activities. Each roadway section was evaluated, a decrease in PCI from one year to the next was found (evidence of maintenance), the segment was broken into two, both starting at time (t) = 0. Each of the broken segments were used in the model, and they were individually shifted by a time factor to move to the appropriate lateral location on the sigmoidal curve. The sigmoidal curve was fit to best represent the data. This model was developed as a tool to benefit the pavement management of a roadway network and the prioritization of maintenance activity.

The sigmoidal curve and time shifting methodology discussed above was further developed and modified in this research to reflect pavement roughness deterioration.

3. METHODOLOGY

3.1 Process

The methodology described in this section utilizes historical pavement roughness data, typically collected from a local, regional, or state transportation agency. The measured roughness data is collected regularly using consistent calibrated equipment and standardized techniques. A sufficient timespan of data, reflecting pavement performance over time, is necessary to develop a performance curve, and pavements of varying age should be considered. Ideally, the modeling process would include roadway sections which were regularly measured over 25 years, from the time the roadway was open to traffic. In practical applications this is not always possible. In these cases, it is important to capture a sufficient quantity of roadway sections in various phases of the deterioration or performance curve. For example, developing a reliable model of lifetime pavement deterioration is not possible if only data of road sections of one to five years in age are considered.

This modeling approach produces a prediction tool for pavement roughness conditions if no further maintenance or reconstructed efforts are implemented. In addition, the constructed performance curve only considers the deterioration on roadway sections in between maintenance intervention. The process separates the complete timespan of collected IRI data on a roadway segment into multiple series. For example, if maintenance occurred at year 5, 8, 12, and 15, there are five separate series for modeling (years 0-5, years 5-8, years 8-12, years 12-15, and years 15+). If maintenance has not been adequately documented within the data, maintenance can be generally identified by a significant drop in IRI between two dates of collected measurements.

The best source of historical data for the modeling effort is from routine profilometers measurements. The data should be stored in a database which also documents material, construction, drainage, traffic, maintenance, and climatic (based on roadway network size) information. This additional information is used to create several specific models for parts of the roadway network with similar characteristics, which provides more accurate prediction. Asphalt Concrete (AC) and Portland Cement Concrete (PCC) sections should have distinct predictive models, as the timeline and process in which they deteriorate is different. In a large network of diverse roadway sections, a more accurate prediction for a particular roadway segment will come from a performance model that is built with sections of the same subgroup (i.e., sections with similar traffic levels or sections within the same climatic region).

A group of hypothetical roadway sections will be used to demonstrate the modeling process used in this methodology chapter. This example will extend through the other subsections within Chapter 3. The "measured" IRI data of the hypothetical five roadway sections of similar characteristics are presented in Table 2, which represent data throughout the service life of a typical pavement section. For example, Roadway Section 1 includes data from 1987 to 2006 and includes 20 IRI measurements (on average, one measurement every 12 months). The other 4 roadway sections include data which span different time periods.

Table 2: Data Demonstration – IRI Measurements of Five Roadway Segments

Roadway Section	Date of Measurement	Measured IRI (m/km)	Roadway Section	Date of Measurement	Measured IRI (m/km)	Roadway Section	Date of Measurement	Measured IRI (m/km)	Roadway Section	Date of Measurement	Measured IRI (m/km)	Roadway Section	Date of Measurement	Measured IRI (m/km)
1	11/11/1987	1.00	2	5/2/2001	3.00	3.00	9/13/1999	3.50	4	8/9/1993	2.50	5	10/31/1974	2.10
	9/9/1988	1.10		8/7/2001	3.20		10/4/2001	3.50		3/27/1995	2.70		5/29/1975	2.30
	5/24/1989	1.10		12/4/2002	3.40		2/11/2003	3.60		10/10/1995	2.80		6/28/1976	2.80
	1/16/1990	1.20		7/7/2003	3.70		4/3/2003	3.65		4/2/1996	2.90		1/31/1977	3.00
	6/27/1990	1.20		3/15/2004	2.00		6/10/2003	3.70		8/13/1996	3.00		7/1/1977	3.40
	2/5/1992	1.30		8/9/2004	2.10		10/30/2003	3.70		8/31/1998	3.10		10/21/1977	3.70
	11/10/1993	1.50		3/9/2005	2.20		7/6/2004	3.80		2/29/2000	3.30		12/14/1977	4.00
	3/17/1995	1.80		4/26/2005	2.40		1/17/2005	3.80		10/25/2000	3.70		7/6/1978	1.00
	7/21/1995	2.00		1/2/2006	2.60		1/27/2005	3.90		6/22/2001	3.90		8/24/1978	1.00
	12/12/1995	2.40		4/6/2007	3.20		6/1/2006	4.00		11/22/2001	4.10		3/30/1979	1.00
	2/23/1996	0.90		7/23/2007	3.50		3/20/2007	2.50		12/24/2001	1.00		2/4/1980	1.20
	9/13/1996	1.00		9/12/2008	3.70		10/2/2007	2.70		4/22/2002	1.02		10/15/1980	1.30
	7/10/1998	1.20		12/24/2009	3.80		10/2/2008	2.90		7/24/2002	1.05		3/18/1981	1.40
	5/17/1999	1.25		1/20/2010	1.50		9/11/2009	3.10		8/5/2003	1.05		10/2/1981	1.45
	3/9/2000	1.30		12/14/2011	1.60		12/17/2009	3.50		7/7/2004	1.06		11/16/1981	1.45
	11/24/2000	1.40		8/13/2012	1.60		9/9/2011	3.60		3/7/2005	1.07		1/15/1982	1.60
	3/22/2002	1.60		12/5/2013	1.70		12/27/2011	1.50		11/10/2005	1.10		11/3/1982	2.00
	9/14/2004	1.80		1/17/2014	1.80		9/19/2012	1.50					12/22/1982	0.75
	5/2/2005	2.20		4/10/2014	1.90		3/25/2013	1.60					6/6/1984	0.80
	4/18/2006	2.40		4/14/2014	2.00		4/3/2013	1.60					7/27/1984	0.85
				9/29/2014	2.40		11/13/2013	1.70					1/23/1985	0.85
				2/5/2015	2.60		3/23/2014	1.70					7/21/1987	0.90
				8/4/2015	2.90		10/27/2014	1.80					2/15/1988	1.00
							1/12/2015	1.90					8/19/1988	1.10
							6/23/2015	1.90					1/2/1989	1.12
							10/6/2015	2.00					7/24/1989	1.15
													4/3/1991	1.20

Figure 4 visually describes this data; each section begins and ends at a unique location. In practical applications, the information of a roadway section may be limited. For example, if there is only a small series of IRI data known for a particular roadway segment but the open-to-traffic date is unknown, it is difficult to determine the appropriate location on the lifetime performance curve. The methodology described in this section utilizes a time shifting process to shift series of IRI measurements to their appropriate location on the performance curve.

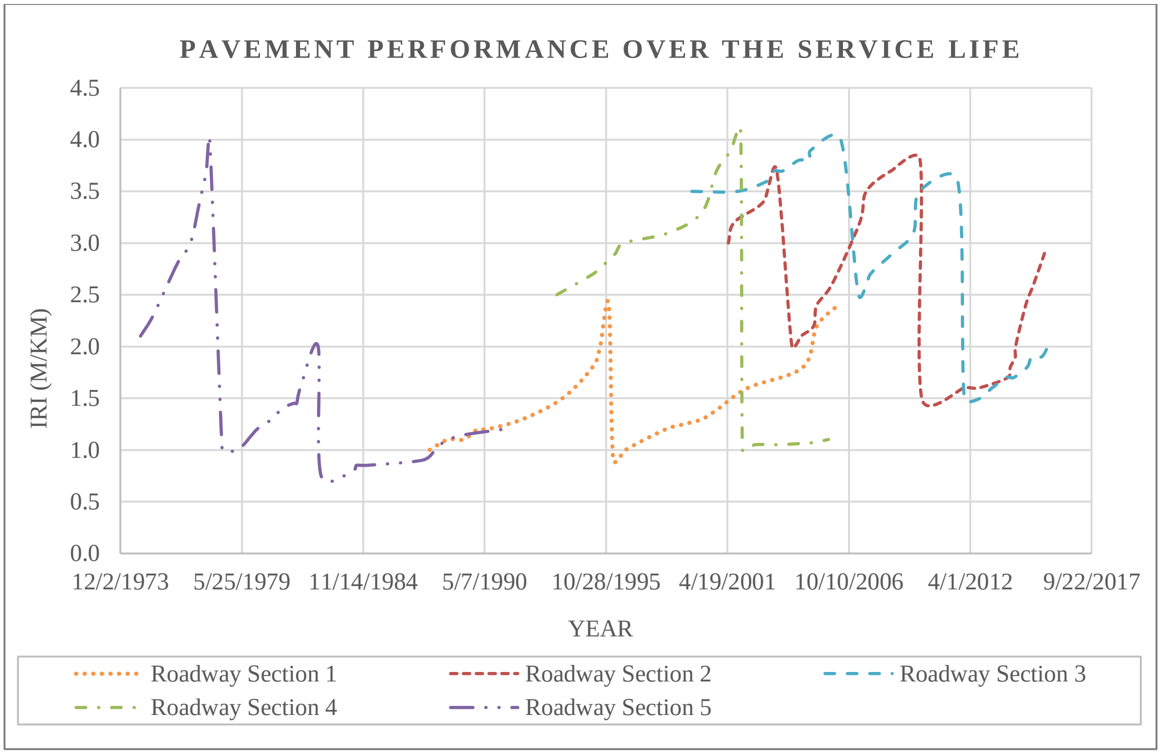

Figure 4: Data Demonstration – IRI Measurements of Five Roadway Segments

3.2 Data Preparation

The next step in the data preparation process is to standardize the time scale, which allows the measurements of roadway sections of various time periods to be analyzed together. In this step, all roadway segments are modified to begin at "Time = 0". All subsequent time measurements are indicated in units of years. If the first measurement was on 11/11/1987 and the second measurement was on 9/9/1998, this converts to Time = 0 and Time = 0.83, respectively. The five roadway sections with standardized time is shown in Table 3. This is displayed graphically in Figure 5, where all roadway segments are set to begin at "Time = 0".

Table 3: Data Demonstration – IRI Measurements using Standardized Time

Roadway Section	Standardized Time (Years)	Measured IRI (m/km)	Roadway Section	Standardized Time (Years)	Measured IRI (m/km)	Roadway Section	Standardized Time (Years)	Measured IRI (m/km)	Roadway Section	Standardized Time (Years)	Measured IRI (m/km)	Roadway Section	Standardized Time (Years)	Measured IRI (m/km)
1	0.00	1.00	2	0.00	3.00	3	0.00	3.50	4	0.00	2.50	5	0.00	2.10
	0.83	1.10		0.27	3.20		2.06	3.50		1.63	2.70		0.58	2.30
	1.53	1.10		1.59	3.40		3.42	3.60		2.17	2.80		1.66	2.80
	2.18	1.20		2.18	3.70		3.56	3.65		2.65	2.90		2.25	3.00
	2.63	1.20		2.87	2.00		3.74	3.70		3.01	3.00		2.67	3.40
	4.24	1.30		3.27	2.10		4.13	3.70		5.06	3.10		2.98	3.70
	6.00	1.50		3.85	2.20		4.82	3.80		6.56	3.30		3.12	4.00
	7.35	1.80		3.99	2.40		5.35	3.80		7.22	3.70		3.68	1.00
	7.70	2.00		4.67	2.60		5.38	3.90		7.87	3.90		3.82	1.00
	8.09	2.40		5.93	3.20		6.72	4.00		8.29	4.10		4.41	1.00
	8.29	0.90		6.23	3.50		7.52	2.50		8.38	1.00		5.27	1.20
	8.85	1.00		7.37	3.70		8.06	2.70		8.71	1.02		5.96	1.30
	10.67	1.20		8.65	3.80		9.06	2.90		8.96	1.05		6.38	1.40
	11.52	1.25		8.73	1.50		10.00	3.10		9.99	1.05		6.93	1.45
	12.33	1.30		10.62	1.60		10.27	3.50		10.92	1.06		7.05	1.45
	13.05	1.40		11.29	1.60		12.00	3.60		11.58	1.07		7.21	1.60
	14.37	1.60		12.60	1.70		12.30	1.50		12.26	1.10		8.01	2.00
	16.85	1.80		12.72	1.80		13.03	1.50					8.15	0.75
	17.48	2.20		12.95	1.90		13.54	1.60					9.61	0.80
	18.45	2.40		12.96	2.00		13.56	1.60					9.75	0.85
				13.42	2.40		14.18	1.70					10.24	0.85
				13.77	2.60		14.53	1.70					12.73	0.90
				14.27	2.90		15.13	1.80					13.30	1.00
							15.34	1.90					13.81	1.10
							15.79	1.90					14.18	1.12
							16.07	2.00					14.74	1.15
													16.43	1.20

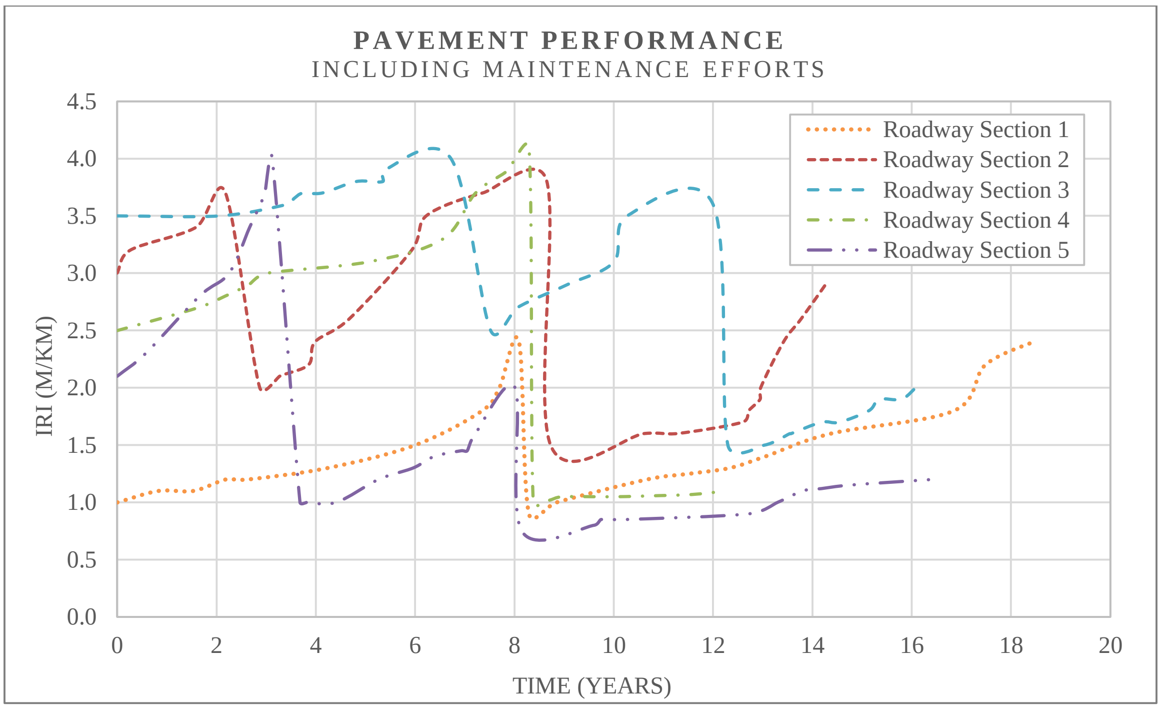

Figure 5: Data Demonstration – IRI Measurements using Standardized Time

The IRI data, provided in Table 3 and Figure 5, depicts periods of roughness increase followed by a significant decrease in IRI. This pattern describes regular pavement maintenance performed to extend the service life, which can include pothole patching, crack sealing, and overlays. In this stage of the process the datasets are still in the "raw" format, as it includes maintenance efforts. The objective is to develop a model that describes how a pavement section would deteriorate in the absence of any maintenance intervention. This is accomplished by studying the deterioration patterns in between maintenance efforts, and superimposing these smaller sections to understand the lifetime behavior. In Table 3, red bars separate the IRI data of each roadway section into smaller series. These locations are identified by a significant decrease in IRI between two periodic measurements, which indicate maintenance activity between the two readings. These smaller subsections are separated in Table 4, and are hereafter referred to as "series".

Table 4: Data Demonstration – IRI Measurements using Standardized Time, Separated by Maintenance Efforts

Roadway Section	Standardized Time (Years)	Measured IRI (m/km)	Roadway Section	Standardized Time (Years)	Measured IRI (m/km)	Roadway Section	Standardized Time (Years)	Measured IRI (m/km)	Roadway Section	Standardized Time (Years)	Measured IRI (m/km)	Roadway Section	Standardized Time (Years)	Measured IRI (m/km)
1A	0.00	1.00	2A	0.00	3.00	3A	0.00	3.50	4A	0.00	2.50	5A	0.00	2.10
	0.83	1.10		0.27	3.20		2.06	3.50		1.63	2.70		0.58	2.30
	1.53	1.10		1.59	3.40		3.42	3.60		2.17	2.80		1.66	2.80
	2.18	1.20		2.18	3.70		3.56	3.65		2.65	2.90		2.25	3.00
	2.63	1.20	2B	0.00	2.00		3.74	3.70		3.01	3.00		2.67	3.40
	4.24	1.30		0.40	2.10		4.13	3.70		5.06	3.10		2.98	3.70
	6.00	1.50		0.98	2.20		4.82	3.80		6.56	3.30		3.12	4.00
	7.35	1.80		1.12	2.40		5.35	3.80		7.22	3.70	5B	0.00	1.00
	7.70	2.00		1.80	2.60		5.38	3.90		7.87	3.90		0.13	1.00
	8.09	2.40		3.06	3.20		6.72	4.00		8.29	4.10		0.73	1.00
1B	0.00	0.90		3.36	3.50	3B	0.00	2.50	4B	0.00	1.00		1.58	1.20
	0.56	1.00		4.50	3.70		0.54	2.70		0.33	1.02		2.28	1.30
	2.38	1.20		5.78	3.80		1.54	2.90		0.58	1.05		2.70	1.40
	3.23	1.25	2C	0.00	1.50		2.48	3.10		1.61	1.05		3.24	1.45
	4.04	1.30		1.90	1.60		2.75	3.50		2.54	1.06		3.37	1.45
	4.76	1.40		2.56	1.60		4.48	3.60		3.20	1.07		3.53	1.60
	6.08	1.60		3.88	1.70	3C	0.00	1.50		3.88	1.10		4.33	2.00
	8.56	1.80		3.99	1.80		0.73	1.50				5C	0.00	0.75
	9.19	2.20		4.22	1.90		1.24	1.60					0.73	0.80
	10.16	2.40		4.23	2.00		1.27	1.60					1.58	0.85
				4.69	2.40		1.88	1.70					2.28	0.85
				5.05	2.60		2.24	1.70					2.70	0.90
				5.54	2.90		2.84	1.80					3.24	1.00
							3.05	1.90					3.37	1.10
							3.49	1.90					3.53	1.12
							3.78	2.00					4.33	1.15
													4.47	1.20

For example, there is evidence of two individual maintenance efforts within the Roadway Segment 2 dataset. The significant decreases in IRI (maintenance efforts) are shown in Figure 6 in the shaded regions. Based on the maintenance efforts, Roadway Section 2 is separated into three series. In order to standardize the time scale and analyze each series as a separate piece of data, each new series is also shifted to begin at "Time = 0".

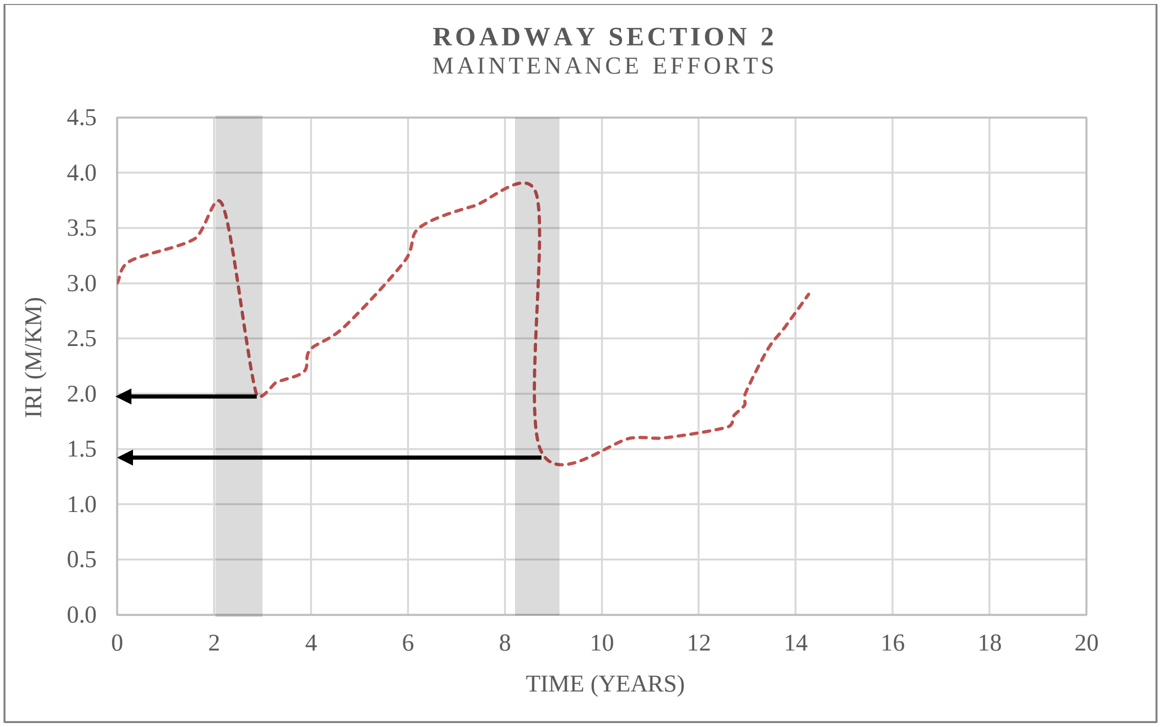

Figure 6: Data Demonstration – Roadway Section 2 Maintenance Efforts

Figure 7 shows the separated series within Roadway Section 2 shifted to begin at "Time = 0". This process is continued for the other four roadway sections, and their separated series are shown together in Figure 8.

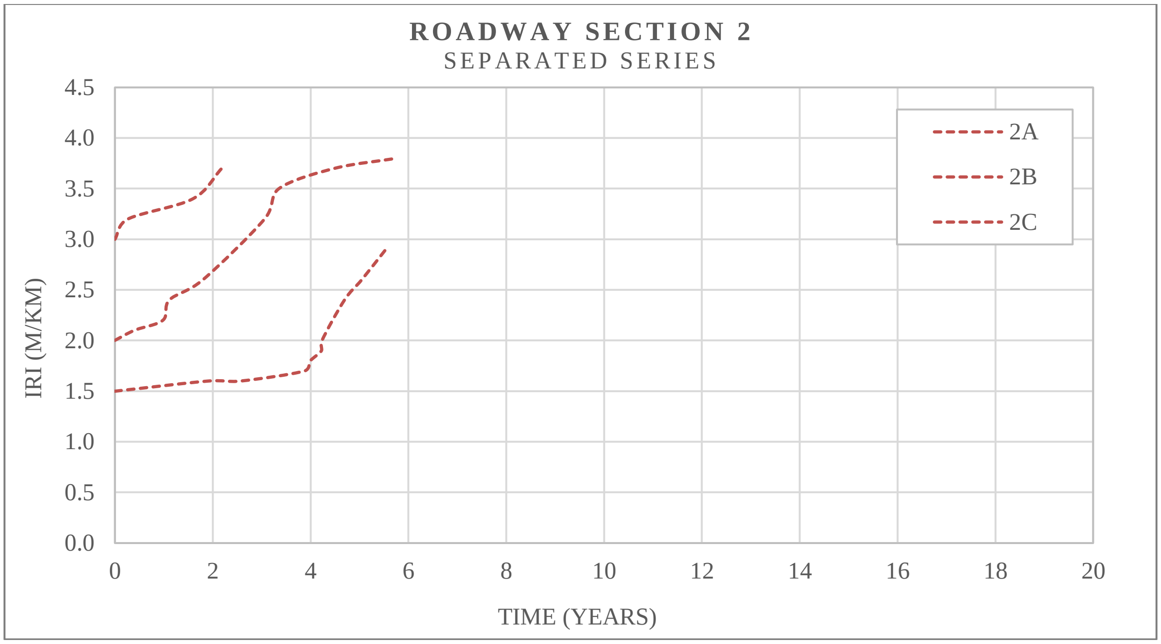

Figure 7: Data Demonstration – Roadway Section 2 Separated Series

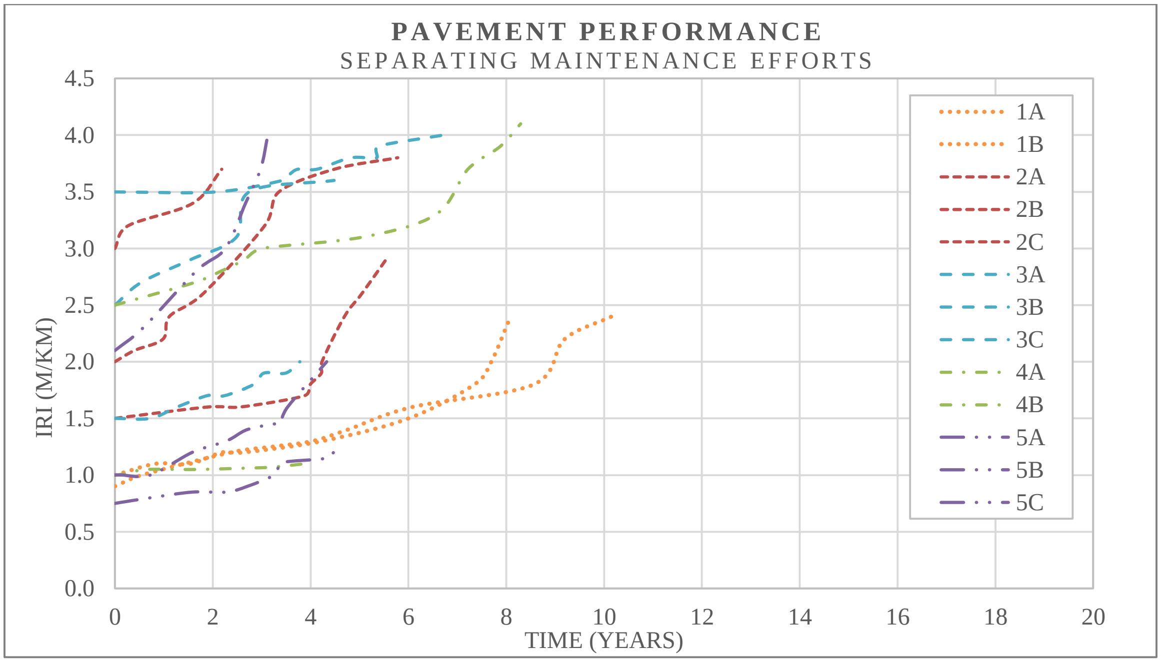

Figure 8: Data Demonstration – Pavement Performance, Separating Maintenance Efforts

Each IRI data series must be in the standardized time format, shown in Table 4 and Figure 8, to continue with the next step of the methodology.

3.3 Development of Performance Curves

3.3.1 Sigmoidal Function

Similar to the PCI sigmoidal decay function (Equation 3), the appropriate Sigmoidal Growth Function used in this research effort is shown below (Equation 4). Essentially, the difference is in the negative coefficient a_3 which reverses the shape of the classical sigmoidal function.

Equation 4: Sigmoidal Growth Function

$$IRI = a_1 + \frac{a_2}{1+e^{(-a_3*t+a_4)}}$$

Where:

IRI	=	International Roughness Index (m/km)
a_1	=	Lower IRI Limit
a_2	=	Factor affecting the IRI Upper Limit (Upper IRI Limit = a_1+a_2)
a_3	=	Factor affecting the rate of deterioration
a_4	=	Factor affecting the start time and rate of deterioration
t	=	Offset Time (Years)

3.3.2 Excel Solver Optimization

The parameters, a_1, a_2, a_3, and a_4, were used to develop a unique sigmoidal function based on the group of separated series. Excel Solver was used to individually shift each series and minimize the difference between the series location and the best-fit sigmoidal curve.

To facilitate the sigmoidal parameter fitting in Excel Solver, several parameter constraints were used. The parameter constraints are shown in Table 5. Based on the sigmoidal growth function selected for the analysis, all four parameters (a_1, a_2, a_3, and a_4) are required to be positive. Another constraint was placed on parameter a_2, which affects the upper IRI limit. The upper IRI limit in the model is the sum of parameters a_1 and a_2. Although true pavement roughness deterioration does not have an absolute limit, a maximum value was selected for consistency across the various simulated models. A maximum value ($a_1 + a_2$) of IRI was assumed to be between 4 and 5 meters per kilometer. The most roughness data is available when the offset time (t) is zero, and it was observed that many of the sections began at an IRI between 0.5 and 1.0 meters per kilometer (a_1). Therefore, the a_2 parameter was constrained to be less than or equal to 3.5 meters per kilometer.

Table 5: Parameters used in Sigmoidal Model Fitting

Parameter	Constraints Used
a1	≥ 0
a2	≥ 0 , ≤ 3.5
a3	≥ 0
a4	≥ 0

The Excel spreadsheet template used to develop each sigmoidal curve is provided in Figure 9. This specific spreadsheet was used to determine the sigmoidal curve for the data demonstration of the five roadway sections explained in this chapter. The data for each series (as shown in Table 4) is inputted directly into Columns A-D, which is shown in orange and green blocks. Due to constraints in excel, each series must be equal to or less than 10 measurements (also referred to as data points) If any series is greater than 10 data points, the additional data is added to the subsequent block. This additional "series" can have the same "ROAD No.", but must begin at "Time = 0". Columns K-N essentially compress the data. Each row within these columns refers to a separate series. It details the IRI of the first data point of the series, and the appropriate lateral time shift (optimized by Excel). Column G explains the "Error", or difference, in the location of the fitted curve and each individual data series. Excel Solver is set to minimize the sum of errors (P1) by changing the model parameters (P2:P5) and the individual shift factor of each series (L2:L14).

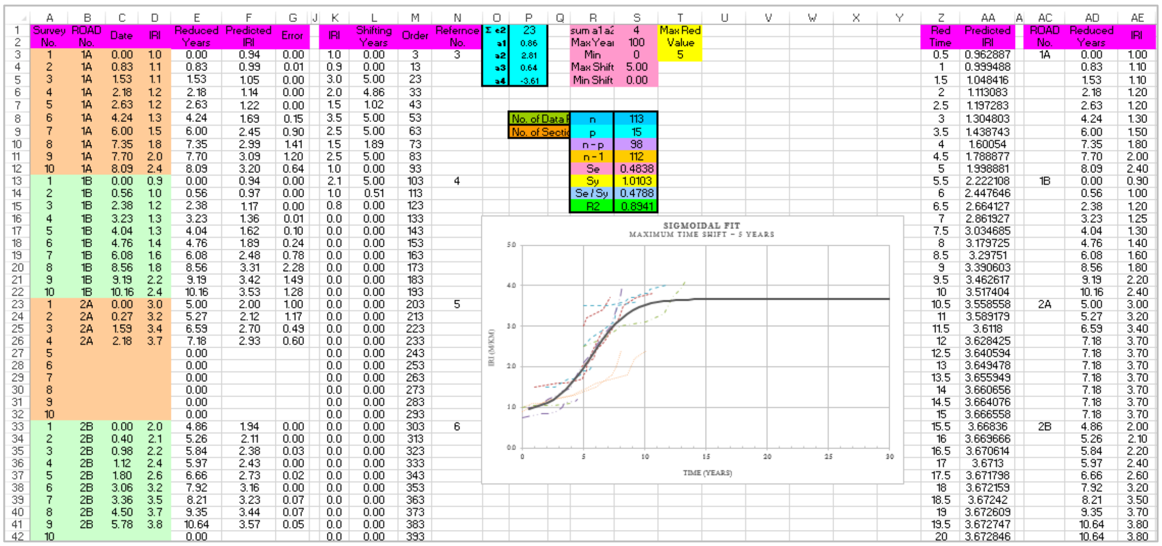

Figure 9: Excel Optimization Spreadsheet

This process finds the best sigmoidal curve to fit the data within a set maximum time shift. Several iterations of maximum time shift are conducted to determine the optimal maximum time shift, which is a related to the rate of deterioration and the length of a pavement's service life. Generally, pavement section groups with greater optimal maximum time shifts (i.e., 30-35) are more ideal than those with lower time shifts (i.e., 10-15 years). If the optimal fit is reached in a short time shift, it indicates that poor condition is reached in a short period of time. Longer optimal time shifts indicate that the poor condition sections occur later in the pavement's lifetime.

Figures 9, 10, and 11, explain the time shifting process for the hypothetical roadway sections explained in this section. Figure 10 allows for a maximum time shift of only 5 years. This first curve is not the best fit, as some of the sections with high IRI (3 – 4 m/km), could still benefit from a greater time shift.

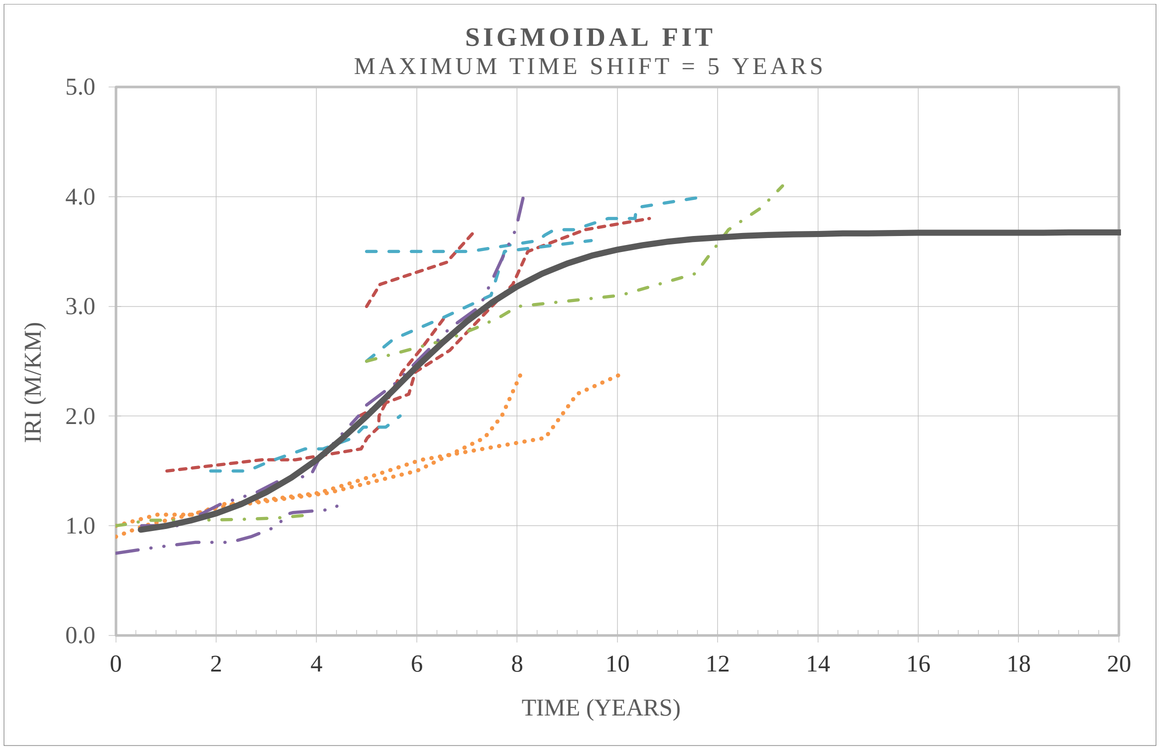

Figure 10: Data Demonstration – Sigmoidal Fit using a 5 Year Maximum Time Shift

Figure 11 shows the same data, but this time with a maximum time shift of 10 years. With the additional allowable shift time, the individual series are able to shift more closely to the fitted curve.

Figure 11: Data Demonstration – Sigmoidal Fit using a 10 Year Maximum Time Shift

Figure 12 shows the next iteration, with a maximum time shift of 15 years. In this methodology, providing a greater allowable time shift will always result in a model with a better fit, until a threshold value is reached.

Figure 12: Data Demonstration – Sigmoidal Fit using a 15 Year Maximum Time Shift

3.3.3 Model Accuracy and Fit

The optimal allowable time shift for each data group is determined as the time shift iterations reach the threshold value for model accuracy. The relative accuracy ration (Se/Sy) and the coefficient of determination, R^2 were used as statistical measures of the goodness of fit between the master curve and the shifted segments. Se being the standard error of estimate, Sy being the standard deviation. Se/Sy values are good if less than 0.5; and marginal if greater than 0.75. The R^2 value can be used if computed based on the Se/Sy ratio as follows (Equation 5):

Equation 5: Coefficient of Determination

$$R^2 = 1 - \left(\frac{n-v}{n-1}\right) * [Se/Sy]^2$$

Where:

n = Number of samples

ν = Number of regression coefficients

As the maximum time shift increased, the segments had the ability to shift to a more optimal position, and the Se/Sy and R^2 improved. The maximum time shift is incrementally increased to reach the best fit. The optimal time shift is determined after R^2 and Se/Sy reach a threshold value and no longer significantly increase. This threshold is the smallest incremental increase of R^2 between two time shift curves that results in essentially the same goodness of fit. This incremental increase threshold for R^2 must be consistent while developing models for a dataset; for example, a roadway network of either local or statewide, where the data was collected using the same process, equipment, and frequency. This threshold values should only be modified if analyzing two unique datasets; for example, two statewide agencies data with different data collection processes, equipment, and frequency. The modified model sensitivity value may be a better fit for analyzing the comparison of curves of the second network based on the data collection characteristics. Using this technique, it is valuable to compare the optimal time shift curves of pavement groups within a dataset, but not valuable to comparing the time shift of groups in different datasets (i.e., states). The optimal time shift is an indicator of the service life of the pavement, and how quickly it deteriorates to a poor quality.

In this example, it is assumed that the optimal time shift is reached if the next time shift results in R^2 value that is less than or equal to 0.005 greater than the previous R^2 value. This assumption is based on previous modeling efforts of historical data. The three time shift curves developed as part of the hypothetical data modeling are shown in Figure 13, with the optimal time shift of 10 years shown in green.

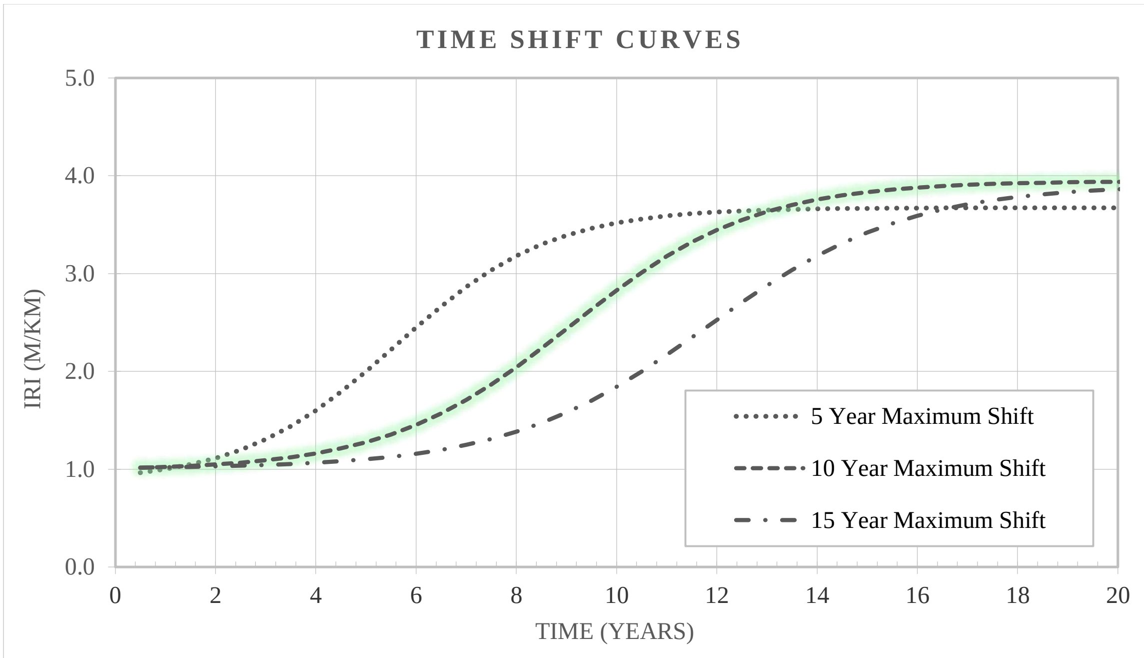

Figure 13: Data Demonstration – Time Shift Curves

An optimal time shift of 10 years was determined by evaluating the measures of fit for each time shift curve. The incremental increase in the R^2 value from the 10 year shift to the 15 year shift is less than or equal to 0.005 (0.0041), which indicates that the 10 year shift is the optimal time shift. After the optimal time shift is determined, there is no benefit in analyzing additional time shift periods, which is why only the 5, 10, and 15 year time shifts are analyzed in this hypothetical example. In other data groups, it is necessary to continue to 45 years to reach the threshold value of less than 0.005 in model fit.

Table 6: Data Demonstration - Time Shift Model Coefficients and Measures of Fit

5 Year Shift		10 Year Shift		15 Year Shift	
a1	0.862	a1	0.987	a1	1.008
a2	2.811	a2	2.959	a2	2.903
a3	0.645	a3	0.545	a3	0.5
a4	-3.61	a4	-4.952	a4	-5.876
Se/Sy	0.4788	Se/Sy	0.2044	Se/Sy	0.1807
R2	0.8941	R2	0.9816	R2	0.9856

4. CASE STUDY 1: LTPP PAVEMENT ROUGHNESS DATA

4.1 Introduction

The Long Term Pavement Performance (LTPP) InfoPave Database was developed as a part of the Strategic Highway Research Program (SHRP) in 1987. The database was created as a system to document pavement attributes, conditions, maintenance activities, and reconstruction efforts over a period of time. Each roadway included in the database has a unique section number, which identifies the location, roadway classification, and material and structure thickness properties. The database will routinely document indicators of pavement performance deterioration, including distresses and roughness, and monitor the conditions over the life of each pavement section.

There are a total of 2509 sections available in the InfoPave database which are located within the United States and Canada. There are five primary categories of information available for each pavement section; these can be used to filter the data and extract only pavement information of interest.

In the *General* data, the pavement age, experiment type, study group, section name, monitoring status, location, roadway classification, and maintenance and rehabilitation efforts and are identified. The *Structure* data lists the material types for the surface, base, and subgrade layers. In this category, Asphalt Concrete (AC) and Portland Cement Concrete (PCC) sections can be separated. The *Climatic* data allows the user to separate pavement sections into the following climate regions: Dry/Freeze, Dry/Non-Freeze, Wet/Freeze, Wet/Non-Freeze. This section also records the annual freezing index, precipitation, and temperature which is experienced by the pavement section. The *Traffic* data records the annual average daily traffic (AADT) and the annual average daily truck traffic (AADTT). The final grouping of data are the *Performance* measures. The deflection, cracking, faulting, and roughness are regularly observed and recorded.

The InfoPave database is useful in conducting pavement performance research. Pavement experiments were conducted to determine the various effects that structure, materials, traffic, climate, and maintenance have on the pavement condition over time.

4.2 Data Summary

In the LTPP InfoPave Database there are a total of 146 roadway sections in Arizona; 95 of which are "Asphalt Concrete Pavement" sections. These sections are to be referred to in this document as "asphalt" sections, or more simply, "AC" sections. The roadway sections in the LTPP database are primarily highways and interstates, as a majority of the data collection has been in partnership with state transportation agencies. Local roads are not included in the database. Some roadway sections began data collection at the time it was opened to traffic, while other section studies began after a roadway segment was in operation.

The Arizona roadway sections in the LTPP InfoPave database are within one of two climatic regions: Dry, Non-Freeze or Dry, Freeze. Traffic loading is reported annually in several forms in the LTPP database; however, the traffic data used in this analysis is in the form of equivalent single axle loads (ESALs or represented as KESAL for 1000 units). The Arizona data ranges from 300-4,450 KESALs.

The roughness data is reported in meters per kilometer (m/km). These measurements were recorded using profilometers, vehicles equipped with sensors to detect the longitudinal profile variation of the pavement. The measurements were collected regularly (approximately once every 6-18 months) over the period of 5-20 years. The roughness data was measured in two locations, on the left and right wheel paths. This method of measurement is to best replicate the ride quality of the travelling public.

The LTPP data also specifies the type and frequency of maintenance activity. The maintenance actions are referred to as a new "construction number" (CN) in the database. For example, new pavement sections begin as CN 1, and after a chip seal the section becomes a CN 2. The CN increases with each maintenance activity and continues over the entire duration that data is collected for the section. The maintenance information is important, as the analysis aims to standardize the data to model roughness deterioration without the effects of maintenance. The construction number is used to distinguish between phases of each section. Within each phase, or CN, there are no effects of maintenance. These phases are used to create individual, standardized datasets for modeling.

The IRI data of the asphalt sections was separated into subgroups based on the climatic region and intensity of traffic loading. The goal of the analysis is to demonstrate the sigmoidal curve methodology, and additionally to show that deterioration trends can be observed when comparing multiple related pavement characteristic groups. The modeling process of analyzing and constructing sigmoidal curves was conducted for the following pavement section groups in Table 7.

Table 7: LTPP Data Grouping Summary

Data Source	Comparison	Name	Number of Sections
LTPP	N/A	Asphalt Sections	87
LTPP	Climatic Region	Asphalt Sections, Dry/Non-Freeze Climate	72
LTPP		Asphalt Sections, Dry/Freeze	15
LTPP	Traffic Level	Asphalt Sections, High Traffic Level (> 2000 KESALS)	44
LTPP		Asphalt Sections, Low Traffic Level (< 2000 KESALS)	43

A list of the individual LTPP roadway segments and attributes of each data group is provided in Appendix A: LTPP and MnROAD Analysis.

4.3 Data Extraction and Preparation

The pavement data was extracted using the 'Data' tab within LTPP InfoPave. A filtering tool allows for only the data of interest to be selected. After data was selected, it was extracted to a downloadable Microsoft Excel file. In this analysis, one group of data was extracted: Arizona Asphalt Concrete Sections. The extracted Excel file contained the left and right wheel path IRI measurement, the construction number, and the date of measurement. Climate and traffic loading data for each section was collected directly from the LTPP InfoPave website, using the 'Section Summary' tab.

Data extracted from the LTPP database requires manual reformatting to be prepared for analysis. To first simplify the large dataset, the average of the two wheel path readings was used as the sole IRI value for a particular measurement date. The data was then time standardized so all sections began at "Time = 0". Next, all construction numbers were identified, and any series with a new construction number was also standardized to begin at "Time = 0". For all series, the time scale was converted from specific dates to the number of years from the beginning of each series. The individual series were inserted into the modeling spreadsheet for further analysis and model optimization.

4.4 Development of Sigmoidal Curves

In this section, the development of sigmoidal curves is explained using the LTPP Asphalt Sections data group as an example. Figure 14 shows each separated series for each asphalt section, which were determined by the construction number, or date in which maintenance was performed. These series were inserted into the modeling spreadsheet to determine the optimal sigmoidal time shift curve. Figure 14 shows this data before any time shifting, with all series beginning at “Time = 0”. This data group includes 165 individual series within the 87 pavement sections, which means that on average, there are approximately 2 series per section.

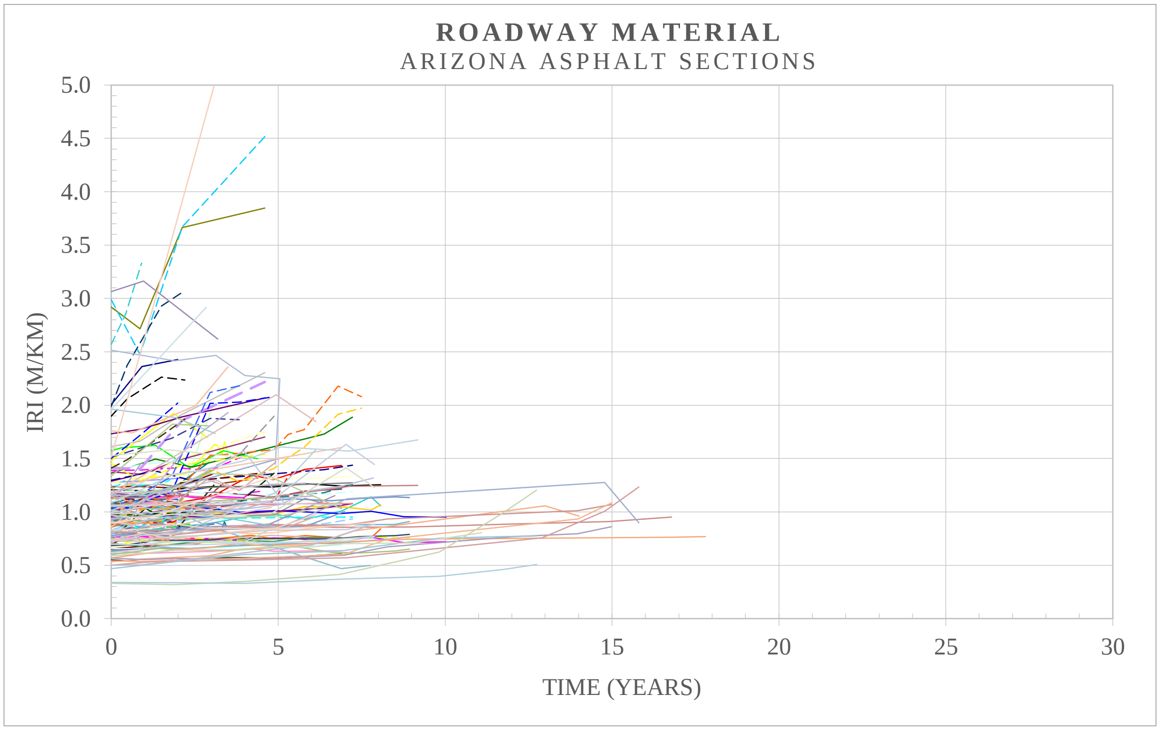

Figure 14: LTPP Data - Raw Asphalt Sections before Time Shifting

The data is optimized to minimize the error between the series and the sigmoidal function. The fitted sigmoidal curve of the 5 year maximum time shift is provided in Figure 15. The time shift process is repeated iteratively until the incremental increase of R^2 is less than or equal to 0.005.

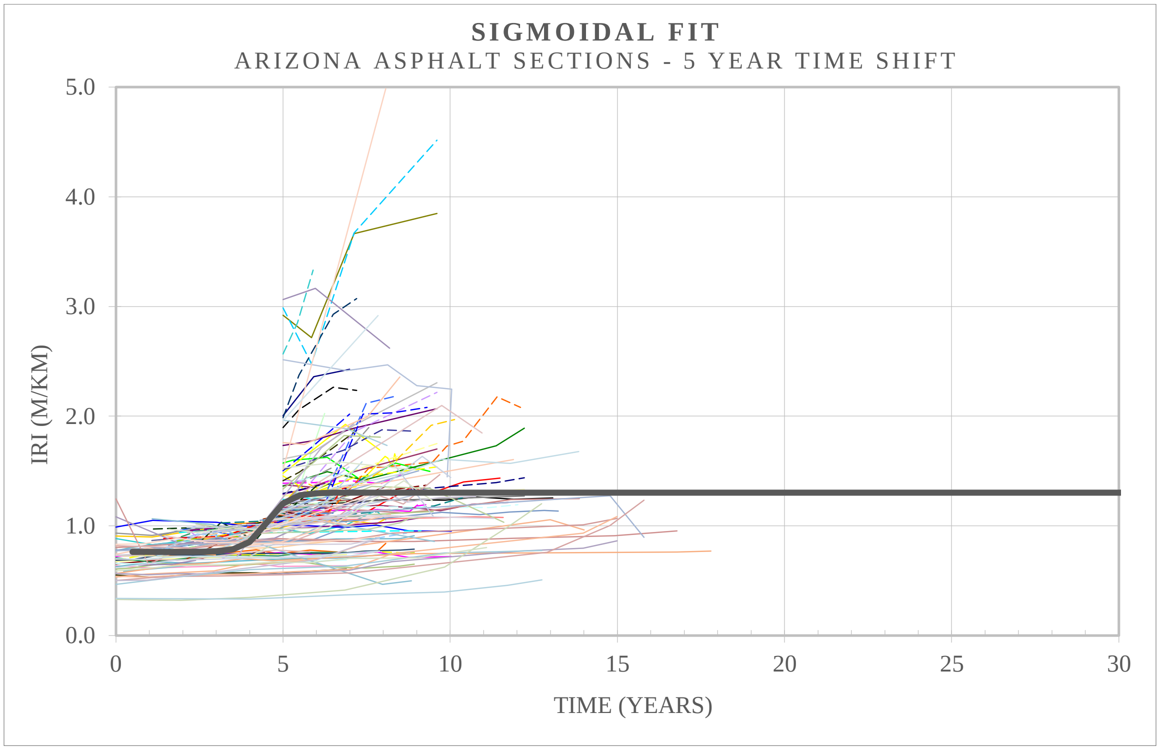

Figure 15: LTPP Data – Asphalt Sections, 5 Year Maximum Time Shift

The fitted curves for 10, 15, 20, 25 and 30 year time shifts are shown in Figures 16, 17, 18, 19, and 20, respectively.

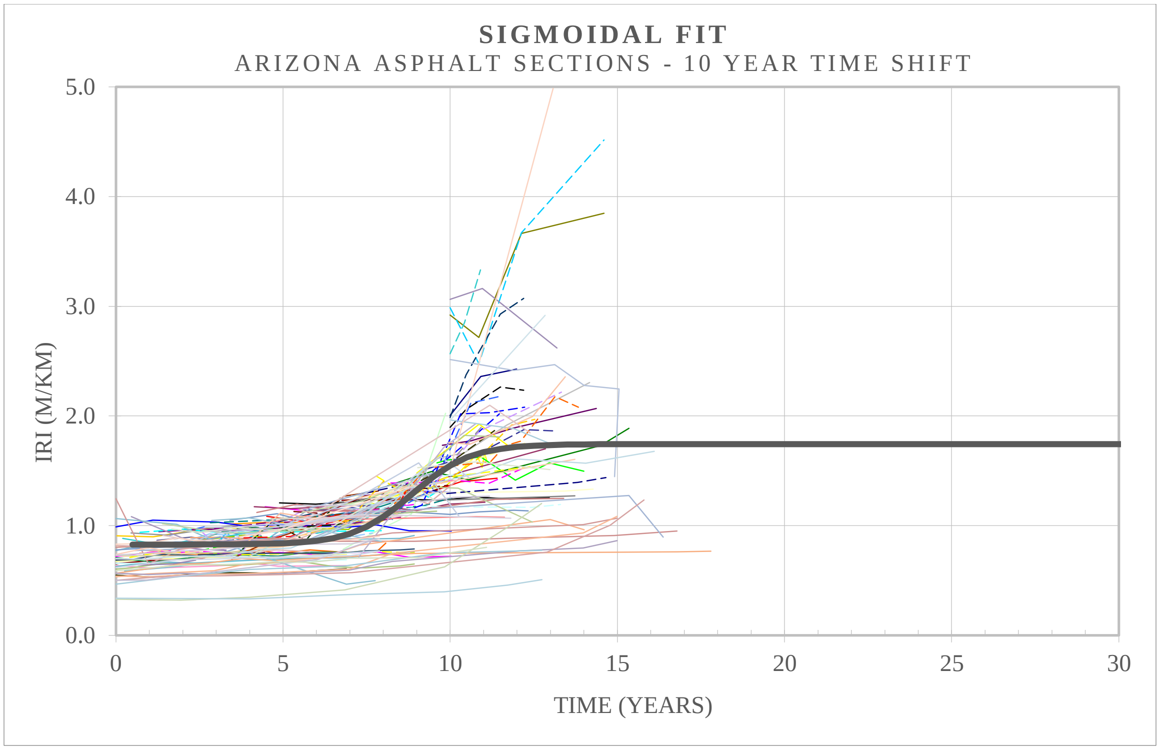

Figure 16: LTPP Data – Asphalt Sections, 10 Year Maximum Time Shift

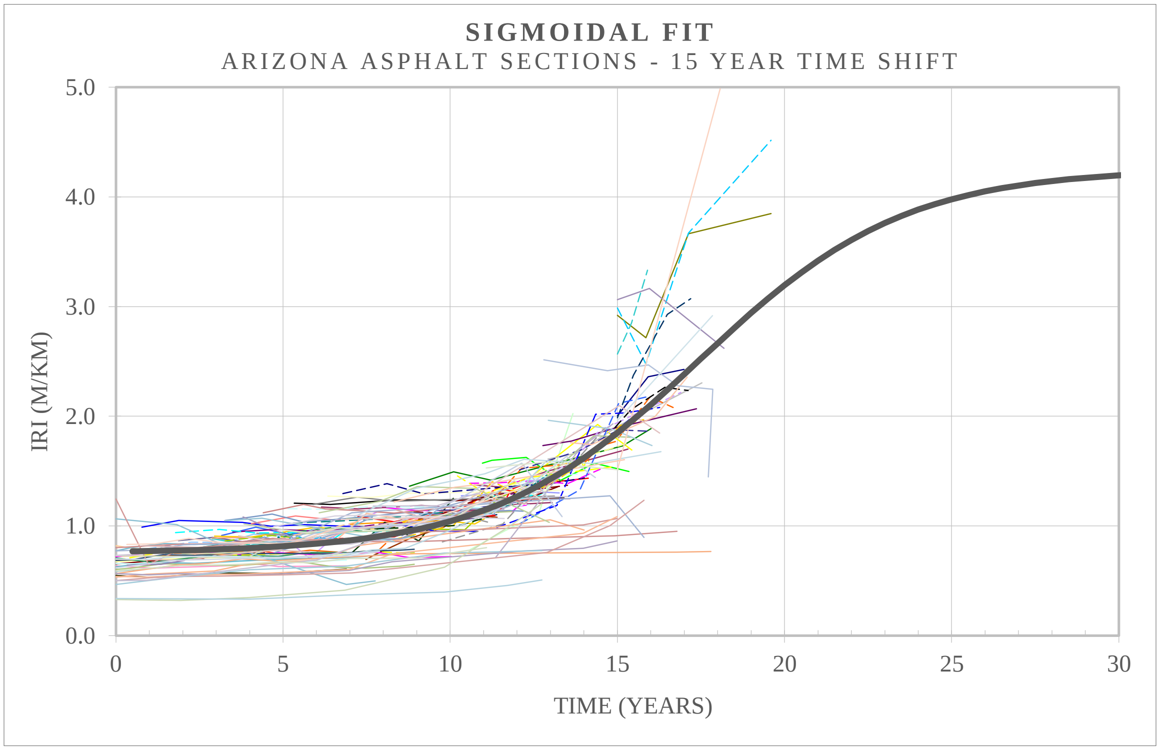

Figure 17: LTPP Data – Asphalt Sections, 15 Year Maximum Time Shift

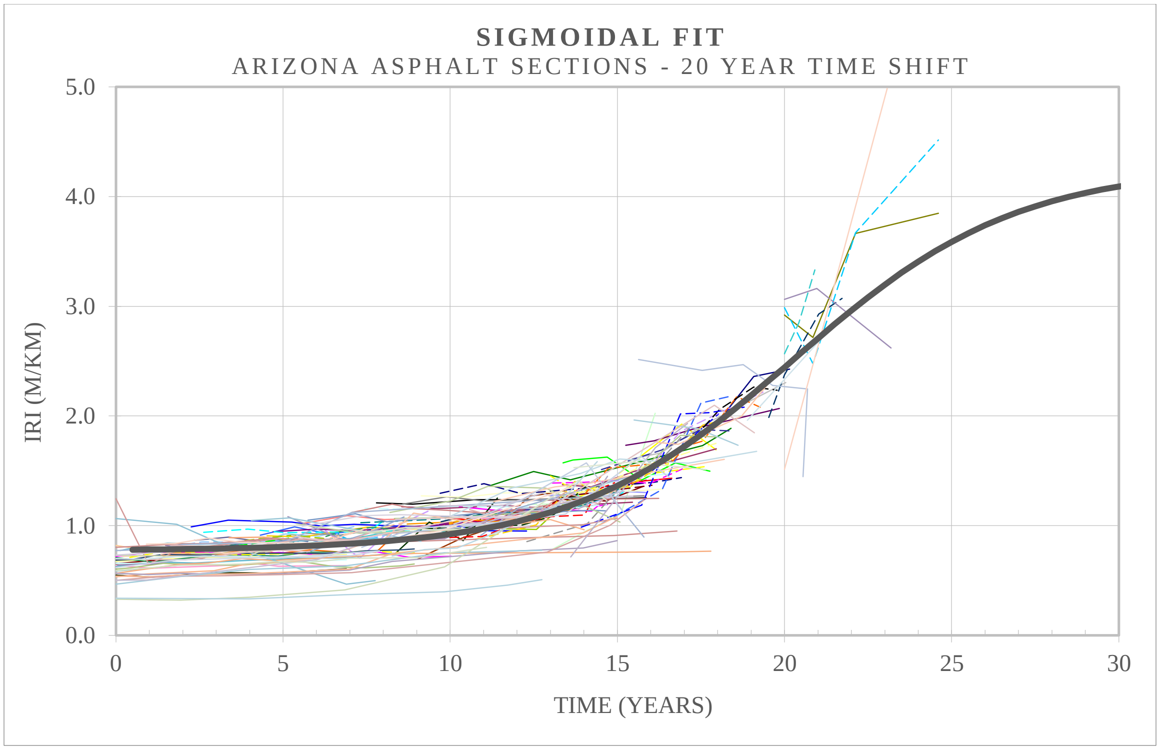

Figure 18: LTPP Data – Asphalt Sections, 20 Year Maximum Time Shift

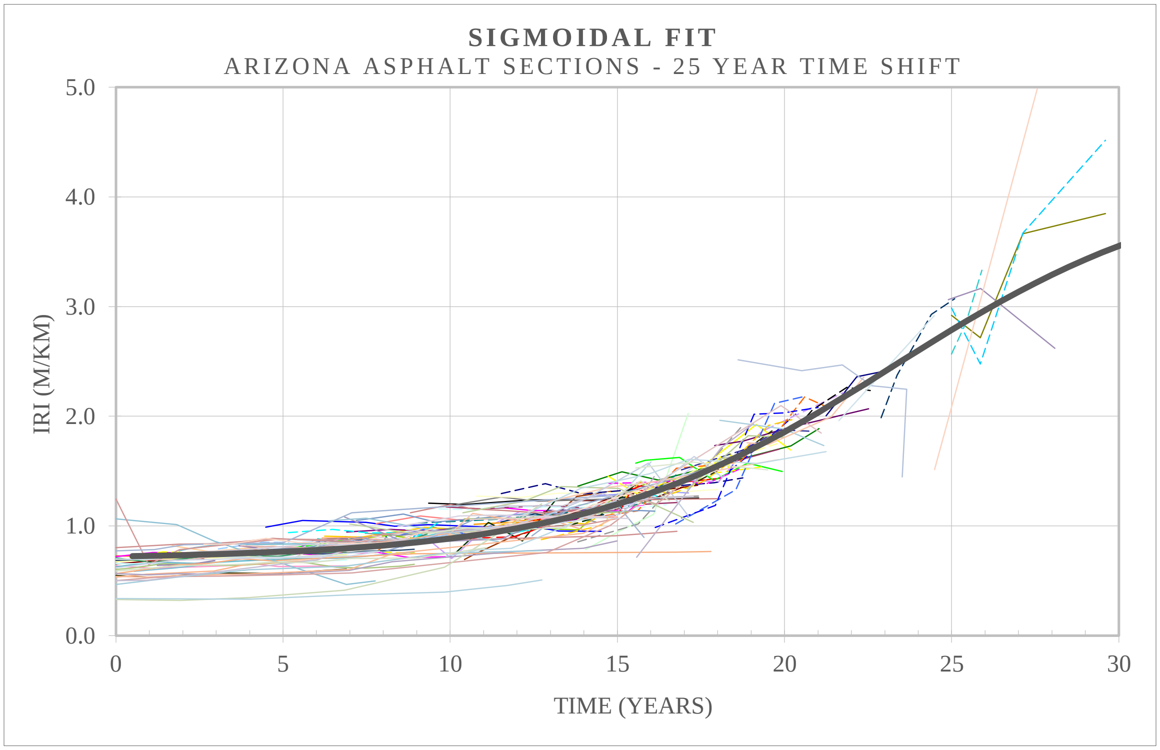

Figure 19: LTPP Data – Asphalt Sections, 25 Year Maximum Time Shift

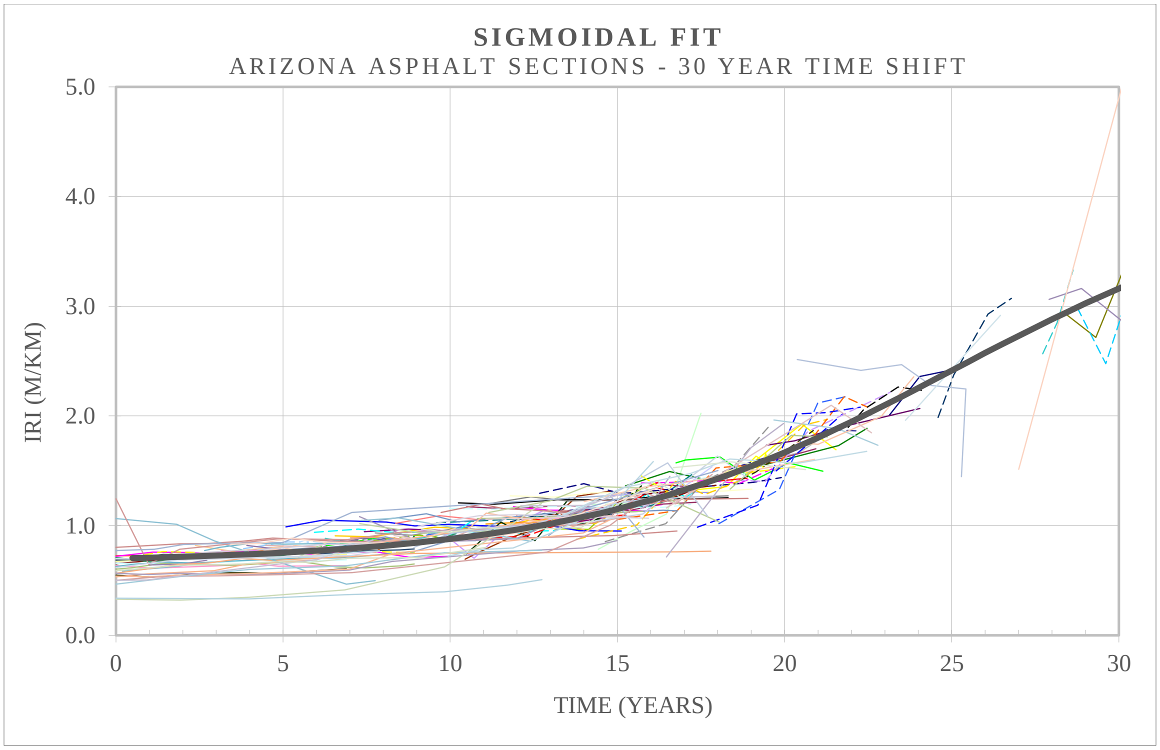

Figure 20: LTPP Data – Asphalt Sections, 30 Year Maximum Time Shift

As the pavement series are allowed a greater maximum time shift, an improved sigmoidal fit is achieved. Modeling efforts did not extend beyond 30 years because a threshold was reached where the measures of model fit no longer increased as the time shift increased. The time shift iteration process is summarized in Figure 21 and Table 8. In Figure 21, the optimized sigmoidal curves of each maximum time shift are superimposed to demonstrate how the shape of the curve changes during the iterative process.

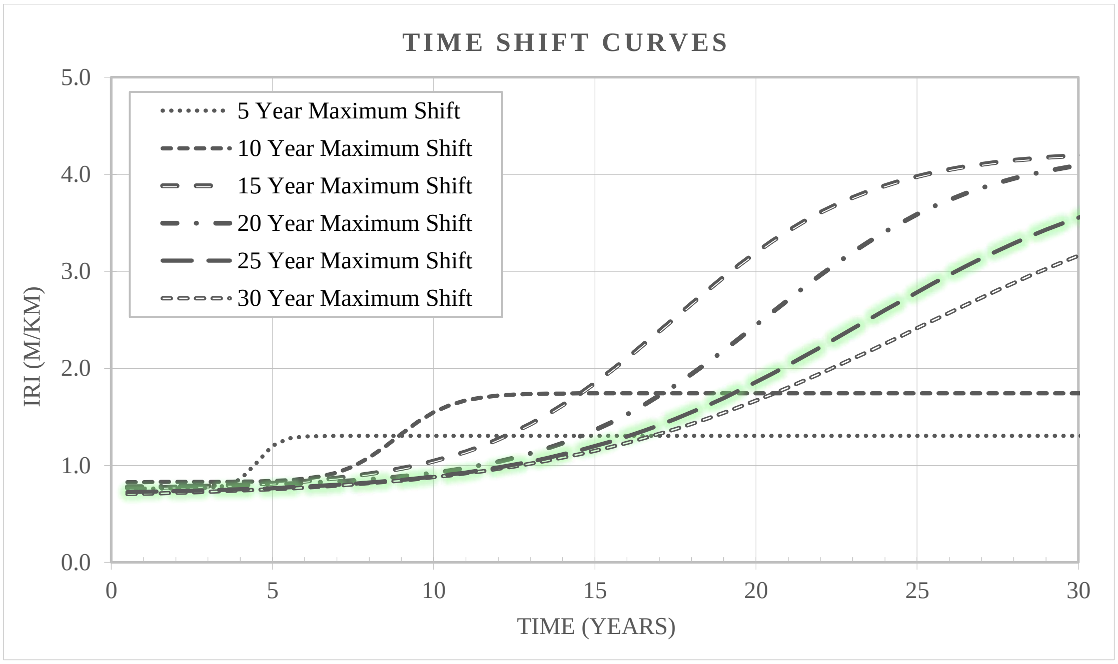

Figure 21: LTPP Data – Time Shift Curves, Asphalt Sections

The model coefficients and measures of fit of each time shift iteration is provided in Table 8. As the maximum allowable time shift increases, the measures of fit (Se/Sy and R^2) improve until a threshold is reached. This model accuracy was reached at the 25 year time shift. The incremental increase in R^2 between the 25 and 30 year time shifts was less than 0.005, which indicates that the threshold was reached. The 25 year time shift was determined to be the optimal time shift, and it is highlighted in Table 8 and Figure 21 in green.

Table 8: LTPP Data – Time Shift Model Coefficients and Measures of Fit, Asphalt Sections

5 Year Shift		10 Year Shift		15 Year Shift		20 Year Shift		25 Year Shift		30 Year Shift	
a1	0.762	a1	0.828	a1	0.754	a1	0.771	a1	0.702	a1	0.665
a2	0.542	a2	0.915	a2	3.5	a2	3.5	a2	3.5	a2	3.5
a3	3.045	a3	1.14	a3	0.324	a3	0.301	a3	0.219	a3	0.182
a4	-13.76	a4	-10.094	a4	-5.653	a4	-6.103	a4	-5.082	a4	-4.561
Se/Sy	0.974	Se/Sy	0.812	Se/Sy	0.61	Se/Sy	0.457	Se/Sy	0.397	Se/Sy	0.384
R2	0.477	R2	0.681	R2	0.835	R2	0.911	R2	0.934	R2	0.938

4.5 Results

The sigmoidal curve development in Section 4.4 was a demonstration of how the individual series of the asphalt sections were shifted to the optimal location on the deterioration curve. For each data group listed in Table 8 this process was replicated to determine the optimal time shift curve to best fit the data.

Climate

Figure 22 and Table 9 depict the comparison of pavement deterioration between roadways in two different climatic regions. In this comparison, the optimal time shift curves have already been determined, and only the final curve is displayed for each data group. The orange dotted line represents the optimal time shift curve for the Dry, Freeze sections, and the blue dotted line represents the optimal time shift curve for the Dry, Non-Freeze sections.

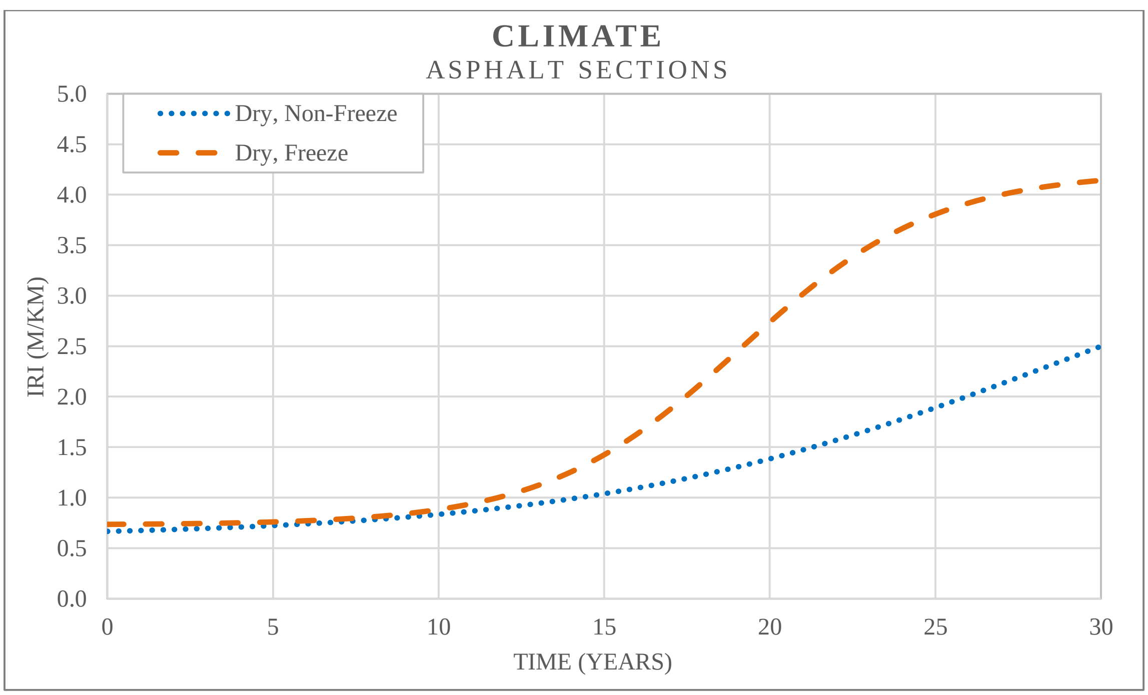

Figure 22: LTPP Asphalt Sections, Climate Comparison

The results of this figure indicate that new pavements in both climatic regions behave very similarly in the first 10 years of pavement life. After this phase, it is observed that the Dry-Freeze sections deteriorated at a much faster rate (greater slope) than the Dry, Non-Freeze sections. The reduced pavement performance of the Dry, Freeze sections can be attributed to damaging internal freeze-thaw effects repeatedly experienced in pavements within this region.

Table 9: LTPP Asphalt Sections, Climatic Comparison

Case Study - Comparison:	LTPP - Asphalt Sections - Climatic Comparison	
Data Set:	Dry, Non-Freeze	Dry, Freeze
Optimal Maximum Time Shift:	35	20
Number of Roadway Sections:	72	15
Number of Data Points:	707	177
Number of Series:	132	34
Se / Sy	0.390	0.238
R2	0.936	0.977
a1	0.608	0.729
a2	3.500	3.500
a3	0.142	0.338
a4	-4.090	-6.472

As shown in Table 9, the optimal time shift for the Dry, Non-Freeze and Dry, Freeze sections was determined to be 35 and 20 years, respectively. The lower optimal time shift value of the Dry, Freeze sections also supports the conclusion of a more rapid deterioration pattern. The final sigmoidal curve of each data group showed strong correlation with the respective data series, with R^2 values of 0.936 and 0.977, and Se/Sy values of 0.390 and 0.238.

Figure 23 and Table 10 show the relationship between high and low traffic levels on asphalt pavement sections. Although the lower traffic sections show earlier deterioration, the sections with greater traffic levels show more rapid deterioration.

Figure 23: LTPP Asphalt Sections, Traffic Level Comparison

It is important to note that although these datasets are grouped by traffic level, the other properties within each group may not be consistent. For example, a pavement section may experience greater traffic levels, but also exhibit superior performance over time due to better quality material and structural properties intentionally designed to compensate for the forecasted loading.

A summary of the optimal time shift curves for each traffic loading group is provided in Table 10 Both groups resulted in an optimal time shift of 30 years. A high correlation exists between the fitted sigmoidal curves and the individual data series.

Table 10: LTPP Asphalt Sections, Traffic Loading Comparison

Case Study - Comparison:	LTPP - Asphalt Sections - Traffic Loading Comparison	
Data Set:	AC > 2000 KESALS	AC < 2000 KESALS
Optimal Maximum Time Shift:	30	30
Number of Roadway Sections:	44	43
Number of Data Points:	415	469
Number of Series:	77	90
Se / Sy	0.403	0.238
R2	0.931	0.977
a1	0.738	0.594
a2	3.500	3.500
a3	0.291	0.145
a4	-7.157	-3.520

The LTPP data shows a practical application of the sigmoidal modeling methodology for IRI data. It was also demonstrated that narrowing the characteristics of the dataset into smaller groups can provide improved model fit. In this case study, the optimal curve of the asphalt sections (Table 8) with an R^2 of 0.934 and Se/Sy of 0.397 can be considered the baseline model. As the roadway sections were categorized into subgroups, three of the four optimized curves showed improved model correlation. Sorting by climatic region and traffic loading are examples of the subgrouping that could be performed to improve deterioration prediction capabilities.

4.6 Summary

The case study utilized data from the LTPP database and focused on asphalt pavement sections located in Arizona. This investigation demonstrated that the sigmoidal function was a suitable model for pavement roughness prediction. Through the analysis of asphalt sections in Arizona, it was shown that the developed sigmoidal curves of some subgroups deteriorated more rapidly than others. Sections located in climates that experience periodic freezing temperatures deteriorated more quickly than sections that did not. It was also observed that sections with a higher traffic level resulted in higher deterioration; however the other pavement characteristics (e.g., layer material and structure) must be known to ensure the results highlight the desired property rather than a combination of characteristics. In addition, this case study concluded that a more accurate model can be developed by narrowing the selection of pavement sections to a more specific group.

5. CASE STUDY 2: MnROAD PAVEMENT ROUGHNESS DATA

5.1 Introduction

The Minnesota Road Research Project (MnROAD) is a pavement research facility developed by the Minnesota Department of Transportation. Construction began in 1991, and the completed test track was opened to traffic in 1994 (Tompkins et al 2007). The test track is comprised of individual cells, or pavement sections, with various material, structural, and traffic conditions. The test track was designed as an ongoing experimental study, with 14 primary objectives. Several of the research goals included the evaluation of empirical and mechanistic design methods, the development of mechanistic models, frost prediction modeling, freeze-thaw characteristics, subgrade and subbase performance, and the reliability and variation in pavement performance (Newcomb et al. 1990).

There are more than 50 experimental sections, each designed and constructed for a specific research purpose. A 3.5 mile Mainline (interstate) track and a 2.5 mile Low Volume Road track were designed to collect pavement data using over 9,500 sensors located in within the pavement (Tompkins et. al 2007) (Engstrom & Worel, 2015).The MnROAD test sections are shown in Figure 24 (Tompkins et. al 2007). The MnROAD research facility provides pavement performance data for research use to continue developments in pavement engineering.

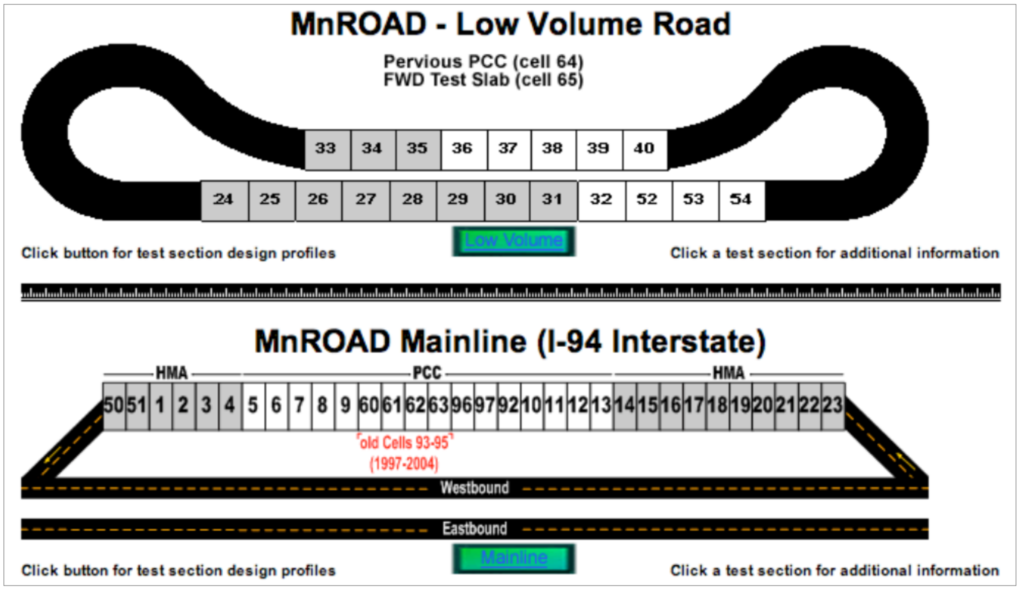

Figure 24: MnROAD Test Track Sections (Tompkins et. al 2007)

5.2 Data Summary

The IRI data was collected using the Lightweight Inertial Surface Analyzer (LISA). This technology consists of laser profilers and sensors equipped to a utility vehicle. LISA measurements are recorded while the vehicle is in motion. On average, LISA measurements are collected three times per year (MnROAD, 2009). The LISA equipment is regularly calibrated and tested for reliability and accuracy of the data collection.

The pavement roughness data is available on the MnROAD website, using the "MnROAD Data" and "Field Monitoring" links. International roughness index data is available for 95 cells, which includes asphalt, concrete, and composite pavement sections. Some sections were excluded from analysis due to limited sample size. A total of 65 sections were analyzed; 31 asphalt sections, 33 concrete sections, and 3 composite sections. Additional information is provided for the sections, including Roadway Classification, Layer Material (Surface, Base, Subbase), Layer Thickness, Lane Type (Inside/Outside, Driving/Passing), Lane Width, and Drainage information.

For the purpose of this case study, the IRI data of the pavement sections was separated into subgroups based on the pavement type, roadway classification, lane type, lane width, and drainage condition. The goal of the analysis was to demonstrate the sigmoidal curve methodology, and additionally to show that deterioration trends can be observed when comparing multiple related pavement characteristic groups. The modeling process of analyzing and constructing sigmoidal curves was conducted for the following pavement section groups in Table 11.

Table 11: MnROAD Data Grouping Summary

Data Source	Comparison	Name	Number of Sections
MnROAD	Pavement Type	Asphalt Sections	31
MnROAD		Composite Sections	3
MnROAD		Concrete Sections	33
MnROAD	Roadway Classification	Asphalt Low Volume Road Sections	15
MnROAD		Asphalt Mainline Sections	16
MnROAD		Concrete Low Volume Road Sections	14
MnROAD		Concrete Mainline Sections	19
MnROAD	Lane Type	Asphalt Low Volume Road, Inside Lane Sections	15
MnROAD		Asphalt Low Volume Road, Outside Lane Sections	15
MnROAD		Asphalt Mainline, Driving Lane Sections	16
MnROAD		Asphalt Mainline, Passing Lane Sections	16
MnROAD		Concrete Low Volume Road, Inside Lane Sections	14
MnROAD		Concrete Low Volume Road, Outside Lane Sections	14
MnROAD		Concrete Mainline, Driving Lane Sections	19
MnROAD		Concrete Mainline, Passing Lane Sections	19
MnROAD	Lane Width	Asphalt Low Volume Road, Sections with 12 FT Lane Width	7
MnROAD		Asphalt Low Volume Road, Sections with 13 - 14 FT Lane Width	8
MnROAD		Concrete Mainline, Sections with 12 FT Lane Width	14
MnROAD		Concrete Mainline, Sections with 13-14 FT Lane Width	5
MnROAD	Drainage Condition	Concrete Mainline, Sections with Drainage	5
MnROAD		Concrete Mainline, Sections without Drainage	14

A list of the individual MnROAD roadway segments and attributes of each data group is provided in Appendix A.

5.3 Data Preparation

The IRI data spreadsheet includes measurements for the left and right wheel path. During each date of measurement, three LISA trials were conducted to ensure reliability of the readings. To prepare the data, the average of the left and right wheel paths was used as the IRI value for each trial. The next step was to determine the average of the three trials on each date of measurement. Each pavement section was simplified to one IRI value for each date.

The process described in the methodology and the LTPP case study was completed for the MnROAD data, where the each section was time standardized to begin at "Time = 0". Significant decreases in IRI value within a roadway section were identified as maintenance intervention, and separated into series, which were also standardized to begin at "Time = 0". For all series, the time scale was converted from specific dates to the number of years from the beginning of each series. The individual series were inserted into the modeling spreadsheet for further analysis and model optimization.

5.4 Development of Performance Models

In this section, the development of sigmoidal performance curves is explained using the MnROAD Asphalt Sections data group as an example. Figure 25 shows each separated series for each asphalt section, which were determined by the date in which maintenance was performed. These series were inserted into the modeling spreadsheet to determine the optimal sigmoidal time shift curve. Figure 25 shows this data before any time shifting, with all series beginning at "Time = 0". This data group includes 184 individual series within the 31 pavement sections, which means that on average, there are approximately 6 series per section.

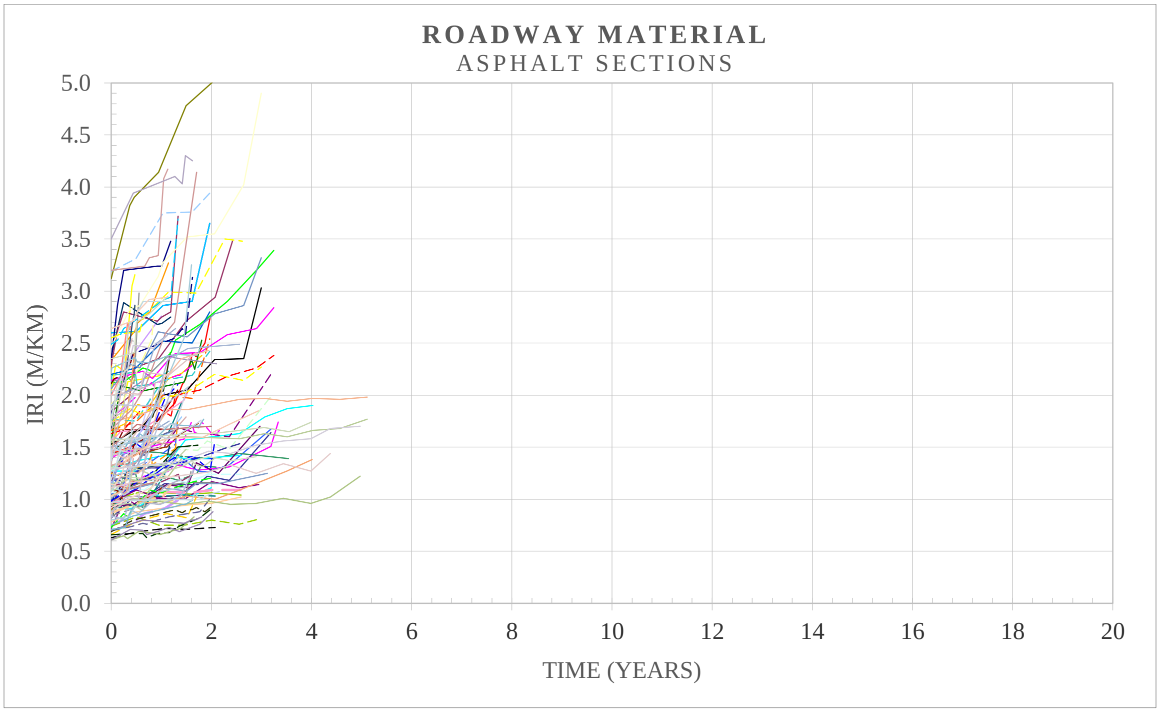

Figure 25: MnROAD Data - Raw Asphalt Sections before Time Shifting

The time shift process is repeated iteratively until the incremental increase of R^2 is less than or equal to 0.001. This value is smaller than the threshold increase value used for the LTPP database. This lower threshold value for the MnROAD data is due to higher accuracy of the data. The MnROAD data was collected as part of one research effort, in the same location, using the same equipment, and consistent measurement frequency. The LTPP data was gathered as part of a larger research program and many data collection efforts, using several equipment, and measuring sections slightly less frequently. The results of the MnROAD time shift curves required a more precise incremental increase value, therefore the value of 0.001 was used. The fitted sigmoidal curve of the 5 year maximum time shift is provided in Figure 26.

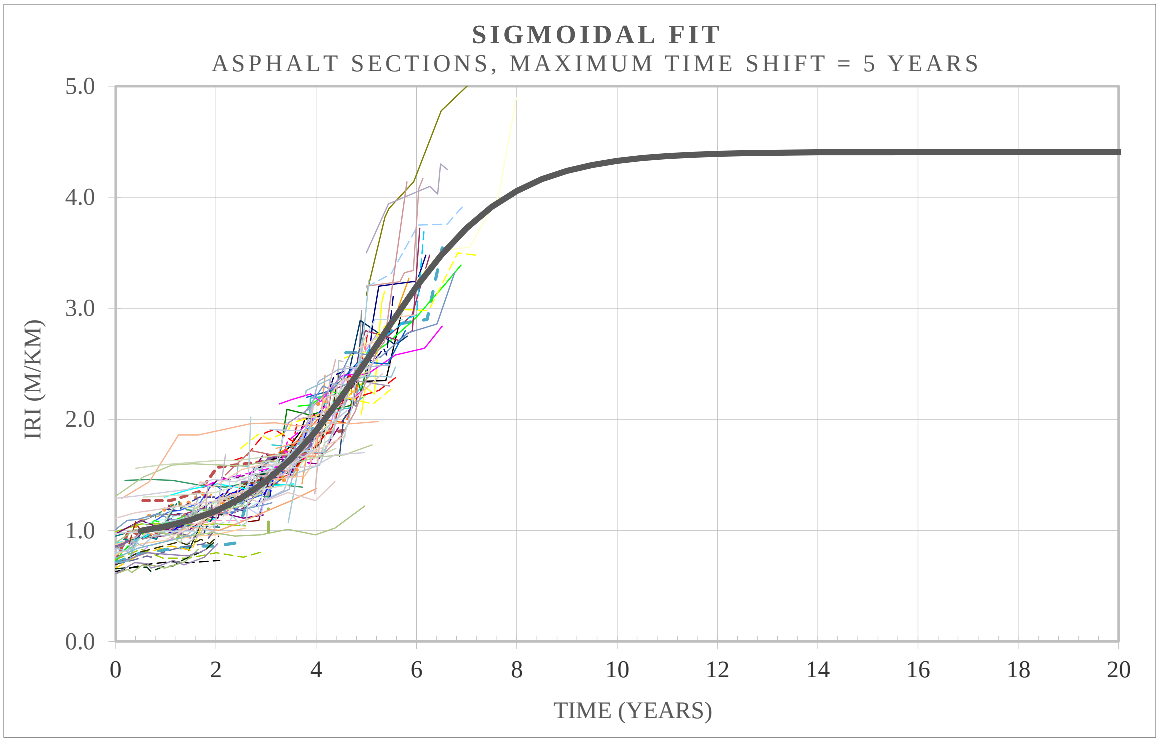

Figure 26: MnROAD Data – Asphalt Sections, 5 Year Maximum Time Shift

The fitted curves for 10, 15, and 20 year time shifts are shown in Figures 27, 28, and 29, respectively. Similarly to the methodology example and LTPP case study, a better model fit is achieved with a greater maximum time shift, until a threshold accuracy limit is reached.

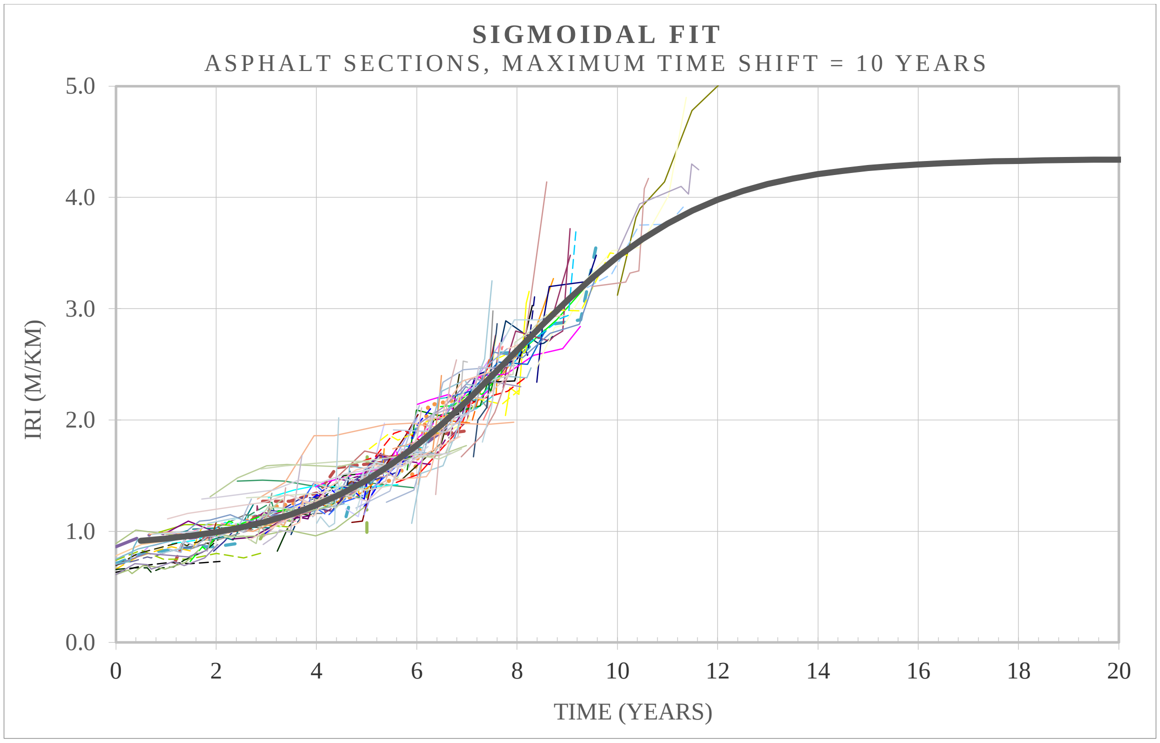

Figure 27: MnROAD Data – Asphalt Sections, 10 Year Maximum Time Shift

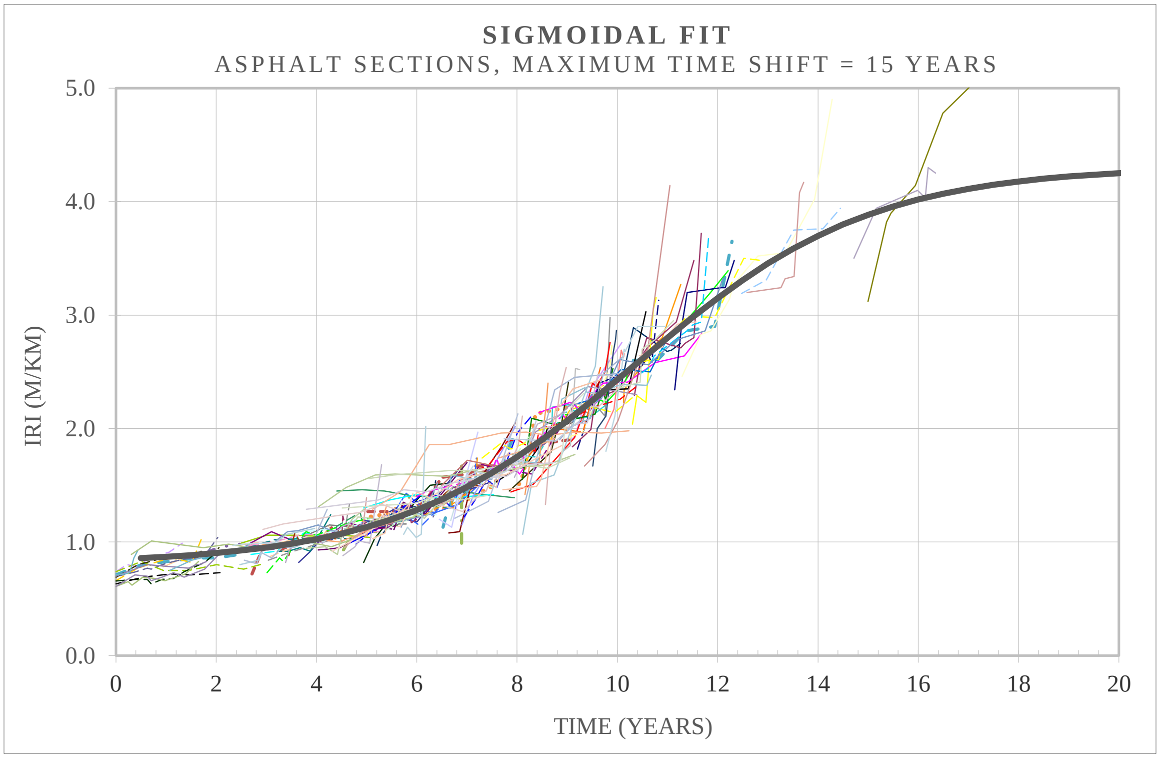

Figure 28: MnROAD Data – Asphalt Sections, 15 Year Maximum Time Shift

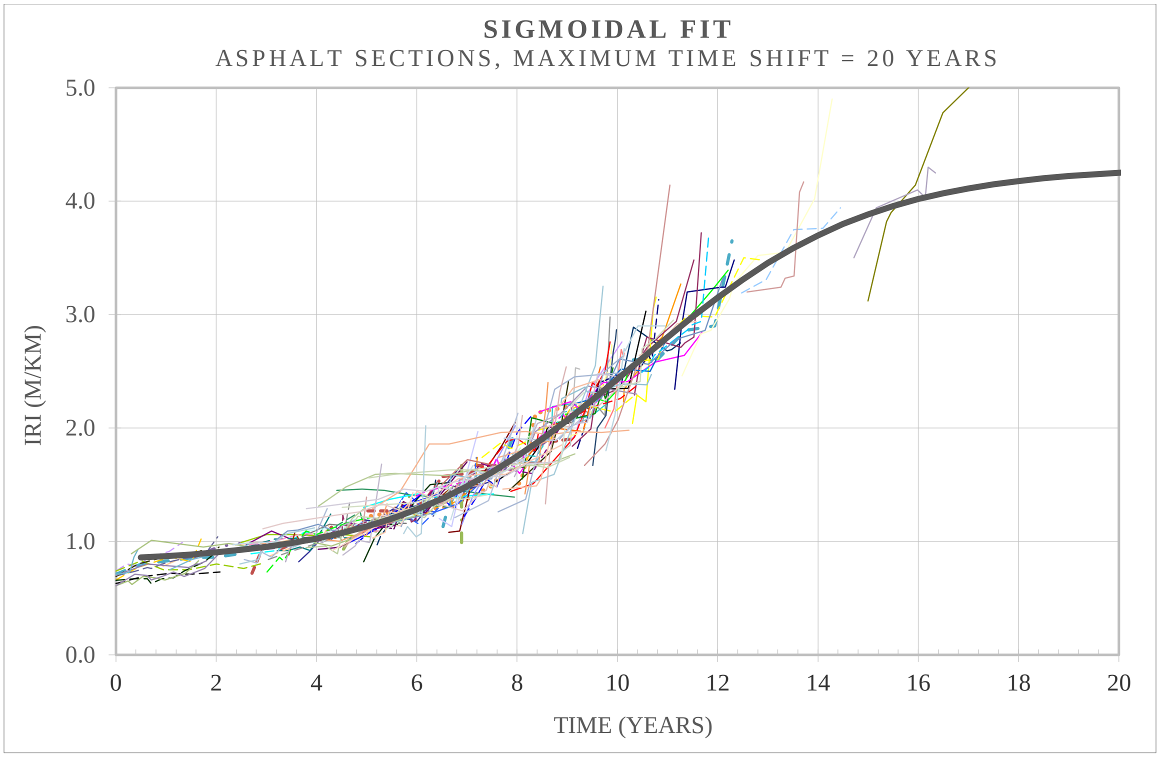

Figure 29: MnROAD Data – Asphalt Sections, 20 Year Maximum Time Shift

Modeling efforts did not extend beyond 30 years because a threshold was reached, where the measures of model fit no longer increased as the time shift increased. The time shift iteration process is summarized in Figure 30 and Table 12. In Figure 30, the optimized sigmoidal curves of each maximum time shift are superimposed to demonstrate how the shape of the curve changes during the iterative process.

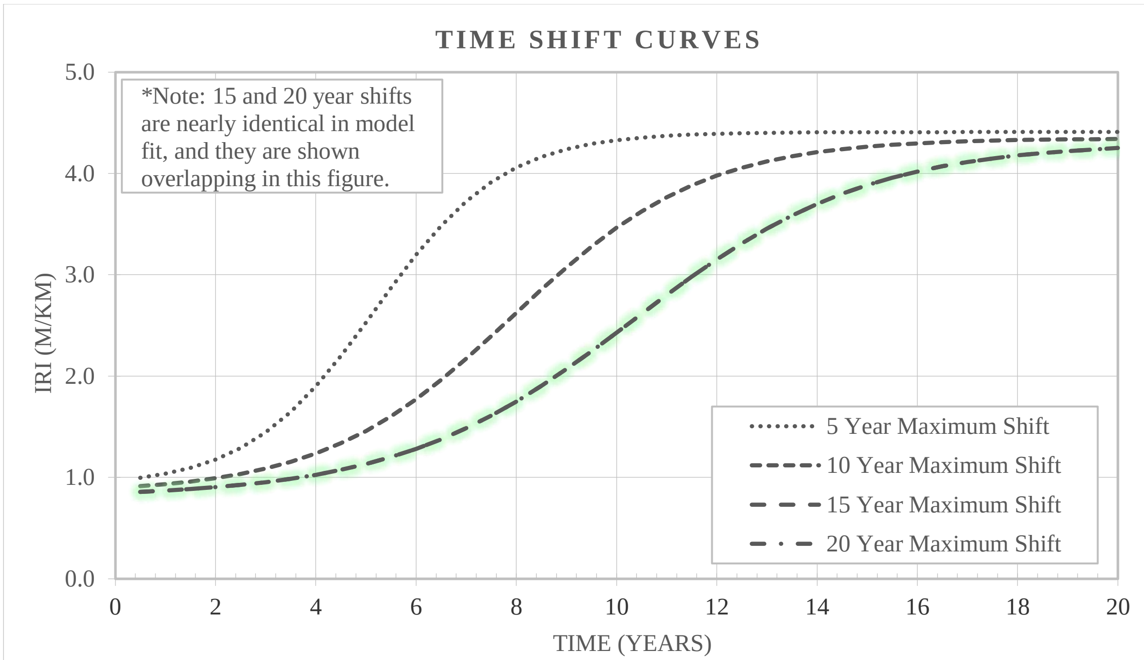

Figure 30: MnROAD Data – Time Shift Curves, Asphalt Sections

The model coefficients and measures of fit of each time shift iteration is provided in Table 12. As the maximum allowable time shift increases, the measures of fit (Se/Sy and R^2) improve until a threshold is reached. This model accuracy was reached at the 15 year time shift. The incremental increase in R^2 between the 15 and 20 year time shifts was less than 0.001, which indicates that the threshold was reached. The 15 year time shift was determined to be the optimal time shift, and it is highlighted in Table 12 and Figure 30 in green. The fit of the 15 and 20 year time shift is nearly identical, which is why the curves overlap in the figure.

Table 12: MnROAD Data – Time Shift Model Coefficients and Measures of Fit, Asphalt Sections

5 Year Shift		10 Year Shift		15 Year Shift		20 Year Shift	
a1	0.908	a1	0.846	a1	0.806	a1	0.806
a2	3.500	a2	3.500	a2	3.500	a2	3.500
a3	0.781	a3	0.528	a3	0.426	a3	0.426
a4	-4.055	a4	-4.189	a4	-4.407	a4	-4.407
Se/Sy	0.394	Se/Sy	0.288	Se/Sy	0.274	Se/Sy	0.274
R2	0.932	R2	0.964	R2	0.968	R2	0.968

5.5 Results

The sigmoidal curve development in Section 5.4 was a demonstration of how the individual series of the asphalt sections were shifted to the optimal location on the deterioration curve. For each data group listed in Table 11, this process was replicated to determine the optimal time shift curve to best fit the data. This includes comparisons within the following categories: Pavement Type, Roadway Classification, Lane Type, Lane Width, and Drainage Condition. The curves displayed in these comparison graphs are the determined optimal time shift curve for each data group.

Pavement Type

Figure 31 and Table 13 depict the comparison of pavement deterioration between roadways of different pavement types. The asphalt and concrete groups resulted in similar performance, however delayed deterioration was observed in the composite sections.

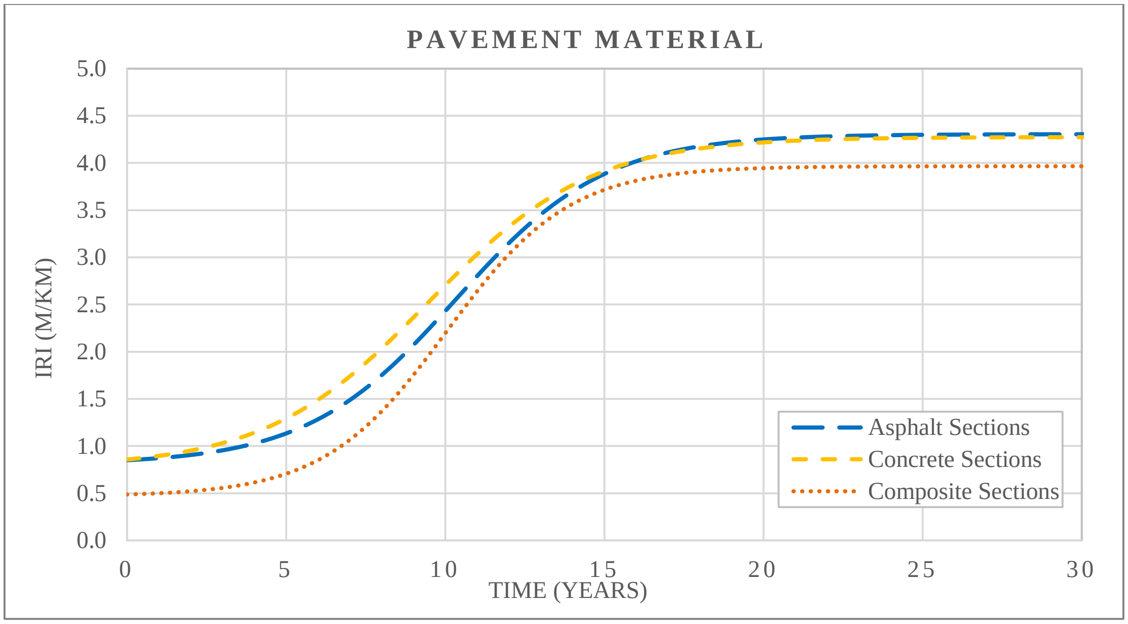

Figure 31: MnROAD Roadway Sections, Pavement Type Comparison

In Table 13, the composite section reached the optimal time shift in 10 years rather than 15 years in the case of asphalt and concrete sections mainly due to the smaller sample size. Due to the limited availability of composite data, this group is excluded from further subgrouping and analysis. The pavement material groups resulted in good correlation between the individual data series and fitted curve, with the best model fit in the Asphalt section group.

Table 13: MnROAD Sections - Pavement Type Comparison

Case Study - Comparison:	MnROAD - Pavement Type Comparison		
Data Set:	Asphalt	Composite	Concrete
Optimal Maximum Time Shift:	15	10	15
Number of Roadway Sections:	31	3	33
Number of Data Points (n):	1199	293	1051
Number of Series (p):	184	69	180
Se / Sy	0.274	0.317	0.362
R2	0.968	0.961	0.944
a1	0.806	0.467	0.802
a2	3.500	3.500	3.500
a3	0.426	0.518	0.393
a4	-4.407	-4.416	-4.243

The comparison of pavement type groups demonstrates that by using a large quantity of roadway sections (with various sub-properties), the resulting curves will be general. More detailed modeling is possible when the data group is narrowed to pavement sections with more similar characteristics, which is shown in the next sections of this chapter.

Roadway Classification

Figure 32 and Table 14 describe the comparison between the various roadway classifications of asphalt pavements. Mainline sections are intended to replicate interstate highways, with more intensive traffic loading but also with stronger pavement materials and structure. The Low Volume Road (LVR) sections are intended to replicate local arterials, with reduced traffic levels and appropriately matched pavement structure. In Figure 32, the Mainline group deteriorated sooner and faster than the LVR group. Although the pavement structure of the Mainline sections are of greater strength and quality, the overwhelming difference in traffic loading is the cause for the Mainline deterioration trends.

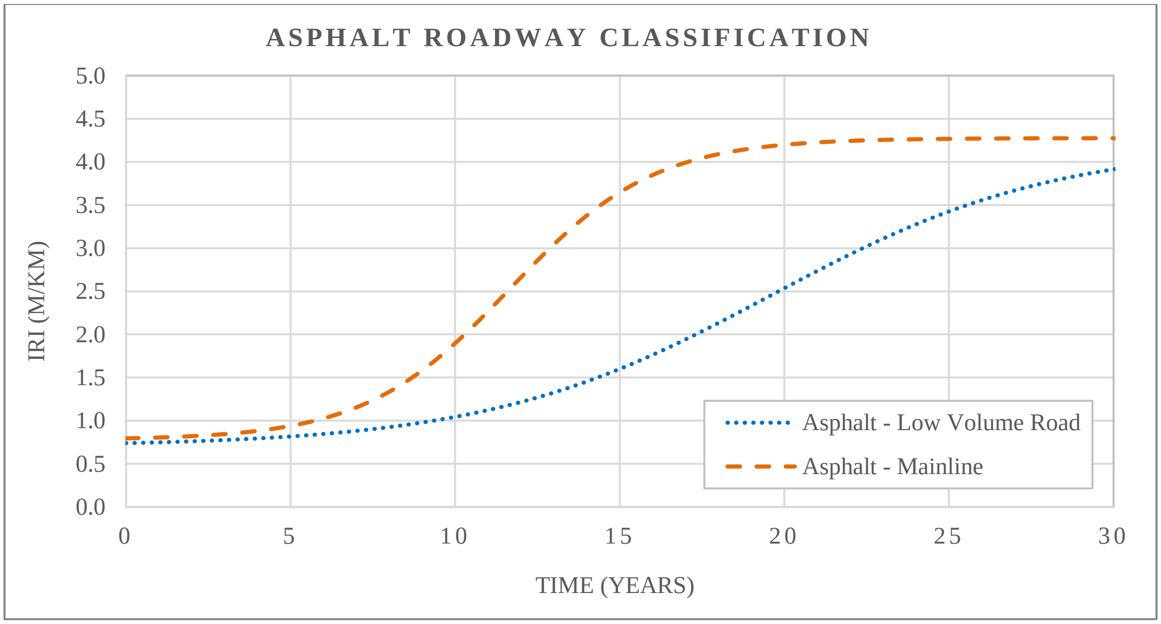

Figure 32: MnROAD Asphalt Sections, Roadway Classification Comparison

The sample sizes of each group are similar; however the optimal time shift was determined to be 30 and 15 years for the LVR and Mainline groups, respectively. This indicates that the LVR sections take more time to reach severe deterioration. The model correlation of the two groups, shown in Table 14, which is consistent with the baseline group (Asphalt Sections, Table 12).

Table 14: MnROAD Asphalt Sections, Roadway Classification Comparison

	MnROAD - Asphalt Sections - Roadway Classification Comparison	
Data Set:	Low Volume Road	Mainline
Optimal Maximum Time Shift:	30 Years	15 Years
Number of Roadway Sections:	15	16
Number of Data Points (n):	482	665
Number of Series (p):	78	103
Se / Sy	0.289	0.241
R2	0.964	0.975
a1	0.702	0.776
a2	3.500	3.500
a3	0.232	0.454
a4	-4.543	-5.296

The next comparison of roadway classification is for concrete sections. Figure 33 shows that the Concrete Mainline sections deteriorate more rapidly than the Concrete LVR sections. These findings are consistent with the Asphalt Roadway Classification results, and are also expected to have been caused by the significantly greater traffic loading on Mainline pavements.

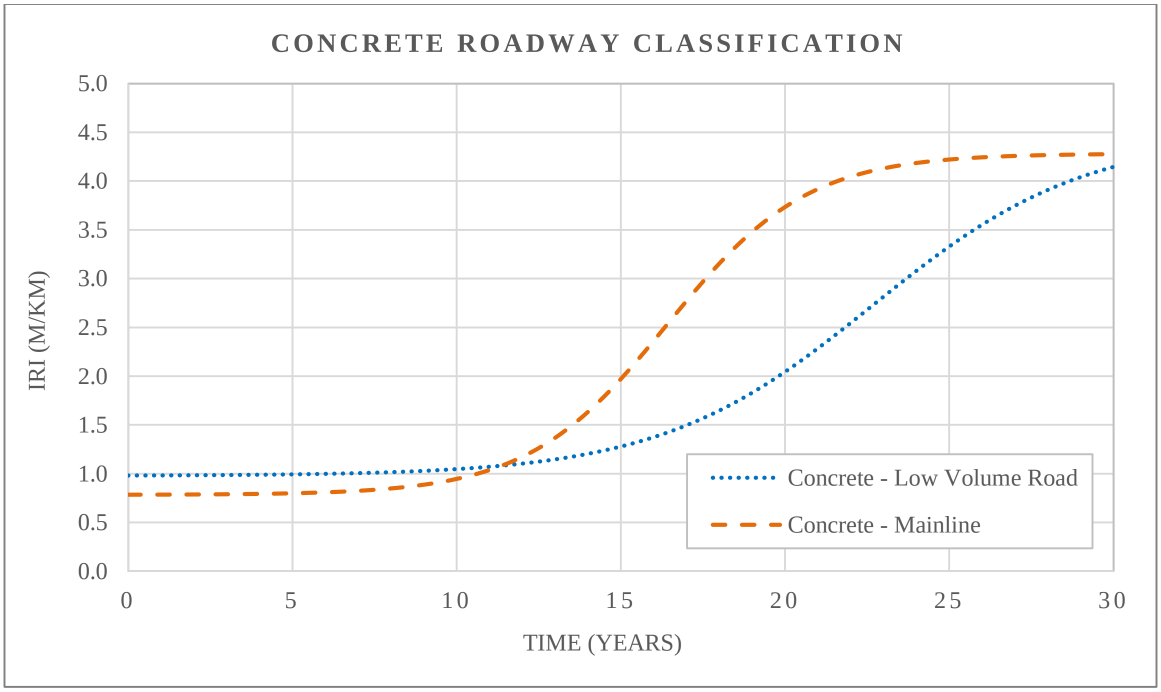

Figure 33: MnROAD Concrete Sections, Roadway Classification Comparison

The optimal time shift was determined to be 35 and 15 years for the LVR and Mainline group, respectively. This indicates that the LVR sections require more time to reach severe deterioration. The model correlation of the LVR sections was slightly stronger than the Mainline sections (Table 15).

Table 15: MnROAD Concrete Sections, Roadway Classification Comparison

	MnROAD - Concrete Sections - Roadway Classification Comparison	
Data Set:	Low Volume Road	Mainline
Optimal Maximum Time Shift:	35 Years	15 Years
Number of Roadway Sections:	14	19
Number of Data Points (n):	516	533
Number of Series (p):	93	89
Se / Sy	0.275	0.418
R2	0.968	0.924
a1	0.976	0.781
a2	3.500	3.500
a3	0.308	0.470
a4	-6.991	-7.715

Lane Type

The next comparison is based on the lane that was measured by the LISA equipment. The right-most lane is generally most utilized due to travel speed considerations and level of access. Highways experience the greatest traffic loading impact in the right-most lane due to slower speeds and high heavy truck utilization. In the United States, it is standard convention to utilize right lanes and reserve left lanes for passing. Similar operation is also observed on local arterials. Right lanes on arterials are also more utilized due to the direct access to complete turns into driveways. In the MnROAD database, different terminology is used for Mainline and LVR sections. IRI data in LVR sections are either Inside (Left) Lanes or Outside (Right) Lanes. The IRI data in Mainline sections is either Passing (Left) Lanes or Driving (Right) Lanes.

The first comparison of Lane Type is for Asphalt LVR sections. Figure 34 shows the deterioration curve for Inside and Outside Lane sections. The Outside (Right) Lane sections are observed to deteriorate earlier in the pavement service life than the Inside (Left) Lane Sections.

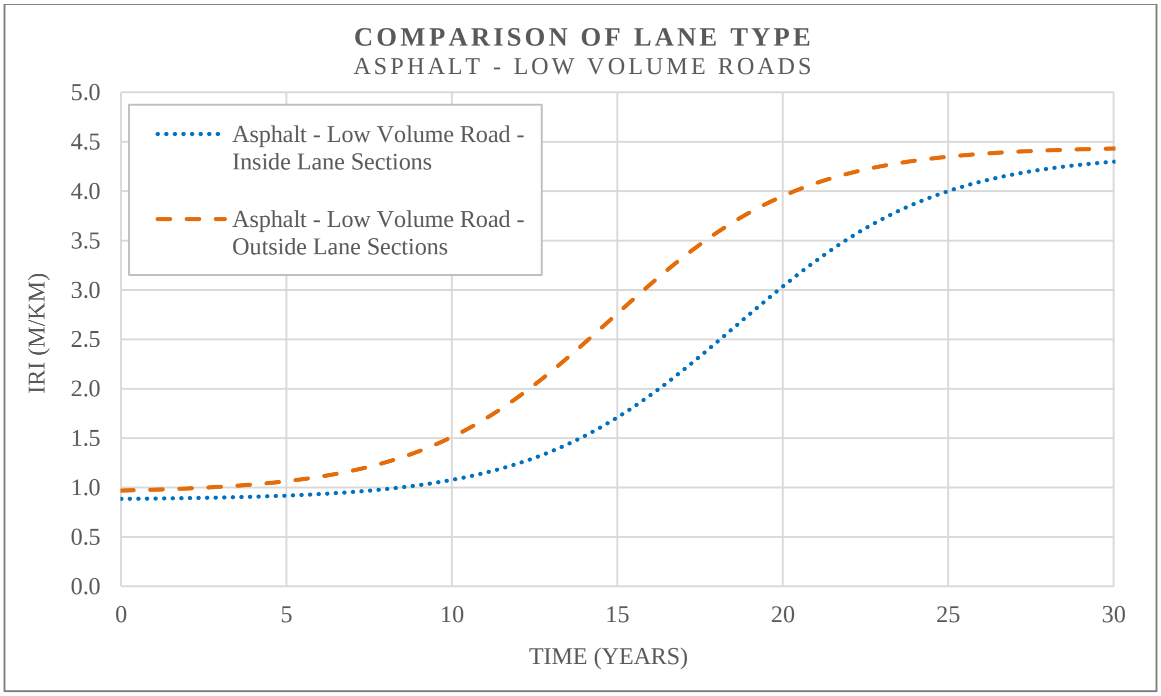

Figure 34: MnROAD Asphalt Low Volume Road Sections, Lane Type Comparison

The optimal time shift was determined to be 35 and 20 years for the Inside and Outside Lane groups, respectively. This indicates that the Inside Lane sections required more time to reach severe deterioration. The measures of fit of the Inside and Outside Lane sections, were essentially the same; with R^2 values of 0.959 and Se/Sy values of 0.310 and 0.308.

Table 16: MnROAD Asphalt Low Volume Road Sections, Lane Type Comparison

	MnROAD - Asphalt Low Volume Road Sections - Lane Type Comparison	
Data Set:	Inside Lane	Outside Lane
Optimal Maximum Time Shift:	35 Years	20 Years
Number of Roadway Sections:	15	15
Number of Data Points (n):	216	277
Number of Series (p):	36	45
Se / Sy	0.310	0.308
R2	0.959	0.959
a1	0.879	0.950
a2	3.500	3.500
a3	0.328	0.345
a4	-6.079	-5.098

The second comparison of Lane Type is for Asphalt Mainline Sections. Figure 35 shows the deterioration curve for Driving and Passing Lane sections. The Driving (Right) Lane sections are observed to deteriorate earlier in the pavement service life than the Passing (Left) Lane Sections.

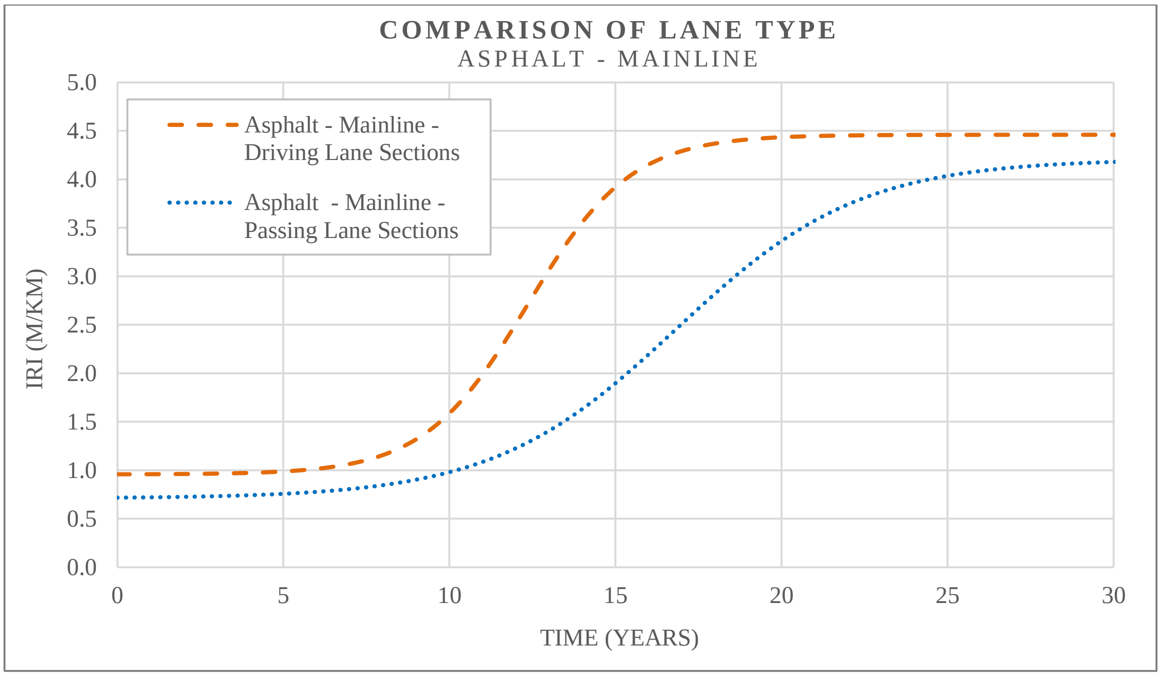

Figure 35: MnROAD Asphalt Mainline Sections, Lane Type Comparison

The optimal time shift was determined to be 20 and 15 years for the Passing and Driving Lane groups, respectively. This indicates that the Passing Lane sections take more time to reach severe deterioration. The model correlation of the both groups is consistent with the baseline group (Asphalt Mainline Sections, Table 14).

Table 17: MnROAD Asphalt Mainline Sections, Lane Type Comparison

	MnROAD - Asphalt Mainline Sections - Lane Type Comparison	
Data Set:	Passing Lane	Driving Lane
Optimal Maximum Time Shift:	20 Years	15 Years
Number of Roadway Sections:	16	16
Number of Data Points (n):	336	351
Number of Series (p):	51	54
Se / Sy	0.247	0.259
R2	0.974	0.971
a1	0.710	0.958
a2	3.500	3.500
a3	0.362	0.644
a4	-6.100	-7.955

The third comparison of Lane Type is for Concrete LVR sections. Figure 36 shows the deterioration curve for Inside and Outside Lane sections. The Outside Lane and Inside Lanes resulted in very similar deterioration trends. The Outside Lane seems to deteriorate at an earlier date, but the rate of deterioration is greater in the Inside Lane sections.

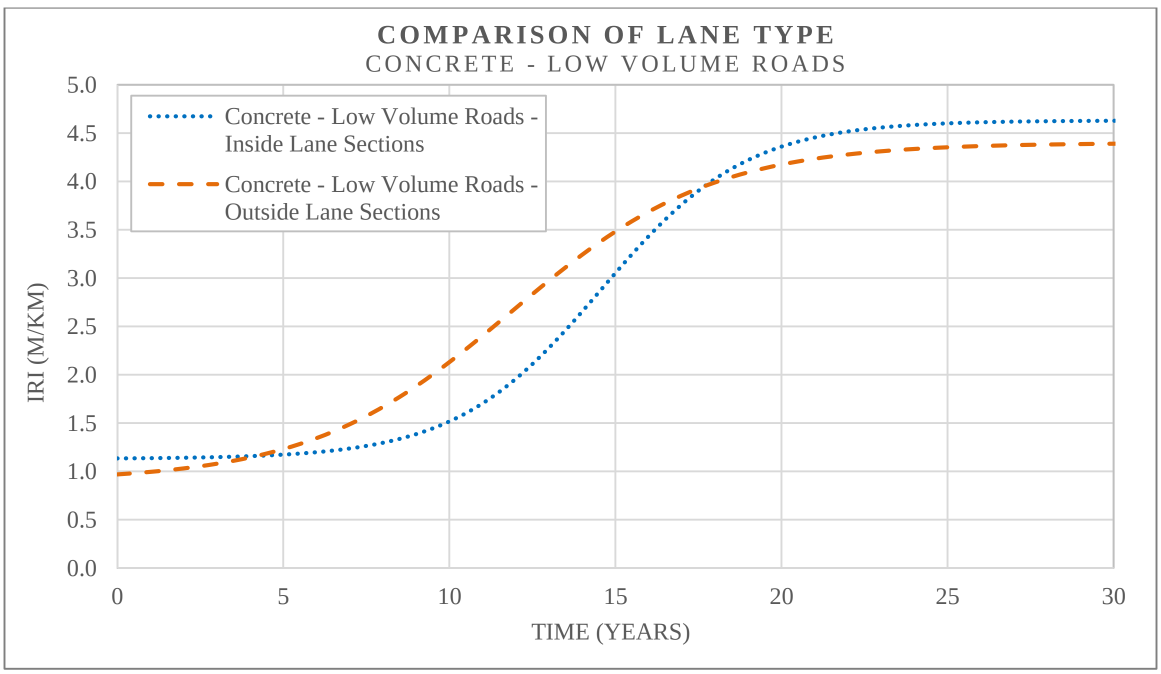

Figure 36: MnROAD Concrete Low Volume Road Sections, Lane Type Comparison

The optimal time shift was determined to be 15 and 20 years for the Inside and Outside Lane groups, respectively, which is contradictory as to what was observed with the Asphalt LVR Sections. The two Concrete LVR groups deteriorated very similarly, and the results are inconclusive in terms of determining the better performing roadway group. These findings may indicate that the lane distribution has less of an impact for Concrete than Asphalt sections in areas of low traffic.

Table 18: MnROAD Concrete Low Volume Road Sections, Lane Type Comparison

	MnROAD - Concrete Low Volume Road Sections - Lane Type Comparison	
Data Set:	Inside Lane	Outside Lane
Optimal Maximum Time Shift:	15 Years	20 Years
Number of Roadway Sections:	14	14
Number of Data Points (n):	259	252
Number of Series (p):	48	47
Se / Sy	0.319	0.255
R2	0.958	0.973
a1	1.131	0.486
a2	3.500	3.500
a3	0.456	0.170
a4	-6.651	-2.214

The final comparison of Lane Type is for Concrete Mainline sections. Figure 37 shows the deterioration curve for Driving and Passing Lane sections. The results show that both curves begin to deteriorate around the same time, but afterwards the rate of deterioration of the Driving Lane group was greater the deteriorations of the Passing Lane group.

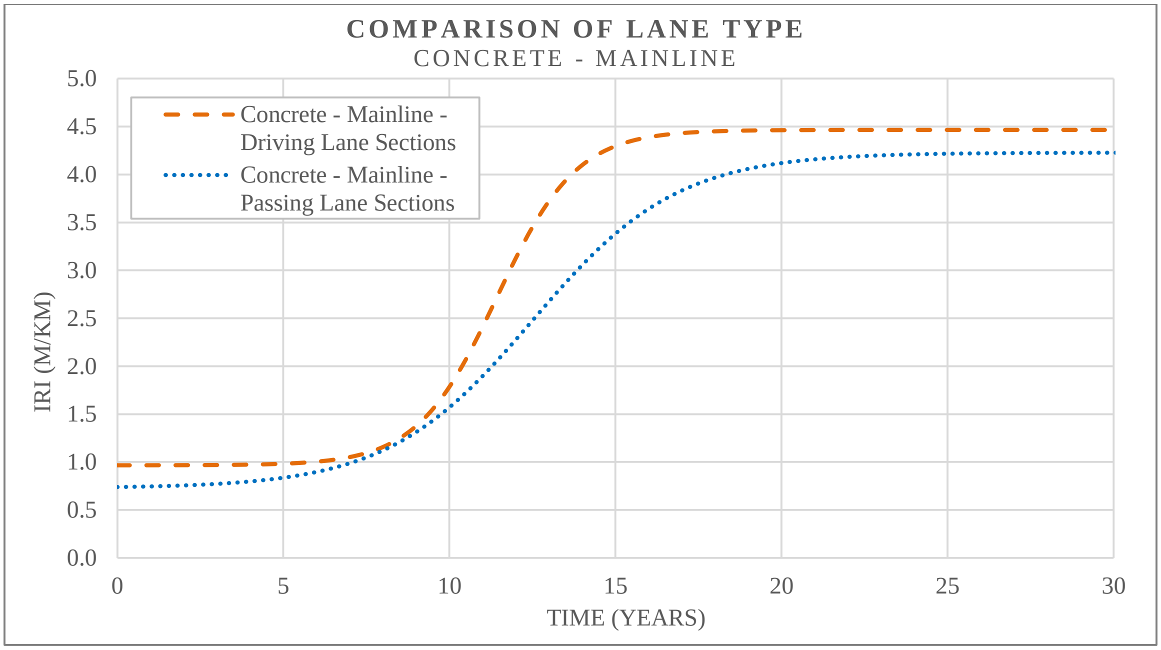

Figure 37: MnROAD Concrete Mainline Sections, Lane Type Comparison

The optimal time shift for both the Passing and Driving Lane groups was determined to be 10 years. This indicates that the Passing Lane sections require more time to reach severe deterioration. The model correlation of the both groups are very similar, and the measures of fit of each group are slightly improved from the baseline group (Concrete Mainline Sections, Table 15).

Table 19: MnROAD Concrete Mainline Sections, Lane Type Comparison

	MnROAD - Concrete Mainline Sections - Lane Type Comparison	
Data Set:	Passing Lane	Driving Lane
Optimal Maximum Time Shift:	10 Years	10 Years
Number of Roadway Sections:	19	19
Number of Data Points (n):	264	271
Number of Series (p):	46	45
Se / Sy	0.400	0.408
R2	0.931	0.928
a1	0.728	0.352
a2	3.500	3.500
a3	0.458	0.233
a4	-5.735	-2.272

In summary, the right (outside or driving) lane was observed to deteriorate more quickly in three of the four comparisons. The results of the Concrete LVR Lane Type comparison were inconclusive, with neither the inside nor outside lane deteriorating at a significantly higher rate. This suggests that the lane distribution does not greatly impact the deterioration of concrete pavements when the traffic level is low.

Lane Width

The purpose of this comparison is to understand if roughness pavement performance is affected by the lane width of a pavement, and if the pavement type also impacts the findings. The pavement sections were separated into two groups, sections of 12 ft lane widths, and sections with lane widths between 13 and 14 ft. All of the MnROAD sections fit into one of these groups. The idea is that wider lanes may better distribute loading, and that the common wheel path will be less restricted. Also, in concrete pavements wider lanes may minimize the effects of curling and warping. This comparison was conducted for Asphalt LVR sections and Concrete Mainline sections. There was insufficient data to complete the analysis for Asphalt Mainline sections and Concrete LVR sections.

Figure 38 shows the comparison of lane width in Asphalt Low Volume Road sections. The results of this comparison are inconclusive; it cannot be clearly determined that one group deteriorates more rapidly than the other.

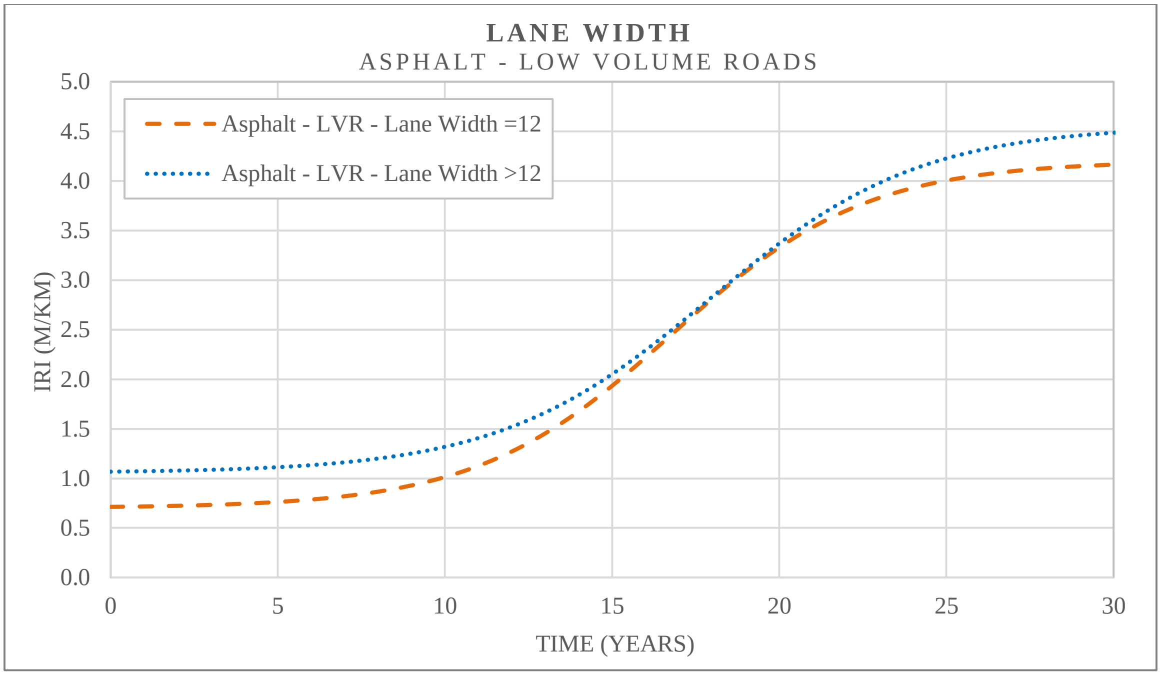

Figure 38: MnROAD Asphalt Low Volume Road Sections, Lane Width Comparison

Further information on the model coefficients and fit is provided in Table 20. The results of this comparison suggest that lane width does not have a significant impact on the pavement performance of asphalt sections in low traffic loading conditions.

Table 20: MnROAD Asphalt Low Volume Road Sections, Lane Width Comparison

	MnROAD - Asphalt Low Volume Road Sections - Lane Width Comparison	
Data Set:	12 Ft Lane Width	13 - 14 Lane Width
Optimal Maximum Time Shift:	15 Years	20 Years
Number of Roadway Sections:	7	8
Number of Data Points (n):	237	262
Number of Series (p):	39	41
Se / Sy	0.400	0.253
R2	0.930	0.973
a1	0.701	1.297
a2	3.500	3.500
a3	0.343	0.592
a4	-5.750	-6.603

Figure 39 shows the deterioration trend for Concrete Mainline sections of the two lane width groups. In this case, the standard lane width of 12 ft does show greater deterioration than the wider sections of 13-14 ft.

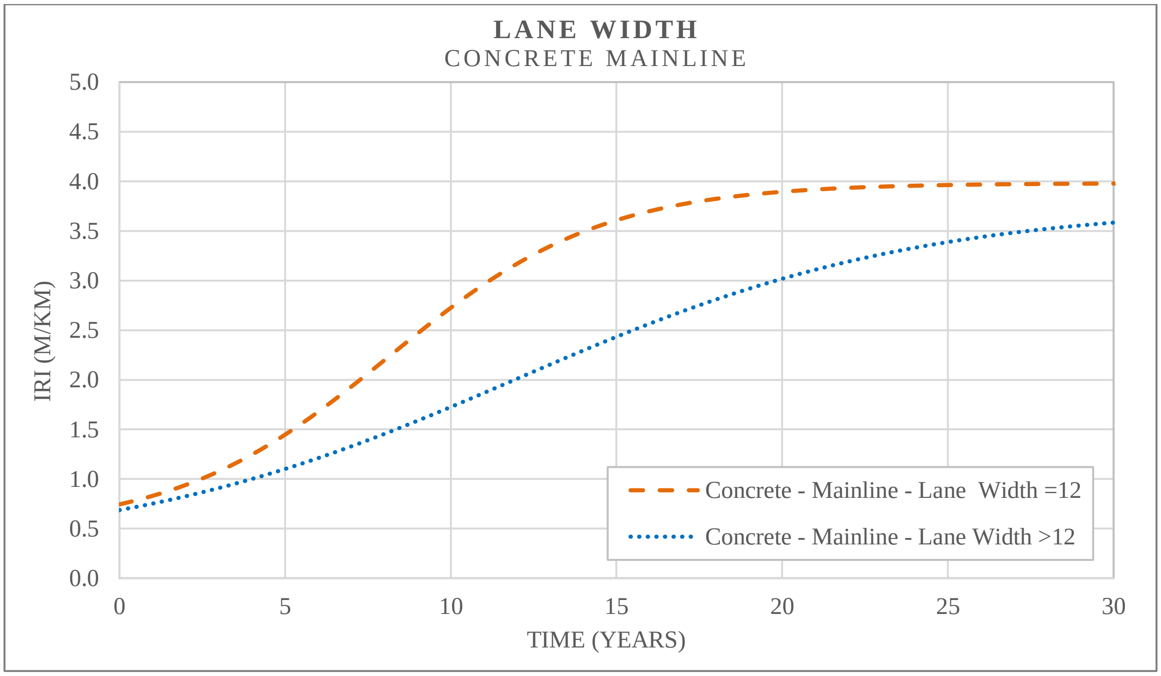

Figure 39: MnROAD Concrete Mainline Sections, Lane Width Comparison

The optimal time shift for both the 12 ft and 13-14 ft lane width groups was determined to be 10 ft. This indicates that the Passing Lane sections take more time to reach severe deterioration. The model correlation of the both groups are consistent are slight improvements from the baseline group (Concrete Mainline Sections, Table 15).

Table 21: MnROAD Concrete Mainline Sections, Lane Width Comparison

	MnROAD - Concrete Mainline Sections - Lane Width Comparison	
Data Set:	12 Ft Lane Width	13 - 14 Lane Width
Optimal Maximum Time Shift:	10 Years	10 Years
Number of Roadway Sections:	14	5
Number of Data Points (n):	262	266
Number of Series (p):	47	43
Se / Sy	0.387	0.409
R2	0.936	0.927
a1	0.482	0.257
a2	3.500	3.500
a3	0.309	0.164
a4	-2.508	-1.967

By Drainage Condition

The final category used to compare datasets is by the presence of pavement drainage components. The drainage systems in the MnROAD roughness database included wick drains, edge drains, porous pavement systems, open graded base, permeable asphalt-stabilized base (with drains), and geocomposite barrier drains. Due to the limited sample size of asphalt sections utilizing these drainage systems, the comparison will focus solely on the comparison of Concrete Mainline sections with and without drainage systems. In Figure 40, the optimal time shift curves for each group is shown. The results demonstrate that concrete sections without drainage systems experience greater deterioration over the pavement life.

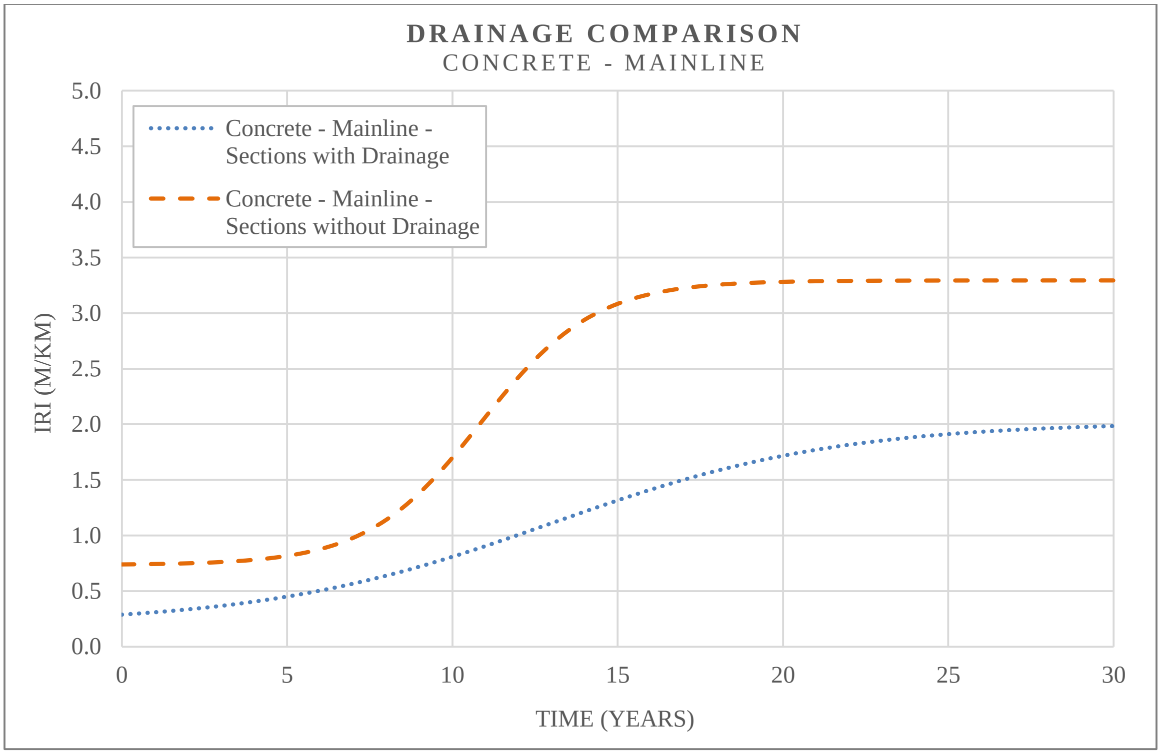

Figure 40: MnROAD Concrete Mainline Sections, Drainage Comparison

These findings are also supported by the optimal maximum time shift, which was 20 years for sections with drainage systems, and 10 years for sections without drainage systems. This indicates that the concrete sections with drainage systems require more time to reach severe deterioration.

Table 22: MnROAD Concrete Mainline Sections, Drainage Comparison

	MnROAD - Concrete Mainline Sections - Drainage Comparison	
Data Set:	Sections with Drainage	Sections Without Drainage
Optimal Maximum Time Shift:	20 Years	10 Years
Number of Roadway Sections:	5	14
Number of Data Points (n):	234	288
Number of Series (p):	39	52
Se / Sy	0.306	0.380
R2	0.960	0.939
a1	0.202	0.734
a2	1.817	2.561
a3	0.230	0.583
a4	-3.000	-6.333

5.6 Summary

The second case study included data from the Minnesota Road Research Project, which involves asphalt, concrete, and composite pavement sections. These sections were further grouped into comparison categories of roadway classification, lane type, lane width, and drainage system. By comparing the fitted sigmoidal curves, predicted trends were observed.

In the comparison of pavement material, it was determined that all three pavement types resulted in very similar deterioration curves, but the composite sections' deterioration was slightly delayed and less severe than the asphalt and concrete section groups. The asphalt, concrete, and composite groups resulted in similar curves primarily due to the large volume of pavement sections used in each group, which actually have many diverse characteristics. Based on this first comparison of pavement type, there was interest in further separating the data into finer subgroups, to determine if stronger conclusions and trends could be found.

In the comparison of roadway classification, pavement sections included in the Mainline group (interstate, high traffic loading) deteriorated more quickly than Low Volume Road (LVR) sections. This pattern was observed in both the asphalt and concrete comparisons of roadway classifications. This deterioration trend is due to the higher volumes and greater truck traffic on interstate highways.

Next, the lane type was investigated. This analysis compared primary lanes and secondary lanes on the same roadway sections. Measurements were taken on both the inside/passing lane and the outside/driving lane. After developing the optimal sigmoidal curve for each group, it was determined that the inside/passing lane deteriorates more slowly than the outside/driving lane. This pattern was observed in Asphalt LVR and Mainline sections, as well as Concrete LVR and Mainline sections.

Pavement groups were also compared by lane width. When comparing the lane widths of Concrete Mainline sections, it was observed that sections with wider lanes (13-14 ft) showed better performance and less deterioration than standard lanes (12 ft). When comparing Asphalt LVR sections, the conclusions were not as distinct. The deterioration curve for each lane width group was similar, indicating that increasing the lane width 1 to 2 inches did not have a significant impact on low volume asphalt roadways.

Lastly, pavement sections were compared to determine the performance differences between Concrete Mainline sections with and without drainage systems. As predicted, the sections without drainage structures showed a higher rate of deterioration which began sooner in the pavement's service life.

Some comparisons showed greater separation between the curves, or deterioration difference between two groups, while other comparisons resulted in very similar curves. Examples of similar curves included the lane type comparison of Concrete LVR sections, and the lane width comparison of Asphalt LVR sections. These results suggest that the comparison property does not significantly impact the IRI pavement performance. Studying deterioration curve separation could be a helpful tool to agencies to identify the characteristics greatly improving pavement performance.

This case study demonstrated the application and suitability of the sigmoidal function in pavement performance modeling.

6. SUMMARY, CONCLUSIONS AND RECOMMENDATIONS

6.1 Summary

The sigmoidal function is a recognized model form for representing pavement performance. The sigmoidal function has been developed for its implementation in Pavement Condition Index (PCI) modeling and other performance applications. The sigmoidal function captures the three phases of a pavement's life; as the pavement starts in good condition, experiences distresses and deterioration, and reaches a threshold for pavement performance loss.

The objective of this research was to develop a methodology to evaluate and predict pavement roughness over the pavement service life. The goal was to demonstrate the application potential of the sigmoidal function for pavement roughness modeling. The research also aimed to document that separating pavement sections of subgroups of similar characteristics can improve the model accuracy. Lastly, studying the deterioration patterns between comparable subgroups was also of interest. The process used in this methodology to develop sigmoidal curves was validated when comparing two subgroups of different attributes (e.g, pavement type, roadway classification, lane type, lane width, or drainage).

This modeling approach provided a prediction tool for pavement roughness conditions if no further maintenance or rehabilitation efforts are employed. Pavement performance is analyzed during the time *in between* maintenance efforts, to understand how a pavement section within a larger group will behave over time.

6.2 Conclusions

Two case studies were included in the research to demonstrate the modeling process and assess the findings. The first case study included data from the Long Term Pavement

Performance (LTPP) InfoPave database. This investigation demonstrated that the sigmoidal function was a suitable model for pavement roughness prediction. Through the analysis of asphalt sections in Arizona, it was demonstrated that the developed sigmoidal curves of some subgroups deteriorated more rapidly than others. Sections located in climates that experience periodic freezing temperatures deteriorated more quickly than sections that did not. In addition, it was concluded that sections with higher traffic levels result in more rapidly deteriorating performance; however, the other pavement characteristics (e.g., layer material and structure) must be known to ensure the data group is *only* comparing one characteristic, which in this case was traffic loading.

The second case study included data from the Minnesota Road Research Project, which includes asphalt, concrete, and composite pavement sections. These sections were further grouped into comparison categories of roadway classification, lane type, lane width, and drainage system. By comparing the fitted sigmoidal curves, predicted trends were observed. Generally speaking, pavement sections without drainage systems, standard lane widths, a higher roadway classification, or measured in the outermost lane were observed to have more rapid deterioration trends than their counterparts.

The four main conclusions of this research study are as follows:

- The sigmoidal growth performance curve methodology for IRI modeling was successfully demonstrated using data from two major databases (case studies): Long Term Pavement Performance (LTPP) and the Minnesota Department of Transportation MnROAD research program.
- The shifting technique utilized along with the quantity of data from each case study was effective to provide adequate section sample size in each phase of the modeled

performance curve. This is a powerful technique when performance data is not available for all phases of the performance curve.

- Separating IRI data into subgroups of similar pavement characteristics resulted in increased model accuracy.
- The ability to compare IRI performance curves of similar data subgroups was demonstrated, which was useful in providing rationality of trends observed and understanding pavement groups expected to have the most rapid deterioration.

6.3 Recommendations

The process of developing the sigmoidal performance function was demonstrated in this study for LTPP and MnROAD data sets. It can be adapted for more specific and practical use by agencies using their sets of collected IRI data. The sigmoidal models have the ability to show the pavement roughness that can be expected over time if there is no maintenance intervention.

It is recommended for agencies to develop more refined models to increase the accuracy of the desired prediction. The modeling efforts in this research serve as a proof of concept of the sigmoidal curve and the methodology. The same framework could be applied to other measures of pavement performance which deteriorate in a similar manner; this could possibly include individual distress, present serviceability rating, and friction loss. In future applications of this framework, it is also possible to model these other performance measures using this methodology and a different mathematical function. Further investigation should be completed to evaluate the suitability of other functions, such as linear or exponential models.

These modeling tools can help an agency allocate funding most effectively by identifying pavement sections or groups that will experience the fastest deterioration. For example, if these pavement sections are identified early, the preventative maintenance budget can be allocated to these sections, while slow deteriorating sections can be identified and maintenance can be delayed. Developing these performance models help to better understand the pavement network and can provide value in asset management and resource allocation planning.

REFERENCES

American Society for Testing and Materials (ASTM). 1999e. “Standard Practice for Computing International Roughness Index of Roads from Longitudinal Profile Measurements.” ASTM Standard Practice E-1926. *Book of ASTM Standards, Volume 04.03*. Philadelphia, PA.

ASTM Standard E950. (2009). "Standard Test Method for Measuring the Longitudinal Profile of Traveled Surfaces with an Accelerometer Established Inertial Profiling Reference," ASTM International, West Conshohocken, PA, 2009.

ASTM Standard E1274. (2012). "Standard Test Method for Measuring Pavement Roughness Using a Profilograph," ASTM International, West Conshohocken, PA, 2012.

Engstrom, G., & Worel, B. (2015). MnROAD: Safer, Smarter, Sustainable Pavements Through Innovative Research. Minnesota Department of Transportation, Saint Paul, Minnesota.

Federal Highway Administration. (1995). Pavement and Road Surface Management for Local Agencies, Participant’s Manual. Washington, D.C.: FHWA.

FHWA. (1999). *1999 Status of the Nation’s Highways, Bridges and Transit: Conditions and Performance*. Report to Congress. Federal Highway Administration, Washington, D.C.

Guide for Mechanistic-Empirical Design of New and Rehabilitated Pavement Structures, Appendix 00-1: Background and Preliminary Smoothness Prediction Models for Flexible Pavements. (2001).

Haas, R., Hundson, W., and Zaniewski, J. (1994). Modern Pavement Management. Krieger Publishing Co., Malabar, Florida.

Kaloush, K. (2014). Roughness and Surface Friction Testing [PowerPoint]. Lecture notes retrieved from Arizona State University, CEE 512: Pavement Performance and Management Blackboard Site.

Minnesota Department of Transportation. (2009). “Lightweight Inertial Surface Analyzer: MnROAD Ride Measurement”. Saint Paul, Minnesota.

Molenaar, A. (2001). Pavement Management Systems. Retrieved from http://goo.gl/rZztCh

Newcomb, D., Johnson, D., Baker, H., and Lund, S. (1990). Minnesota Road Research Project: Work Plan for Research Objectives.” Report. No. MN-RC-1990-03, Minnesota Dept. of Transportation, Saint Paul, Minnesota.

Pais, J., Amorim, S., and Minhoto, M. (2013). "Impact of Traffic Overload on Road Pavement Performance." Journal of Transportation Engineering.

Park, K., Thomas, N., & Lee, K. (2007). Applicability of the International Roughness Index as a Predictor of Asphalt Pavement Condition. Journal of Transportation Engineering, 706-709.

Pavement Management Guide. (2001). American Association of State Highway and Transportation Officials (AASHTO).

Prasad, J., Kanuganti, S., Bhanegaonkar, P., Sarkar, A., & Arkatkar, S. (2013). Development of Relationship between Roughness (IRI) and Visible Surface Distresses: A Study on PMGSY Roads. Procedia - Social and Behavioral Sciences, 322-331.

R3 Consulting Group, Inc. (2008). Trash Services Study, City of Fort Collins, Colorado.

Riggins, M., Lytton, R., & Garcia-Diaz, A. (1984). Developing Stochastic Flexible Pavement Distress and Serviceability Equations. Texas A&M Transportation Institute, College Station, TX.

Sayers, M. W. 1990. "Profiles of Roughness." *Transportation Research Record 1260*. Transportation Research Board, Washington, D.C.

Sebaaly, P., and Bazi, G., (2005). "Impact of Construction Variability on Pavement Performance", Nevada Department of Transportation, Carson City, Nevada.

Sotil, A., & Kaloush, K. (2004). Development of Pavement Performance Models for Delhi Township, Ohio Pavement management System. Compendium of Papers CD-ROM, 73 Meeting of the Transportation Research Board, National Research Council.

Tompkins, D., Khazanovich, L., and Johnson, D. (2007). "Overview of the First Ten Years of the Minnesota Road Research Project." Journal of Transportation Engineering.

Watanatada, T., Harral, C., Paterson, W., Dhareshwar, A., Bhandari, A., & Tsunokawa, K. (1987). The Highway Design and Maintenance Standards Model. Volume 1: Description of the HDM-III Model.

Zubeck, H. and Doré, G. (2009) Introduction to Cold Regions Pavement Engineering. Cold Regions Engineering 2009: pp. 337-345.

APPENDIX A

LTPP AND MNROAD ANALYSIS

Roadway Group Dataset Summary

The roadway sections in each dataset group are included in the respective sigmoidal model.

Long Term Pavement Performance (LTPP) InfoPave Database

Asphalt Sections		**Asphalt Climatic Comparison**			**Asphalt Traffic Comparison**	
		Dry, Non-Freeze		Dry, Freeze	> 2000 KESALS	< 2000 KESALS
0113	0903	0113	1036	0603	0603	0113
0114	1001	0114	1037	0604	0604	0114
0115	1002	0115	1062	0606	0606	0115
0116	1003	0116	1065	0607	0607	0116
0117	1006	0117	6053	0608	0608	0117
0118	1007	0118	6054	0659	0659	0118
0119	1015	0119	6055	0660	0660	0119
0120	1016	0120	6060	0661	0661	0120
0121	1017	0121	A310	0662	0662	0121
0122	1018	0122	A320	0664	0664	0122
0123	1021	0123	A330	0665	0665	0123
0124	1022	0124	A350	0666	0666	0124
0161	1024	0161	A901	0667	0667	0161
0162	1025	0162	A902	0668	0668	0162
0163	1034	0163	A903	0669	0669	0163
0260	1036	0260	B310		1003	0260
0261	1037	0261	B901		1006	0261
0501	1062	0501	B902		1007	501
0502	1065	0502	B903		1015	502
0503	6053	0503	B959		1016	503
0504	6054	0504	B960		1017	504
0505	6055	0505	B961		1018	505
0506	6060	0506	B964		1021	506
0507	A310	0507	C310		1022	507
0508	A320	0508	C330		1024	508
0509	A330	0509	C340		1025	509
0559	A350	0559	C350		1062	559
0560	A901	0560	D310		1065	560
0603	A902	0902			6053	902
0604	A903	0903			6054	903
0606	B310	1001			6055	1002
0607	B901	1002			B310	1034
0608	B902	1003			B901	1036
0659	B903	1006			B902	1037
0660	B959	1007			B903	6060
0661	B960	1015			B959	A310
0662	B961	1016			B960	A320
0664	B964	1017			B961	A330
0665	C310	1018			B964	A330
0666	C330	1021			C310	A350
0667	C340	1022			C330	A901
0668	C350	1024			C340	A902
0669	D310	1025			C350	A903
0902		1034			D310	

Data Set Title:	Asphalt Sections
Case Study:	1
Data Source:	LTPP
Number of Sections:	87
Number of Data Points (n):	884
Number of Series (p):	165
Optimal Maximum Time Shift:	25 Years

Plot of Time Shifting Process:

$$IRI = a_1 + \frac{a_2}{1+e^{(-a_3 * t + a_4)}}$$

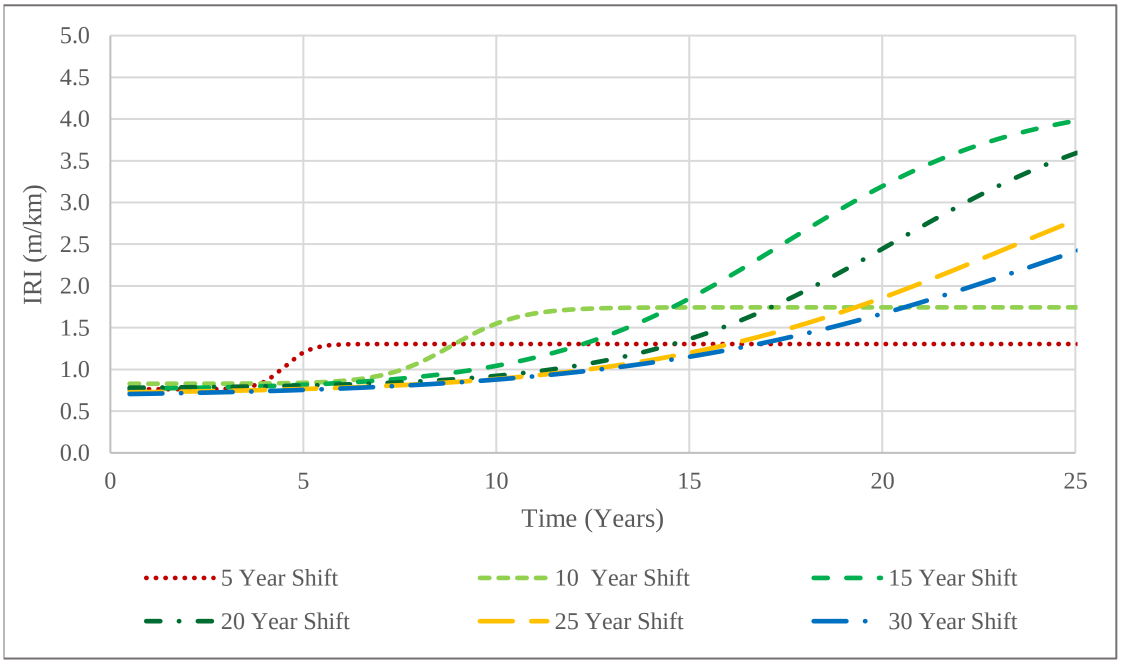

5 Year Shift		10 Year Shift		15 Year Shift		20 Year Shift		25 Year Shift	
a1	0.76236	a1	0.82824	a1	0.75436	a1	0.77144	a1	0.70178
a2	0.54158	a2	0.9152	a2	3.5	a2	3.5	a2	3.5
a3	3.04457	a3	1.14042	a3	0.32437	a3	0.30077	a3	0.21877
a4	-13.76	a4	-10.094	a4	-5.6529	a4	-6.103	a4	-5.0823
Se/Sy	0.97416	Se/Sy	0.81187	Se/Sy	0.60964	Se/Sy	0.45654	Se/Sy	0.39733
R2	0.47673	R2	0.68065	R2	0.83509	R2	0.9112	R2	0.93352

30 Year Shift	
a1	0.66535
a2	3.5
a3	0.18238
a4	-4.5607
Se/Sy	0.38371
R2	0.93814

Note: Green shading represents the optimal maximum time shift

Data Set Title:	Asphalt Dry Non-Freeze Climatic Sections
Case Study:	1
Data Source:	LTPP
Number of Sections:	72
Number of Data Points (n):	707
Number of Series (p):	132
Optimal Maximum Time Shift:	35

Plot of Time Shifting Process:

$$IRI = a_1 + \frac{a_2}{1+e^{(-a_3 * t + a_4)}}$$

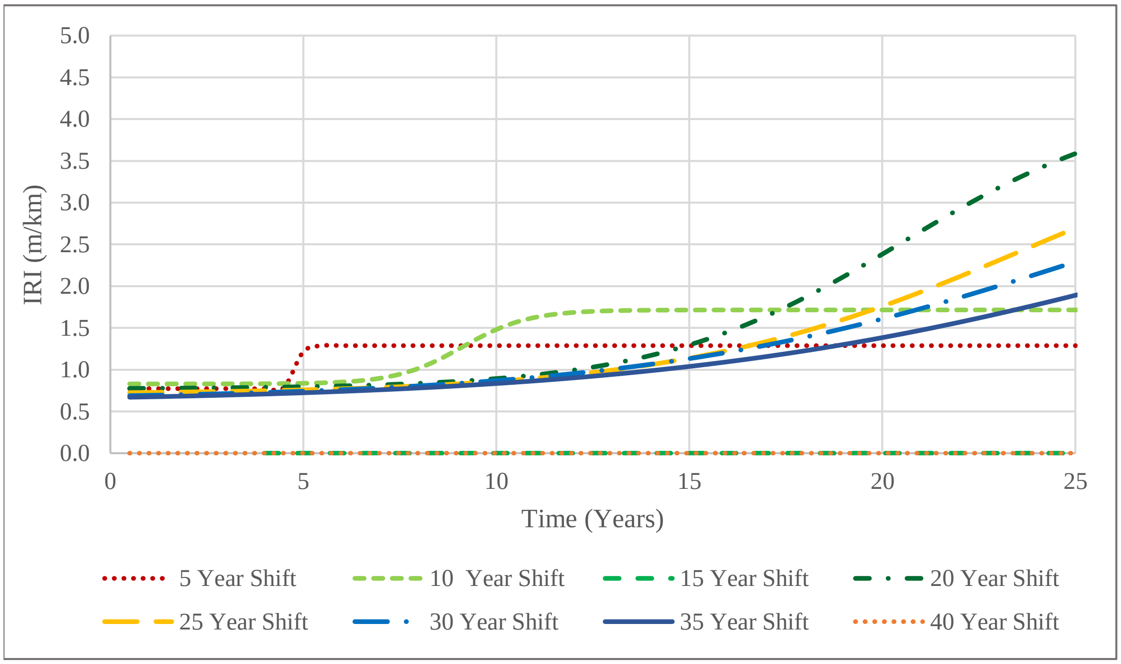

5 Year Shift		10 Year Shift				20 Year Shift		25 Year Shift	
a1	0.77283	a1	0.82937			a1	0.7693	a1	0.70631
a2	0.5149	a2	0.88583			a2	3.5	a2	3.5
a3	10.5226	a3	1.1639			a3	0.31477	a3	0.22357
a4	-50.816	a4	-10.617			a4	-6.4515	a4	-5.3147
Se/Sy	0.97255	Se/Sy	0.83079			Se/Sy	0.49434	Se/Sy	0.42868
R2	0.47921	R2	0.66171			R2	0.89497	R2	0.92213

30 Year Shift		35 Year Shift			
a1	0.64046	a1	0.60823		
a2	3.5	a2	3.5		
a3	0.16976	a3	0.14169		
a4	-4.357	a4	-4.09		
Se/Sy	0.40649	Se/Sy	0.38976		
R2	0.93028	R2	0.93609		

Note: Green shading represents the optimal maximum time shift

Data Set Title:	Asphalt Dry Freeze Climatic Sections
Case Study:	1
Data Source:	LTPP
Number of Sections:	15
Number of Data Points (n):	177
Number of Series (p):	34
Optimal Maximum Time Shift:	20

Plot of Time Shifting Process:

$$IRI = a_1 + \frac{a_2}{1+e^{(-a_3 * t + a_4)}}$$

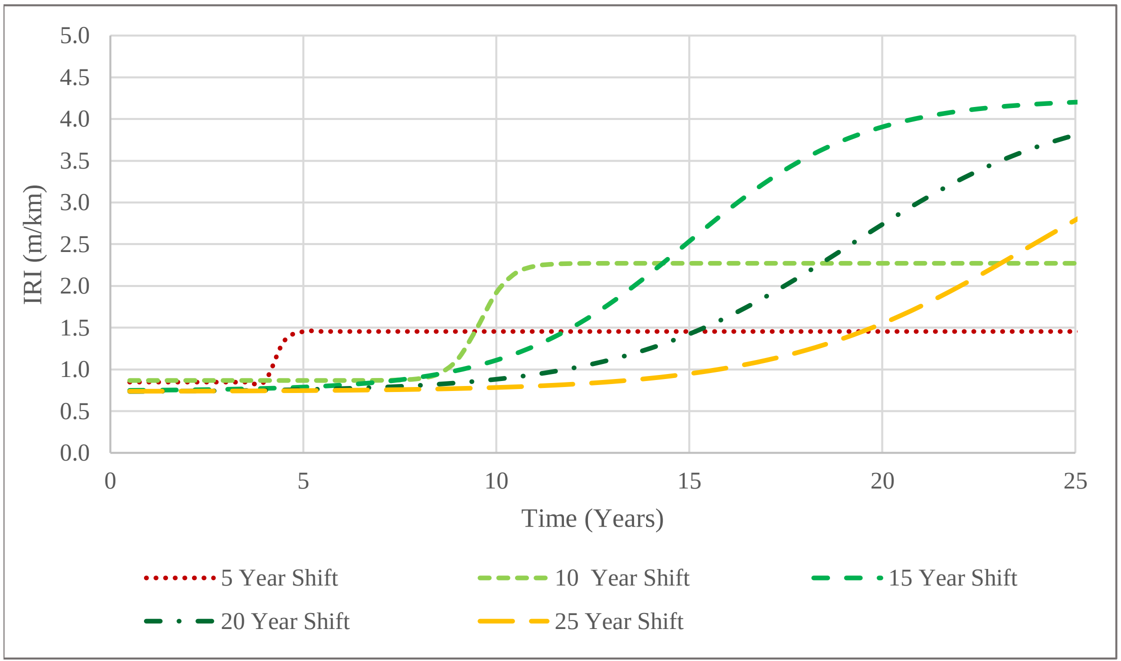

5 Year Shift		10 Year Shift		15 Year Shift		20 Year Shift		25 Year Shift	
a1	0.84773	a1	0.86724	a1	0.74266	a1	0.72921	a1	0.73558
a2	0.60641	a2	1.40406	a2	3.5	a2	3.5	a2	3.5
a3	11.02	a3	2.60063	a3	0.43811	a3	0.33849	a3	0.30882
a4	-48.143	a4	-24.911	a4	-6.523	a4	-6.4724	a4	-7.3697
Se/Sy	0.92313	Se/Sy	0.49623	Se/Sy	0.29053	Se/Sy	0.23792	Se/Sy	0.22829
R2	0.55463	R2	0.89438	R2	0.9651	R2	0.97673	R2	0.9786

Note: Green shading represents the optimal maximum time shift

Data Set Title:	Asphalt Sections, Greater than 2000 KESALS
Case Study:	1
Data Source:	LTPP
Number of Sections:	44
Number of Data Points (n):	415
Number of Series (p):	77
Optimal Maximum Time Shift:	30 Years

Plot of Time Shifting Process:

$$IRI = a_1 + \frac{a_2}{1+e^{(-a_3*t+a_4)}}$$

5 Year Shift		10 Year Shift		15 Year Shift		20 Year Shift		25 Year Shift	
a1	0.68727	a1	0.78672	a1	0.74926	a1	0.76689	a1	0.74515
a2	0.50344	a2	0.80766	a2	3.5	a2	3.5	a2	3.5
a3	1.74763	a3	1.65097	a3	0.39829	a3	0.35056	a3	0.27799
a4	-7.4384	a4	-15.409	a4	-7.0901	a4	-6.9955	a4	-6.4515
Se/Sy	1.00276	Se/Sy	0.83658	Se/Sy	0.65786	Se/Sy	0.47649	Se/Sy	0.42386
R2	0.42316	R2	0.65468	R2	0.80416	R2	0.90257	R2	0.92375

30 Year Shift		35 Year Shift	
a1	0.73803	a1	0.72889
a2	3.5	a2	3.5
a3	0.29075	a3	0.28659
a4	-7.1571	a4	-7.3651
Se/Sy	0.4028	Se/Sy	0.39415
R2	0.93142	R2	0.93443

Note: Green shading represents the optimal maximum time shift

Data Set Title:	Asphalt Sections, Less than 2000 KESALS
Case Study:	1
Data Source:	LTPP
Number of Sections:	43
Number of Data Points (n):	469
Number of Series (p):	90
Optimal Maximum Time Shift:	30 Years

Plot of Time Shifting Process:

$$IRI = a_1 + \frac{a_2}{1+e^{(-a_3 * t + a_4)}}$$

5 Year Shift		10 Year Shift		15 Year Shift		20 Year Shift		25 Year Shift	
a1	0.72472	a1	0.86101	a1	0.80427	a1	0.72501	a1	0.68545
a2	0.85227	a2	3.5	a2	3.5	a2	3.5	a2	3.5
a3	0.65266	a3	0.47266	a3	0.32629	a3	0.22446	a3	0.18942
a4	-3.1631	a4	-5.7675	a4	-5.0146	a4	-4.177	a4	-4.237
Se/Sy	0.95576	Se/Sy	0.64976	Se/Sy	0.48085	Se/Sy	0.40989	Se/Sy	0.365
R2	0.51013	R2	0.81124	R2	0.90153	R2	0.92949	R2	0.94452

30 Year Shift		35 Year Shift	
a1	0.59444	a1	0.54045
a2	3.5	a2	3.5
a3	0.14542	a3	0.12975
a4	-3.5204	a4	-3.2296
Se/Sy	0.34642	Se/Sy	0.34148
R2	0.95017	R2	0.95161

Note: Green shading represents the optimal maximum time shift

Roadway Group Dataset Summary

The roadway sections in each dataset group are included in the respective sigmoidal model.

Minnesota Department of Transportation MnROAD Database

Pavement Type*			**Asphalt Roadway Classification***		**Concrete Road Classification***		**Concrete Mainline Sections***	
Asphalt	Composite	Concrete	Low Volume Road	Mainline	Low Volume Road	Mainline	With Drainage	Without Drainage
1	92	5	24	1	32	5	7	5
2	93	6	25	2	36	6	8	6
3	94	7	26	3	37	7	9	11
4	95	8	27	4	38	8	10	13
14	96	9	28	14	39	9	12	60
15	97	10	29	15	40	10		61
16		11	30	16	41	11		62
17		12	31	17	42	12		63
18		13	33	18	43	13		114
19		32	34	19	44	60		213
20		36	35	20	45	61		214
21		37	54	21	46	62		414
22		38	77	22	52	63		513
23		39	78	23	53	114		614
24		40	79	50		213		
25		41		51		214		
26		42				414		
27		43				513		
28		44				614		
29		45						
30		46						
31		52						
33		53						
34		60						
35		61						
50		62						
51		63						
54		114						
77		213						
78		214						
79		414						
		513						
		614						

*Note: These grouped sections include both lane types. The Low Volume Road sections include the inside and outside lanes, and the Mainline sections include the driving and passing lanes.

Roadway Group Dataset Summary

The roadway sections in each dataset group are included in the respective sigmoidal model.

Minnesota Department of Transportation MnROAD Database

Asphalt Low Volume Road		Asphalt Mainline		Concrete Low Volume Road		Concrete Mainline	
Inside Lane Sections	Outside Lane Sections	Driving Lane Sections	Passing Lane Sections	Inside Lane Sections	Outside Lane Sections	Driving Lane Sections	Passing Lane Sections
24 - I	24 - O	1 - D	1 - P	32 - I	32 - O	5 - D	5 - P
25 - I	25 - O	2 - D	2 - P	36 - I	36 - O	6 - D	6 - P
26 - I	26 - O	3 - D	3 - P	37 - I	37 - O	7 - D	7 - P
27 - I	27 - O	4 - D	4 - P	38 - I	38 - O	8 - D	8 - P
28 - I	28 - O	14 - D	14 - P	39 - I	39 - O	9 - D	9 - P
29 - I	29 - O	15 - D	15 - P	40 - I	40 - O	10 - D	10 - P
30 - I	30 - O	16 - D	16 - P	41 - I	41 - O	11 - D	11 - P
31 - I	31 - O	17 - D	17 - P	42 - I	42 - O	12 - D	12 - P
33 - I	33 - O	18 - D	18 - P	43 - I	43 - O	13 - D	13 - P
34 - I	34 - O	19 - D	19 - P	44 - I	44 - O	60 - D	60 - P
35 - I	35 - O	20 - D	20 - P	45 - I	45 - O	61 - D	61 - P
54 - I	54 - O	21 - D	21 - P	46 - I	46 - O	62 - D	62 - P
77 - I	77 - O	22 - D	22 - P	52 - I	52 - O	63 - D	63 - P
78 - I	78 - O	23 - D	23 - P	53 - I	53 - O	114 - D	114 - P
79 - I	79 - O	50 - D	50 - P			213 - D	213 - P
		51 - D	51 - P			214 - D	214 - P
						414 - D	414 - P
						513 - D	513 - P
						614 - D	614 - P

Note: A particular roadway segment can be further defined by the inside (passing) or outside (driving) lane. MnROAD uses different terminology based on the roadway classification. Low Volume Road sections are defined by either "Inside Lane" or "Outside Lane", and Mainline sections are defined by either "Driving Lane" or "Passing Lane".

Roadway Group Dataset Summary

The roadway sections in each dataset group are included in the respective sigmoidal model.

Minnesota Department of Transportation MnROAD Database

Asphalt Low Volume Road*		Concrete Mainline*	
12 Ft Lane Width	13 - 14 Ft Lane Width	12 Ft Lane Width	13 - 14 Ft Lane Width
24	27	10	5
25	28	11	6
26	33	12	7
29	34	13	8
30	35	60	9
31	77	61	
54	78	62	
	79	63	
		114	
		213	
		214	
		414	
		513	
		614	

*Note: These grouped sections include both lane types. The Low Volume Road sections include the inside and outside lanes, and the Mainline sections include the driving and passing lanes.

Data Set Title:	Asphalt Sections
Case Study:	2
Data Source:	MnRoad
Number of Sections:	31
Number of Data Points (n):	1199
Number of Series (p):	184
Optimal Maximum Time Shift:	15 Years

Plot of Time Shifting Process:

$$IRI = a_1 + \frac{a_2}{1+e^{(-a_3*t+a_4)}}$$

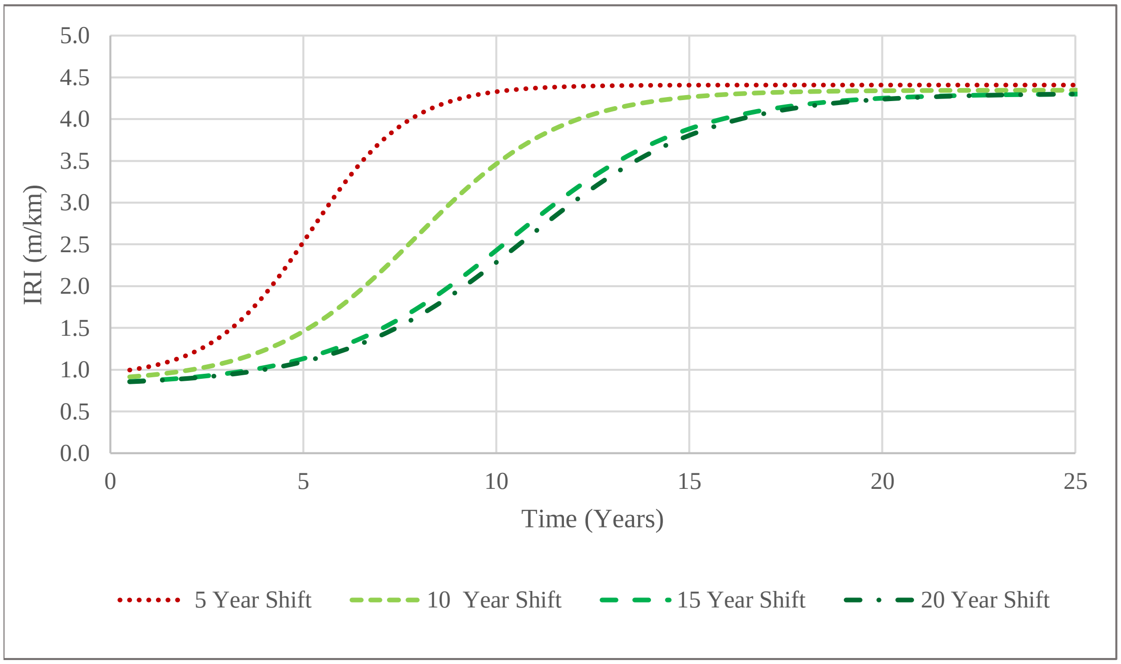

5 Year Shift		10 Year Shift		15 Year Shift		20 Year Shift	
a1	0.90816	a1	0.84593	a1	0.80623	a1	0.80828
a2	3.5	a2	3.5	a2	3.5	a2	3.5
a3	0.7814	a3	0.52769	a3	0.42619	a3	0.42008
a4	-4.0549	a4	-4.1893	a4	-4.4074	a4	-4.5154
Se/Sy	0.39412	Se/Sy	0.28773	Se/Sy	0.2739	Se/Sy	0.27337
R2	0.93188	R2	0.96429	R2	0.9677	R2	0.96782

Note: Green shading represents the optimal maximum time shift

Data Set Title:	Composite Sections
Case Study:	2
Data Source:	MnRoad
Number of Sections:	6
Number of Data Points (n):	293
Number of Series (p):	69
Optimal Maximum Time Shift:	10

Plot of Time Shifting Process:

$$IRI = a_1 + \frac{a_2}{1+e^{(-a_3*t+a_4)}}$$

5 Year Shift		10 Year Shift		15 Year Shift	
a1	0.4801	a1	0.46705	a1	0.46688
a2	3.5	a2	3.5	a2	3.5
a3	0.61036	a3	0.51808	a3	0.51785
a4	-2.6117	a4	-4.4161	a4	-5.2829
Se/Sy	0.32267	Se/Sy	0.31681	Se/Sy	0.31681
R2	0.95924	R2	0.96073	R2	0.96073

Note: Green shading represents the optimal maximum time shift

Data Set Title:	Concrete Sections
Case Study:	2
Data Source:	MnRoad
Number of Sections:	33
Number of Data Points (n):	1051
Number of Series (p):	180
Optimal Maximum Time Shift:	15 Years

Plot of Time Shifting Process:

$$IRI = a_1 + \frac{a_2}{1+e^{(-a_3*t+a_4)}}$$

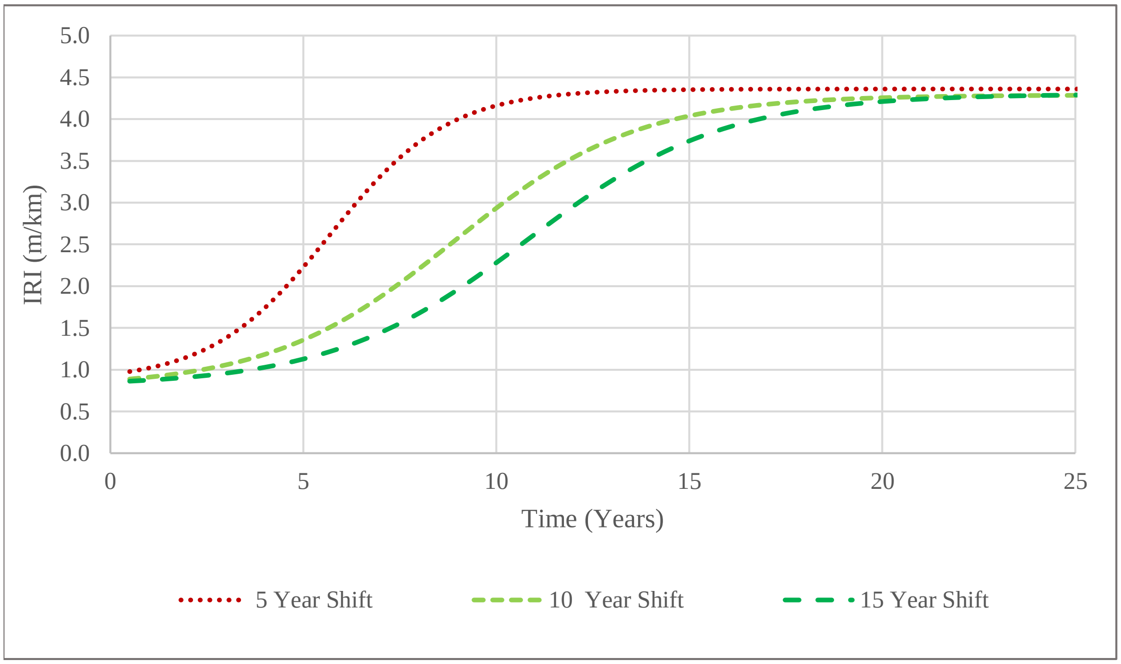

5 Year Shift		10 Year Shift		15 Year Shift	
a1	0.86087	a1	0.78869	a1	0.80188
a2	3.5	a2	3.5	a2	3.5
a3	0.6504	a3	0.42077	a3	0.39305
a4	-3.6962	a4	-3.7471	a4	-4.2428
Se/Sy	0.43342	Se/Sy	0.36533	Se/Sy	0.36223
R2	0.91879	R2	0.94302	R2	0.94401

Note: Green shading represents the optimal maximum time shift

Data Set Title:	Asphalt Low Volume Road Sections
Case Study:	2
Data Source:	MnRoad
Number of Sections:	15
Number of Data Points (n):	482
Number of Series (p):	78
Optimal Maximum Time Shift:	30 Years

Plot of Time Shifting Process:

$$IRI = a_1 + \frac{a_2}{1+e^{(-a_3*t+a_4)}}$$

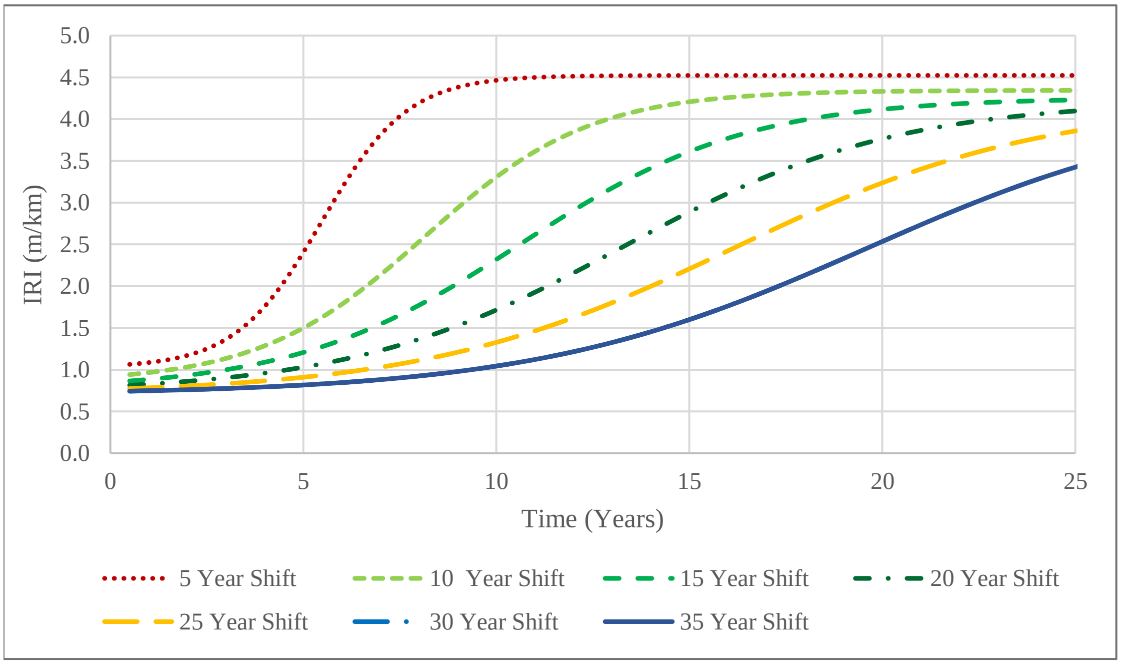

5 Year Shift		10 Year Shift		15 Year Shift		20 Year Shift		25 Year Shift	
a1	1.02359	a1	0.84524	a1	0.75627	a1	0.72101	a1	0.70471
a2	3.5	a2	3.5	a2	3.5	a2	3.5	a2	3.5
a3	0.89777	a3	0.46662	a3	0.34	a3	0.28211	a3	0.24933
a4	-4.9165	a4	-3.8038	a4	-3.6136	a4	-3.7461	a4	-4.0249
Se/Sy	0.52078	Se/Sy	0.35112	Se/Sy	0.31027	Se/Sy	0.29582	Se/Sy	0.29033
R2	0.87875	R2	0.94681	R2	0.95872	R2	0.96255	R2	0.96395

30 Year Shift		35 Year Shift	
a1	0.70171	a1	0.70171
a2	3.5	a2	3.5
a3	0.2319	a3	0.2319
a4	-4.5431	a4	-4.5431
Se/Sy	0.2885	Se/Sy	0.2885
R2	0.96441	R2	0.96441

Note: Green shading represents the optimal maximum time shift

Data Set Title:	Asphalt Mainline Sections
Case Study:	2
Data Source:	MnRoad
Number of Sections:	16
Number of Data Points (n):	665
Number of Series (p):	103
Optimal Maximum Time Shift:	15 Years

Plot of Time Shifting Process:

$$IRI = a_1 + \frac{a_2}{1+e^{(-a_3 * t + a_4)}}$$

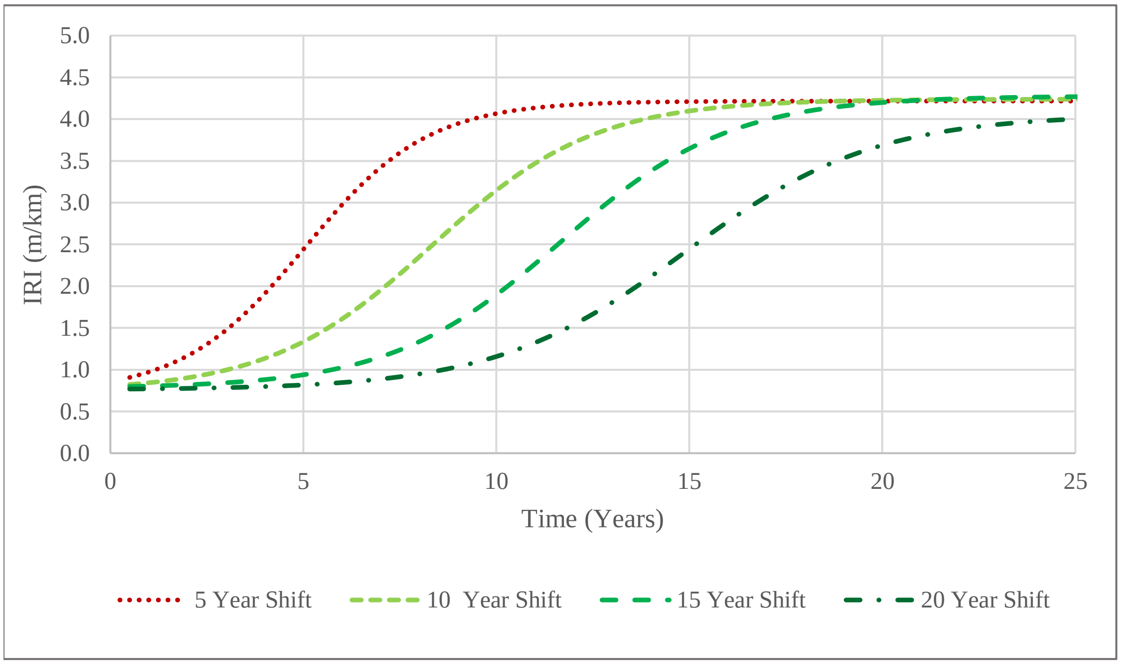

5 Year Shift		10 Year Shift		15 Year Shift		20 Year Shift	
a1	0.7163	a1	0.73912	a1	0.77642	a1	0.75868
a2	3.5	a2	3.5	a2	3.5	a2	3.2954
a3	0.62746	a3	0.4751	a3	0.45419	a3	0.40601
a4	-3.168	a4	-3.9607	a4	-5.296	a4	-6.0433
Se/Sy	0.31181	Se/Sy	0.24527	Se/Sy	0.24145	Se/Sy	0.2507
R2	0.95797	R2	0.97421	R2	0.97502	R2	0.97304

Note: Green shading represents the optimal maximum time shift

Data Set Title:	Concrete Low Volume Road Sections
Case Study:	2
Data Source:	MnRoad
Number of Sections:	14
Number of Data Points (n):	516
Number of Series (p):	93
Optimal Maximum Time Shift:	35 Years

Plot of Time Shifting Process:

$$IRI = a_1 + \frac{a_2}{1+e^{(-a_3*t+a_4)}}$$

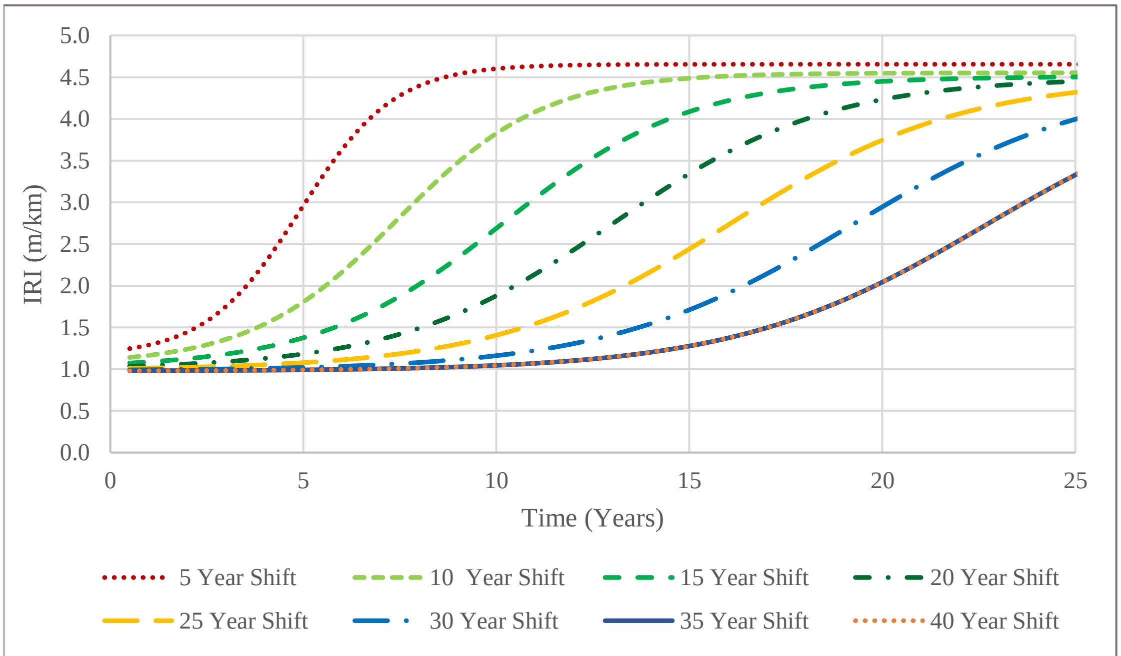

5 Year Shift		10 Year Shift		15 Year Shift		20 Year Shift		25 Year Shift	
a1	1.15559	a1	1.05269	a1	1.0104	a1	0.99637	a1	0.9897
a2	3.5	a2	3.5	a2	3.5	a2	3.5	a2	3.5
a3	0.82166	a3	0.52672	a3	0.41332	a3	0.3593	a3	0.33127
a4	-4.045	a4	-3.9275	a4	-4.2156	a4	-4.6784	a4	-5.3143
Se/Sy	0.41512	Se/Sy	0.31864	Se/Sy	0.29042	Se/Sy	0.28054	Se/Sy	0.27701
R2	0.92653	R2	0.9574	R2	0.96474	R2	0.96714	R2	0.96797

30 Year Shift		35 Year Shift		40 Year Shift	
a1	0.98145	a1	0.97619	a1	0.97619
a2	3.5	a2	3.5	a2	3.5
a3	0.31612	a3	0.30834	a3	0.30834
a4	-6.0764	a4	-6.9908	a4	-6.9908
Se/Sy	0.27574	Se/Sy	0.27529	Se/Sy	0.27529
R2	0.96827	R2	0.96838	R2	0.96838

Note: Green shading represents the optimal maximum time shift

Data Set Title:	Concrete Mainline Sections
Case Study:	2
Data Source:	MnRoad
Number of Sections:	19
Number of Data Points (n):	533
Number of Series (p):	89
Optimal Maximum Time Shift:	15 Years

Plot of Time Shifting Process:

$$IRI = a_1 + \frac{a_2}{1+e^{(-a_3 * t + a_4)}}$$

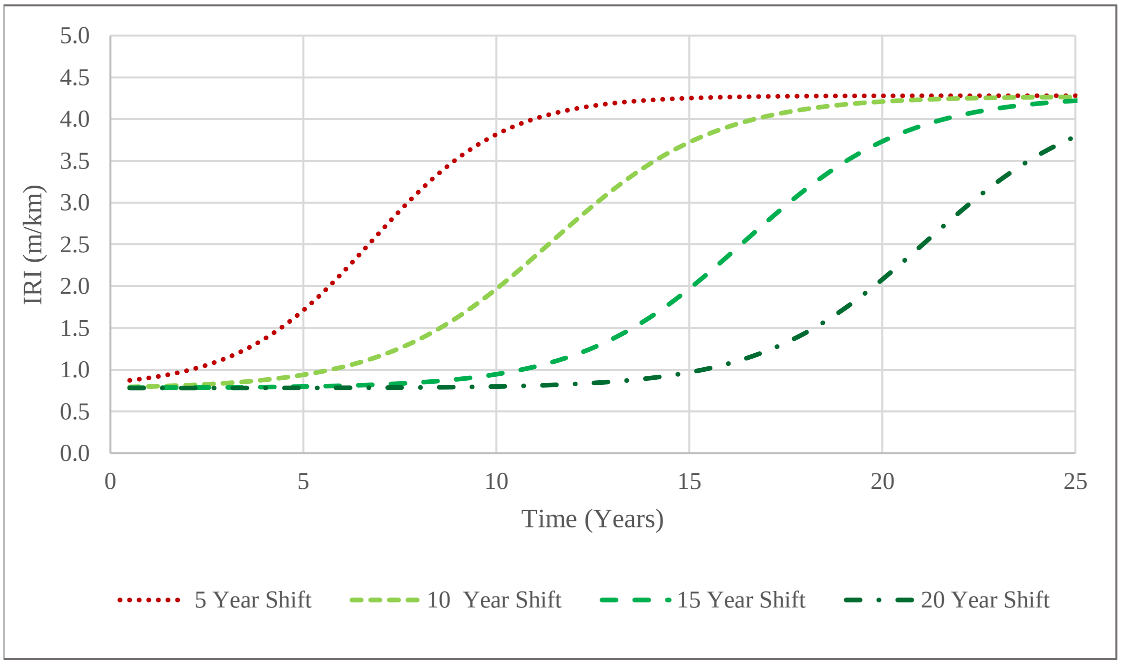

5 Year Shift		10 Year Shift		15 Year Shift		20 Year Shift	
a1	0.78073	a1	0.7719	a1	0.78133	a1	0.77971
a2	3.5	a2	3.5	a2	3.5	a2	3.5
a3	0.57909	a3	0.46797	a3	0.46998	a3	0.46854
a4	-3.9116	a4	-5.3366	a4	-7.7151	a4	-9.8956
Se/Sy	0.44084	Se/Sy	0.4189	Se/Sy	0.41839	Se/Sy	0.41835
R2	0.91532	R2	0.92388	R2	0.92407	R2	0.92409

Note: Green shading represents the optimal maximum time shift

Data Set Title:	Concrete Mainline Sections, with Drainage
Case Study:	2
Data Source:	MnRoad
Number of Sections:	5
Number of Data Points (n):	234
Number of Series (p):	39
Optimal Maximum Time Shift:	20 Years

Plot of Time Shifting Process:

$$IRI = a_1 + \frac{a_2}{1+e^{(-a_3*t+a_4)}}$$

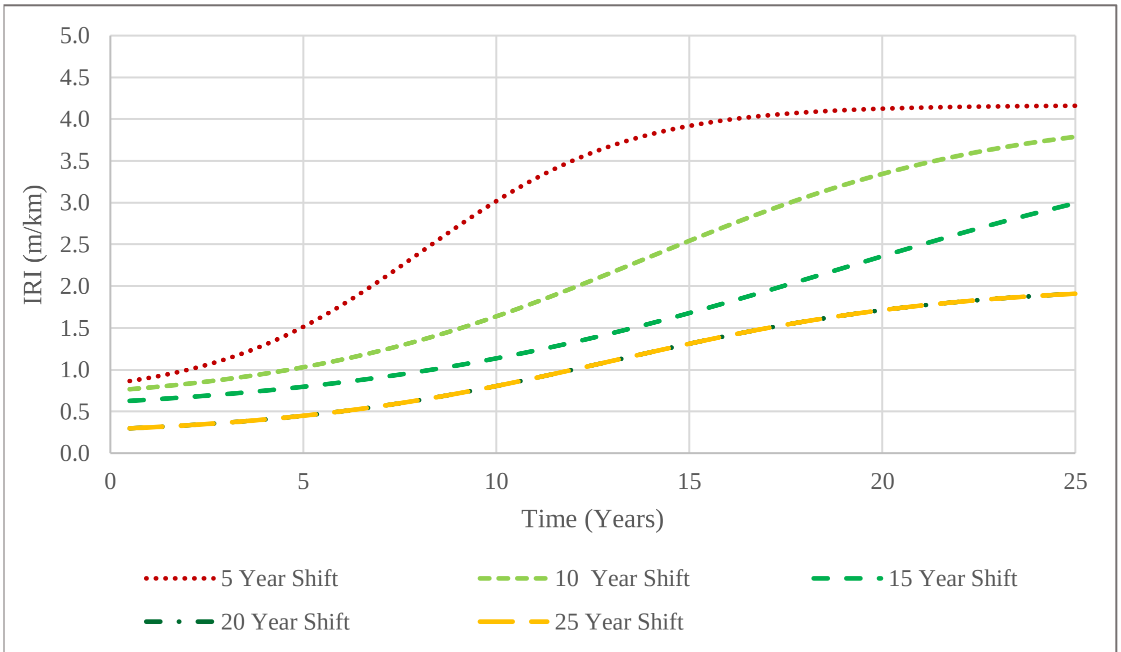

5 Year Shift		10 Year Shift		15 Year Shift		20 Year Shift		25 Year Shift	
a1	0.66607	a1	0.58211	a1	0.44765	a1	0.20182	a1	0.20182
a2	3.5	a2	3.49404	a2	3.49906	a2	1.81706	a2	1.81706
a3	0.37181	a3	0.21639	a3	0.15922	a3	0.2299	a3	0.2299
a4	-3	a4	-3	a4	-3	a4	-3	a4	-3
Se/Sy	0.42027	Se/Sy	0.32576	Se/Sy	0.3132	Se/Sy	0.30617	Se/Sy	0.30617
R2	0.92314	R2	0.95456	R2	0.95807	R2	0.95997	R2	0.95997

Note: Green shading represents the optimal maximum time shift

Data Set Title:	Concrete Mainline Sections, without Drainage
Case Study:	2
Data Source:	MnRoad
Number of Sections:	14
Number of Data Points (n):	288
Number of Series (p):	52
Optimal Maximum Time Shift:	10 Years

Plot of Time Shifting Process:

$$IRI = a_1 + \frac{a_2}{1+e^{(-a_3*t+a_4)}}$$

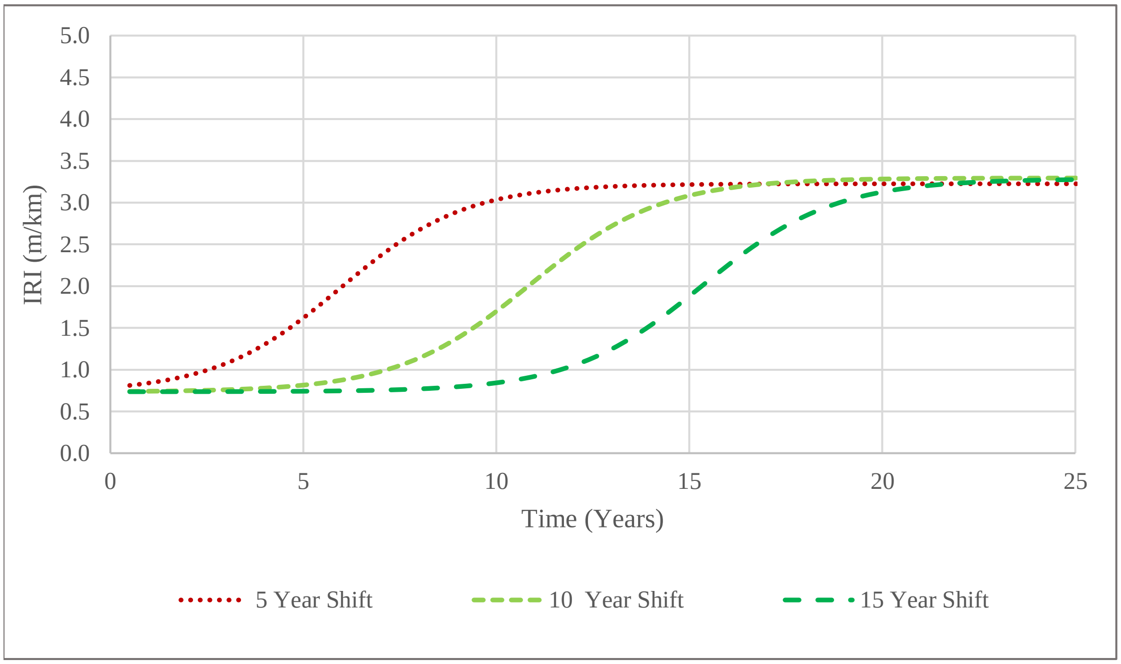

5 Year Shift		10 Year Shift		15 Year Shift	
a1	0.72759	a1	0.73381	a1	0.73584
a2	2.49833	a2	2.56137	a2	2.54866
a3	0.61572	a3	0.58296	a3	0.58573
a4	-3.6679	a4	-6.3327	a4	-8.9895
Se/Sy	0.38398	Se/Sy	0.37991	Se/Sy	0.37991
R2	0.93742	R2	0.93878	R2	0.93879

Note: Green shading represents the optimal maximum time shift

Data Set Title:	Asphalt Low Volume Road - Inside Lane Sections
Case Study:	2
Data Source:	MnRoad
Number of Sections:	15
Number of Data Points (n):	216
Number of Series (p):	36
Optimal Maximum Time Shift:	35 Years

Plot of Time Shifting Process:

$$IRI = a_1 + \frac{a_2}{1+e^{(-a_3*t+a_4)}}$$

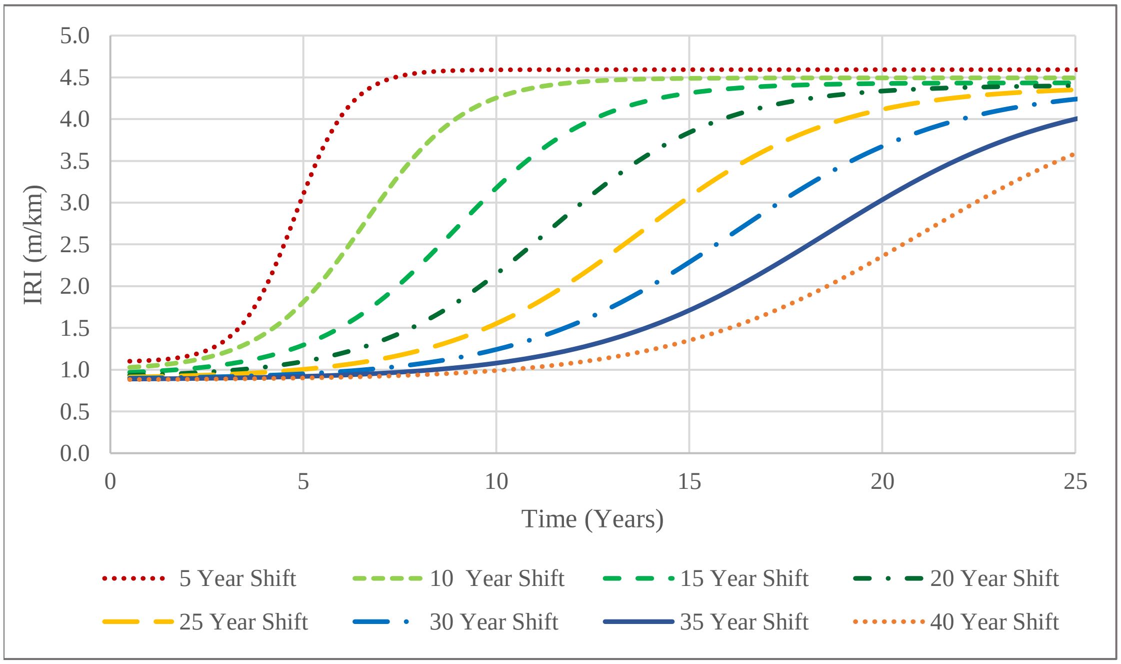

5 Year Shift		10 Year Shift		15 Year Shift		20 Year Shift		25 Year Shift	
a1	1.09242	a1	0.99359	a1	0.93435	a1	0.90604	a1	0.8927
a2	3.5	a2	3.5	a2	3.5	a2	3.5	a2	3.5
a3	1.39559	a3	0.76046	a3	0.54822	a3	0.44938	a3	0.3918
a4	-6.68	a4	-4.9925	a4	-4.9044	a4	-5.0947	a4	-5.3782
Se/Sy	0.53201	Se/Sy	0.37196	Se/Sy	0.34088	Se/Sy	0.32563	Se/Sy	0.31747
R2	0.87352	R2	0.9403	R2	0.95011	R2	0.95458	R2	0.95688

30 Year Shift		35 Year Shift		40 Year Shift	
a1	0.88398	a1	0.87883	a1	0.87556
a2	3.5	a2	3.5	a2	3.5
a3	0.35398	a3	0.32757	a3	0.30862
a4	-5.7114	a4	-6.0791	a4	-6.4804
Se/Sy	0.31288	Se/Sy	0.3102	Se/Sy	0.30861
R2	0.95815	R2	0.95887	R2	0.9593

Note: Green shading represents the optimal maximum time shift

Data Set Title:	Asphalt Low Volume Road - Outside Lane Sections
Case Study:	2
Data Source:	MnRoad
Number of Sections:	15
Number of Data Points (n):	277
Number of Series (p):	45
Optimal Maximum Time Shift:	20 Years

Plot of Time Shifting Process:

$$IRI = a_1 + \frac{a_2}{1+e^{(-a_3*t+a_4)}}$$

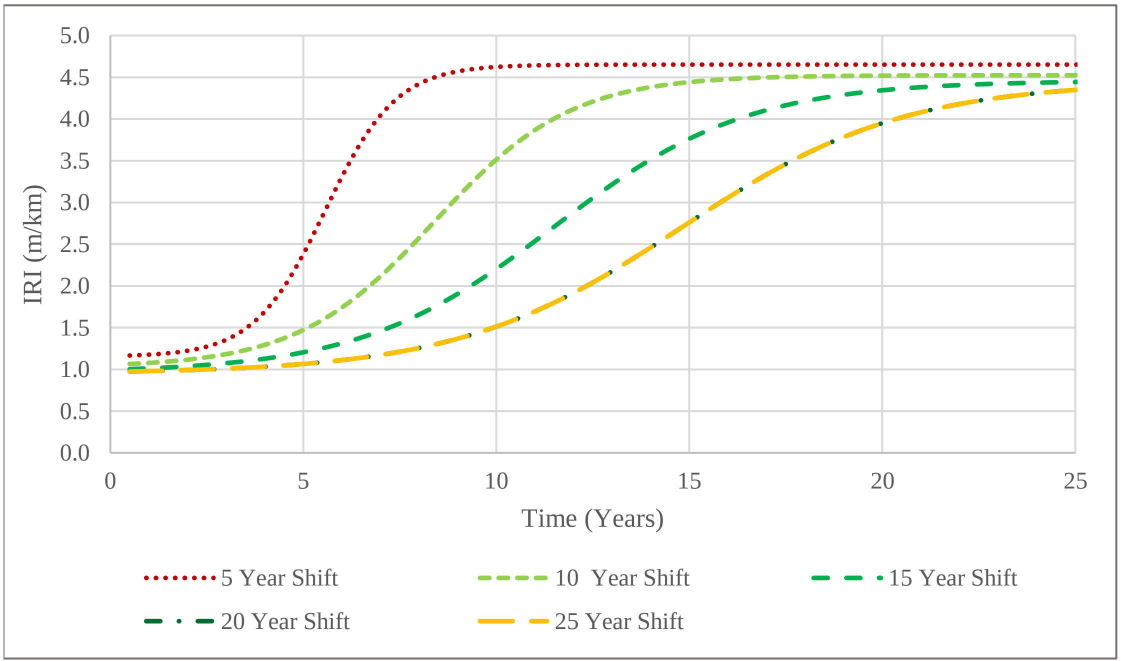

5 Year Shift		10 Year Shift		15 Year Shift		20 Year Shift		25 Year Shift	
a1	1.15223	a1	1.0248	a1	0.95937	a1	0.94971	a1	0.94971
a2	3.5	a2	3.5	a2	3.5	a2	3.5	a2	3.5
a3	1.08724	a3	0.56441	a3	0.3978	a3	0.34454	a3	0.34454
a4	-6.0493	a4	-4.7432	a4	-4.5735	a4	-5.0975	a4	-5.0975
Se/Sy	0.51947	Se/Sy	0.33764	Se/Sy	0.31129	Se/Sy	0.30835	Se/Sy	0.30835
R2	0.8793	R2	0.95088	R2	0.95841	R2	0.95921	R2	0.95921

Note: Green shading represents the optimal maximum time shift

Data Set Title:	Asphalt Mainline - Driving Lane Sections
Case Study:	2
Data Source:	MnRoad
Number of Sections:	16
Number of Data Points (n):	351
Number of Series (p):	54
Optimal Maximum Time Shift:	15 Years

Plot of Time Shifting Process:

$$IRI = a_1 + \frac{a_2}{1+e^{(-a_3 * t + a_4)}}$$

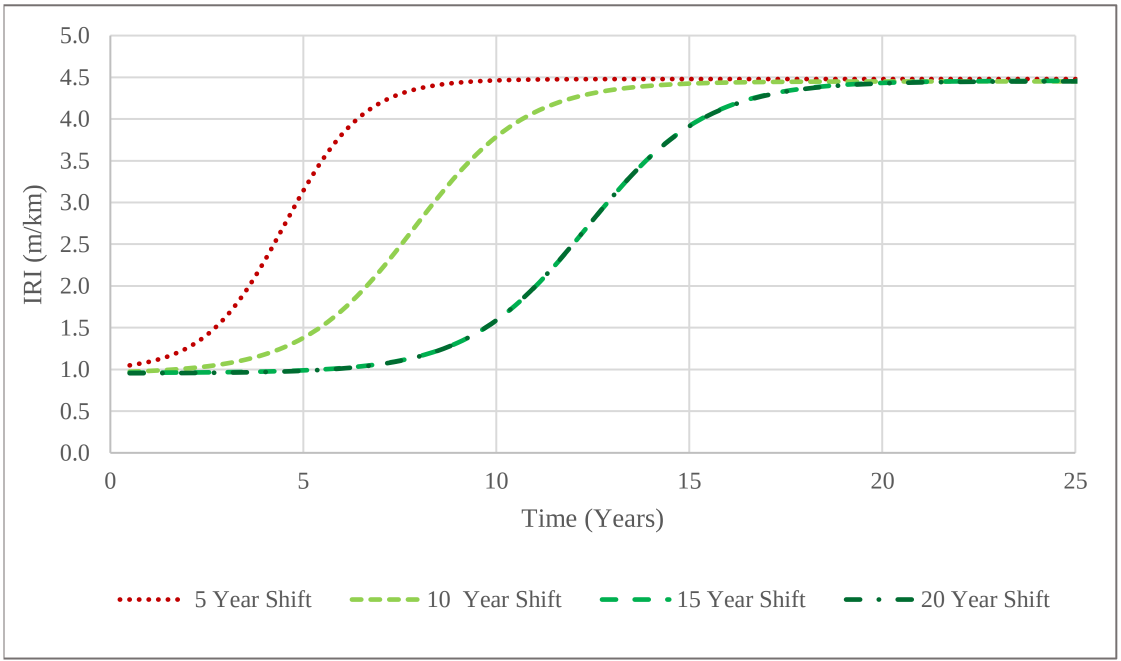

5 Year Shift		10 Year Shift		15 Year Shift		20 Year Shift	
a1	0.97933	a1	0.95087	a1	0.95834	a1	0.95244
a2	3.5	a2	3.5	a2	3.5	a2	3.5
a3	0.97422	a3	0.68542	a3	0.64365	a3	0.64175
a4	-4.3919	a4	-5.4014	a4	-7.9551	a4	-7.9224
Se/Sy	0.32358	Se/Sy	0.2622	Se/Sy	0.2588	Se/Sy	0.25871
R2	0.95454	R2	0.97039	R2	0.97117	R2	0.97119

Note: Green shading represents the optimal maximum time shift

Data Set Title:	Asphalt Mainline - Passing Lane Sections
Case Study:	2
Data Source:	MnRoad
Number of Sections:	16
Number of Data Points (n):	336
Number of Series (p):	51
Optimal Maximum Time Shift:	20 Years

Plot of Time Shifting Process:

$$IRI = a_1 + \frac{a_2}{1+e^{(-a_3*t+a_4)}}$$

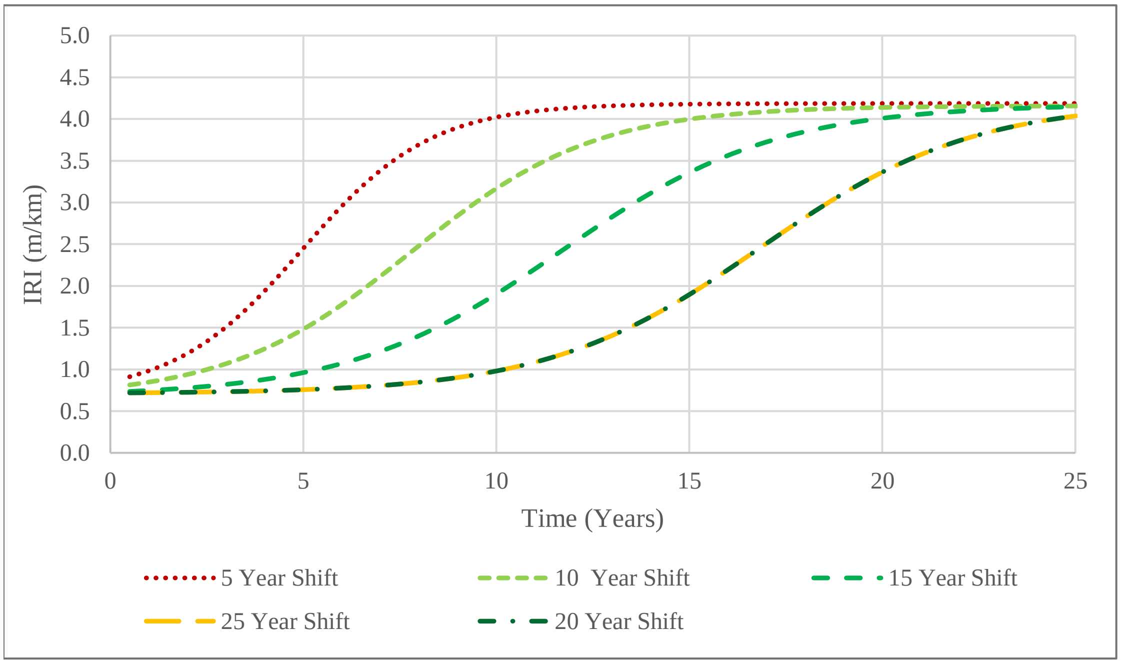

5 Year Shift		10 Year Shift		15 Year Shift		20 Year Shift		25 Year Shift	
a1	0.68661	a1	0.6589	a1	0.67573	a1	0.70968	a1	0.70968
a2	3.5	a2	3.5	a2	3.5	a2	3.5	a2	3.5
a3	0.59855	a3	0.4212	a3	0.36113	a3	0.36215	a3	0.36215
a4	-2.9766	a4	-3.2842	a4	-4.2273	a4	-6.0996	a4	-6.0996
Se/Sy	0.34926	Se/Sy	0.25838	Se/Sy	0.24714	Se/Sy	0.24665	Se/Sy	0.24665
R2	0.94669	R2	0.97119	R2	0.97367	R2	0.97378	R2	0.97378

Note: Green shading represents the optimal maximum time shift

Data Set Title:	Concrete Low Volume Road - Inside Lane Sections
Case Study:	2
Data Source:	MnRoad
Number of Sections:	14
Number of Data Points (n):	259
Number of Series (p):	48
Optimal Maximum Time Shift:	15 Years

Plot of Time Shifting Process:

$$IRI = a_1 + \frac{a_2}{1+e^{(-a_3*t+a_4)}}$$

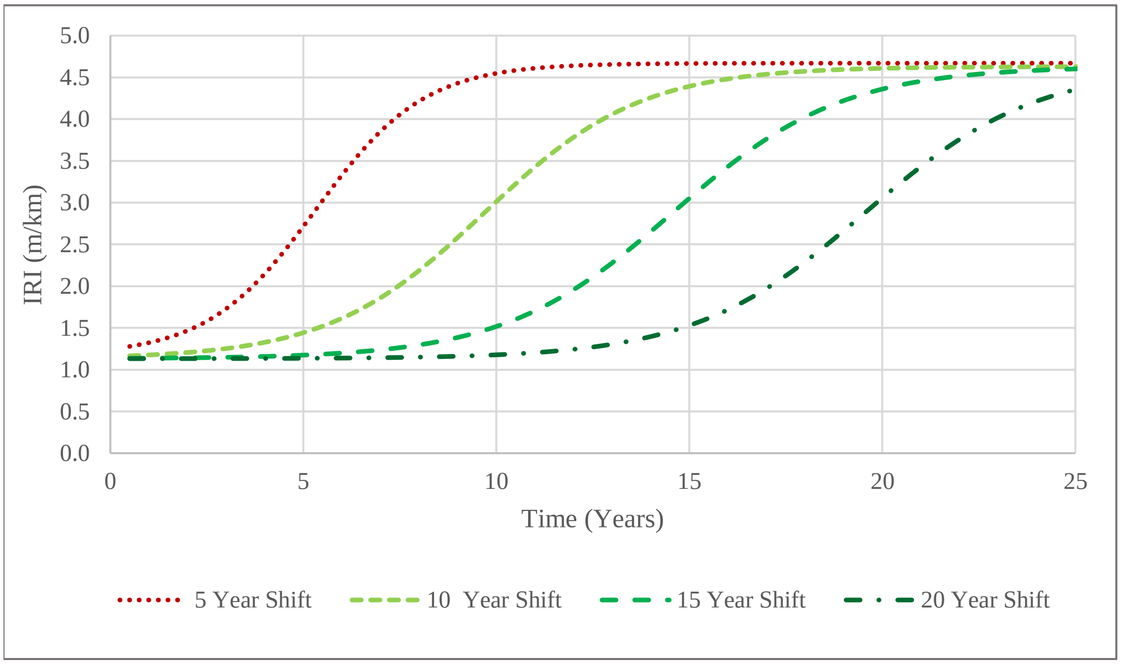

5 Year Shift		10 Year Shift		15 Year Shift		20 Year Shift	
a1	1.16957	a1	1.12931	a1	1.13062	a1	1.13117
a2	3.5	a2	3.5	a2	3.5	a2	3.5
a3	0.71219	a3	0.49434	a3	0.45645	a3	0.45032
a4	-3.7956	a4	-4.7909	a4	-6.6509	a4	-8.8061
Se/Sy	0.36274	Se/Sy	0.32298	Se/Sy	0.31883	Se/Sy	0.31837
R2	0.94466	R2	0.95639	R2	0.95753	R2	0.95765

Note: Green shading represents the optimal maximum time shift

Data Set Title:	Concrete Low Volume Road - Outside Lane Section
Case Study:	2
Data Source:	MnRoad
Number of Sections:	14
Number of Data Points (n):	252
Number of Series (p):	47
Optimal Maximum Time Shift:	20 Years

Plot of Time Shifting Process:

$$IRI = a_1 + \frac{a_2}{1+e^{(-a_3*t+a_4)}}$$

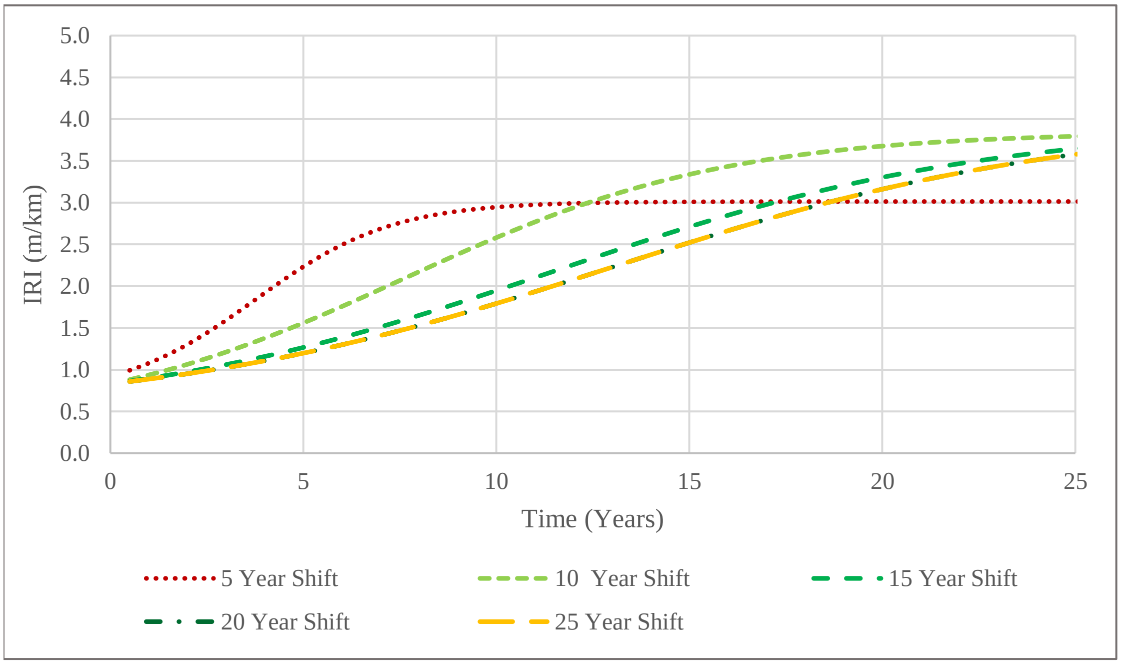

5 Year Shift		10 Year Shift		15 Year Shift		20 Year Shift		25 Year Shift	
a1	0.67255	a1	0.34725	a1	0.43472	a1	0.48638	a1	0.48638
a2	2.34099	a2	3.5	a2	3.5	a2	3.5	a2	3.5
a3	0.56371	a3	0.24045	a3	0.17863	a3	0.16951	a3	0.16951
a4	-2.1263	a4	-1.8367	a4	-2.0597	a4	-2.214	a4	-2.214
Se/Sy	0.38443	Se/Sy	0.27313	Se/Sy	0.25571	Se/Sy	0.25531	Se/Sy	0.25531
R2	0.93771	R2	0.96906	R2	0.97293	R2	0.97302	R2	0.97302

Note: Green shading represents the optimal maximum time shift

Data Set Title:	Concrete Mainline - Driving Lane Sections
Case Study:	2
Data Source:	MnRoad
Number of Sections:	19
Number of Data Points (n):	271
Number of Series (p):	45
Optimal Maximum Time Shift:	10 Years

Plot of Time Shifting Process:

$$IRI = a_1 + \frac{a_2}{1+e^{(-a_3*t+a_4)}}$$

5 Year Shift		10 Year Shift		15 Year Shift	
a1	0.14878	a1	0.35215	a1	0.35215
a2	3.5	a2	3.5	a2	3.5
a3	0.25896	a3	0.23293	a3	0.23293
a4	-1.5913	a4	-2.2716	a4	-2.2716
Se/Sy	0.43108	Se/Sy	0.40821	Se/Sy	0.40821
R2	0.91938	R2	0.92803	R2	0.92803

Note: Green shading represents the optimal maximum time shift

Data Set Title:	Concrete Mainline - Passing Lane Sections
Case Study:	2
Data Source:	MnRoad
Number of Sections:	19
Number of Data Points (n):	264
Number of Series (p):	46
Optimal Maximum Time Shift:	10 Years

Plot of Time Shifting Process:

$$IRI = a_1 + \frac{a_2}{1+e^{(-a_3*t+a_4)}}$$

5 Year Shift		10 Year Shift		15 Year Shift	
a1	0.69717	a1	0.7284	a1	0.7284
a2	3.5	a2	3.5	a2	3.5
a3	0.47757	a3	0.45848	a3	0.45848
a4	-3.5699	a4	-5.7347	a4	-5.7347
Se/Sy	0.40581	Se/Sy	0.40024	Se/Sy	0.40024
R2	0.92925	R2	0.93124	R2	0.93124

Note: Green shading represents the optimal maximum time shift

Data Set Title:	Asphalt Low Volume Road - 12 Ft Lane Width
Case Study:	2
Data Source:	MnRoad
Number of Sections:	7
Number of Data Points (n):	237
Number of Series (p):	39
Optimal Maximum Time Shift:	15 Years

Plot of Time Shifting Process:

$$IRI = a_1 + \frac{a_2}{1+e^{(-a_3*t+a_4)}}$$

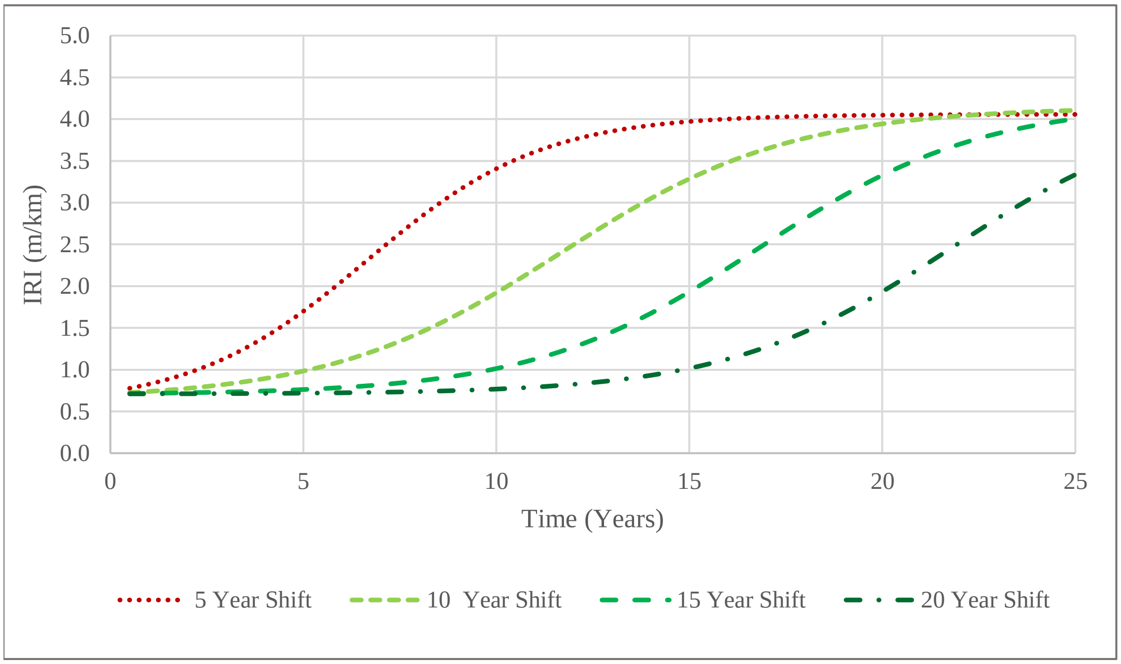

5 Year Shift		10 Year Shift		15 Year Shift		20 Year Shift	
a1	0.55757	a1	0.64381	a1	0.70146	a1	0.70802
a2	3.5	a2	3.5	a2	3.5	a2	3.5
a3	0.44012	a3	0.33542	a3	0.34258	a3	0.34396
a4	-2.926	a4	-3.9085	a4	-5.7504	a4	-7.496
Se/Sy	0.45633	Se/Sy	0.40185	Se/Sy	0.40042	Se/Sy	0.4003
R2	0.90845	R2	0.9298	R2	0.93031	R2	0.93036

Note: Green shading represents the optimal maximum time shift

Data Set Title:	Asphalt Low Volume Road - 13 or 14 Ft Lane Widt
Case Study:	2
Data Source:	MnRoad
Number of Sections:	8
Number of Data Points (n):	262
Number of Series (p):	41
Optimal Maximum Time Shift:	20 Years

Plot of Time Shifting Process:

$$IRI = a_1 + \frac{a_2}{1+e^{(-a_3 * t + a_4)}}$$

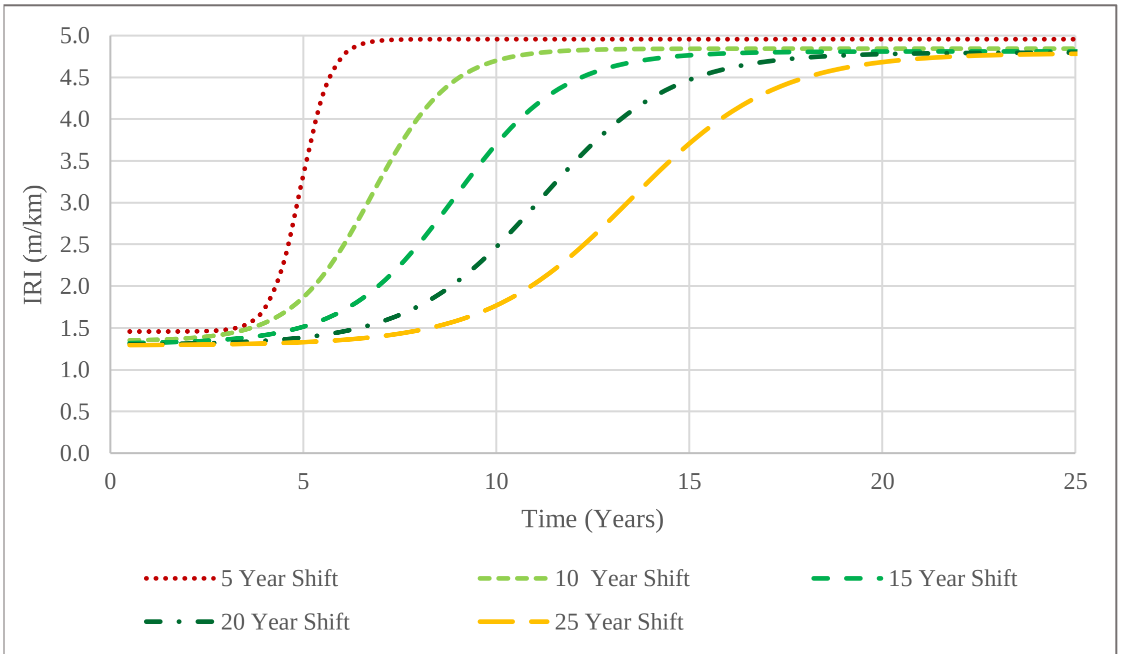

5 Year Shift		10 Year Shift		15 Year Shift		20 Year Shift		25 Year Shift	
a1	1.45664	a1	1.34384	a1	1.31029	a1	1.29654	a1	1.2904
a2	3.5	a2	3.5	a2	3.5	a2	3.5	a2	3.5
a3	2.59131	a3	0.97867	a3	0.7098	a3	0.59179	a3	0.52907
a4	-12.814	a4	-6.6332	a4	-6.3295	a4	-6.6029	a4	-7.1333
Se/Sy	0.48734	Se/Sy	0.28371	Se/Sy	0.26026	Se/Sy	0.25257	Se/Sy	0.2496
R2	0.89381	R2	0.96532	R2	0.9709	R2	0.97262	R2	0.97327

Note: Green shading represents the optimal maximum time shift

Data Set Title:	Concrete Mainline - 12 Ft Lane Width
Case Study:	2
Data Source:	MnRoad
Number of Sections:	14
Number of Data Points (n):	262
Number of Series (p):	47
Optimal Maximum Time Shift:	10 Years

Plot of Time Shifting Process:

$$IRI = a_1 + \frac{a_2}{1+e^{(-a_3*t+a_4)}}$$

5 Year Shift		10 Year Shift		15 Year Shift	
a1	0.49056	a1	0.48182	a1	0.4818
a2	3.5	a2	3.5	a2	3.5
a3	0.34443	a3	0.30887	a3	0.30886
a4	-2.4597	a4	-2.5081	a4	-2.5081
Se/Sy	0.39938	Se/Sy	0.38681	Se/Sy	0.38681
R2	0.93199	R2	0.93635	R2	0.93635

Note: Green shading represents the optimal maximum time shift

Data Set Title:	Concrete Mainline - 13 or 14 Ft Lane Width
Case Study:	2
Data Source:	MnRoad
Number of Sections:	5
Number of Data Points (n):	266
Number of Series (p):	43
Optimal Maximum Time Shift:	10 Years

Plot of Time Shifting Process:

$$IRI = a_1 + \frac{a_2}{1+e^{(-a_3*t+a_4)}}$$

5 Year Shift		10 Year Shift		15 Year Shift	
a1	0.13585	a1	0.25687	a1	0.25314
a2	3.5	a2	3.5	a2	3.5
a3	0.23914	a3	0.1643	a3	0.16362
a4	-1.5628	a4	-1.9666	a4	-2.8292
Se/Sy	0.43868	Se/Sy	0.40902	Se/Sy	0.40902
R2	0.91546	R2	0.92694	R2	0.92694

Note: Green shading represents the optimal maximum time shift